CArbon-14 Source Term
CAST

Final report on results from Work Package 5: Carbon-14 in irradiated graphite (D5.19)

Authors:

Nelly Toulhoat, Nathalie Moncoffre, Ernestas Narkunas, Povilas Poskas, Crina Bucur, Camelia Ichim, Laurent Petit, Stephan Schumacher, Stephane Catherin, Mauro Capone, Natalia Shcherbina, Andrey Bukaemskiy, Marina Rodríguez Alcalá, Enrique Magro, Eva María Márquez, Gabriel Piña, Johannes Fachinger, Viorel Fugaru, Simon Norris, Borys Zlobenko

Editor: Simon Norris

Date of issue of this report: 04/01/18

CAST
Final report on results from Work Package 5:
Carbon-14 in irradiated graphite (D5.19)

CAST – Project Overview

The CAST project (CArbon-14 Source Term) aims to develop understanding of the potential release mechanisms of carbon-14 from radioactive waste materials under conditions relevant to waste packaging and disposal to underground geological disposal facilities. The project focuses on the release of carbon-14 as dissolved and gaseous species from irradiated metals (steels, Zircaloys), irradiated graphite and from ion-exchange materials.
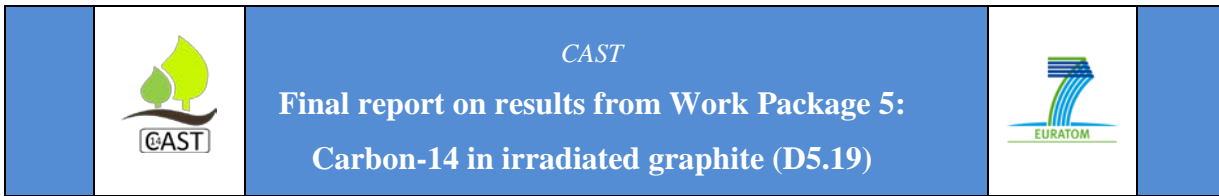
The CAST consortium brings together 33 partners with a range of skills and competencies in the management of radioactive wastes containing carbon-14, geological disposal research, safety case development and experimental work on gas generation. The consortium consists of national waste management organisations, research institutes, universities and commercial organisations.

The objectives of the CAST project are to gain new scientific understanding of the rate of release of carbon-14 (from the corrosion of irradiated steels and Zircaloys and from the leaching of ion-exchange resins and irradiated graphites under geological disposal conditions), its speciation, and how these relate to the carbon-14 inventory and to aqueous conditions. These results will be evaluated in the context of national safety assessments and disseminated to interested stakeholders. The new understanding should be of relevance to national safety assessment stakeholders and will also provide an opportunity for training for early career researchers.

For more information, please visit the CAST website at:
http://www.projectcast.eu

CAST		
Final report on results from Work Package 5: Carbon-14 in irradiated graphite (D5.19)		

CAST		
Work Package: 5	CAST Document no. 5.19	Document type:
Task:	CAST-2017-D5.19	R
Issued by: RWM		Document status:
Internal no. : not applicable		FINAL

Document title
Final report on results from WP5 (D5.19)

## Executive Summary (by organisation)

Work Package 5 involves the contribution of a number of organisations in relation to irradiated graphite (i-graphite)[1] studies. This report summarises their progress in CAST on an organisation-by-organisation basis. Note that the work undertaken by each organisation is affected by the national position in relation to the management of i-graphite, which in some cases involves treatment activities. In this Executive Summary, the top-level output of each organisation in CAST Work Package 5 is presented.

1   CNRS/IN2P3 (IPNL) participates in Task 5.2, named "Characterisation of the ^{14}C inventory in i-graphites" of Work Package 5. This task aims at characterising the ^{14}C inventory in i-graphites because such information is essential in understanding the release. CNRS/IN2P3 (IPNL) develops an indirect approach based on ion-irradiation of ^{13}C-implanted virgin graphites (HOPG model graphite). ^{13}C implantation is used to simulate ^{14}C displaced from its original structural site through nuclear recoil. Ion irradiation is used to simulate neutron irradiation and study the effects of both graphite structure modification and irradiation on the migration of ^{14}C. The results are presented in Deliverable D 5.18.

2   During the first three years of the CAST Project, LEI concentrated on the performance of the Task 5.1 – "Review of CARBOWASTE and other relevant R&D activities to establish the current understanding of inventory and release of ^{14}C from i-graphites" and Task 5.2 – "Characterisation of the ^{14}C inventory in i-graphites". Task 5.5

---

[1] "Irradiated graphite" is referred to in some national programmes as "nuclear graphite".

CAST
Final report on results from Work Package 5:
Carbon-14 in irradiated graphite (D5.19)
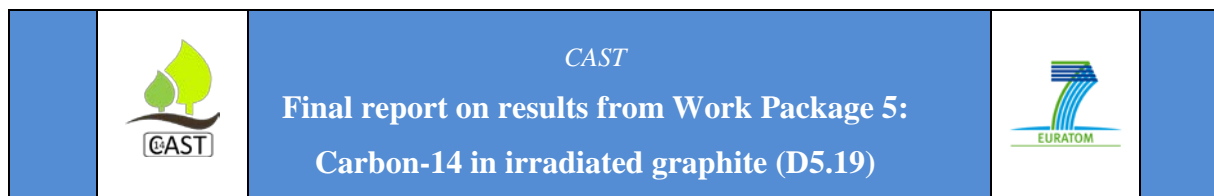
"Data interpretation and synthesis – final report" is a final project year activity. For the Task 5.1, LEI reviewed the outcome of CARBOWASTE Project in the national context and based on that, provided input for deliverable D5.5 "Review of current understanding of inventory and release of ^{14}C from irradiated graphites". For the Task 5.2, LEI modelled the ^{14}C inventory in a RBMK-1500 reactor core using new developed models and experimental data and prepared deliverable D5.17 "Report on modelling of ^{14}C inventory in RBMK reactor core". The Task 5.5 "Data interpretation and synthesis – final report" is the last Task of WP5 that summarises and synthesises in a final report the work undertaken in the previous Tasks by all participants. The outcome of this Task is this deliverable D5.19 "Final report on results from WP5".

3   RATEN ICN was involved in Task 5.1 and Task 5.3. For the Task 5.1, RATEN ICN reviewed the outcome of CARBOWASTE project in the Romanian context as well as the ^{14}C content and speciation and their correlation with impurity content and irradiation history in the MTR i-graphite. The results of the review of the current knowledge achieved in the understanding of the speciation of ^{14}C from irradiated graphite used in research reactors are included in D5.5 "Review of Current Understanding of Inventory and Release of ^{14}C from Irradiated Graphite".

For Task 5.3, RATEN ICN carried out leaching tests, in aerobic and anaerobic conditions, to assess the ^{14}C release as dissolved species in alkaline solution simulating the cementitious environment. The irradiated graphite available for the leaching tests is originating from a brick dismantled in 2000 from the thermal column of the TRIGA research reactor in operation at RATEN ICN. The total ^{14}C measurement in the powder graphite samples taken during mechanical cutting of the specimens used in the leaching tests was achieved by combustion in oxygen reach atmosphere. Also, gamma emitting radionuclides were measured by gamma spectrometry on the same powder graphite samples. For the measurement of inorganic and organic fraction of the ^{14}C released in leachate solutions an analytical method based on acid stripping and wet oxidation was applied. The ^{14}C measurement were carried out by liquid scintillation counting (LSC) using a Tri-Carb® analyser Model 3110 TR. The experimental results obtained from the leaching tests both in aerobic and anaerobic conditions confirm the low ^{14}C release in alkaline environment. Less than 2% from the total ^{14}C inventory in the

CAST
Final report on results from Work Package 5:
Carbon-14 in irradiated graphite (D5.19)

specimens that were subjected to the leaching tests was released as dissolved species. Under aerobic conditions, the ^{14}C released was found to be predominantly in inorganic forms (around 68% from the total ^{14}C released), while in anaerobic conditions, the ^{14}C is released mainly as organic species (around 65% from the total ^{14}C released). These results are presented in D5.10 "Final report on C-14 release and inorganic/organic ratio in leachates from TRIGA irradiated graphite"

4   During the CAST project, Andra and EDF shared some results from studies on French i-graphite. The first step was to review the existing leaching data on carbon-14 in French i-graphites. Deliverable D5.1 was devoted to the synthesis of the leaching rates of carbon-14. In deliverable D5.8, the second step was to study the speciation of the released carbon-14 in the leaching liquor and in the gas phase.

5   ENEA participated in Tasks 5.4 "Exfoliation of irradiated nuclear graphite by treatment with organic solvent assisted by ultrasound", within Work Package 5 (WP5) of the CAST Project. The behaviour of nuclear graphite (NG) through the exfoliation process has been studied, carried out with different organic solvents to remove primarily radiocarbon and estimate the "Removal Efficiency" (as percentage of the recovered activities after treatment in comparison to the original values) of the used solvents, in order to propose a reliable approach to produce graphite for recycling or/and safety disposed as L&ILW.

The exfoliation method is a reliable method to remove some ^{14}C from nuclear graphite, paving the way for the production of graphite for recycling and/or safe disposal. To support this method, a lot of evidence has been collected.

It has been demonstrated that the ratio powder/solvent has a crucial position in the optimization of the whole procedure. The recovery of exfoliated graphite increases when the ratio powder/solvent is low: to maximize the effect of the solvent it could be very useful to operate with a recovery and recycling system, also due to the fact that the solution produced from the exfoliation of nuclear graphite is highly radioactive.

CAST
Final report on results from Work Package 5:
Carbon-14 in irradiated graphite (D5.19)

The extracting abilities of each solvent are quite comparable. Since the partially removed activity is independent of the yield degree, these results can be interpreted on the basis that not all the ^{14}C species in the irradiated graphite are the same and only the ones not chemically bonded or in those forms that have some chemical or physical-chemical affinity with the extracting media are likely to be removed.

These first results are promising enough to promote further investigations in this direction. Furthermore, there is no doubt that the basic aqueous mixture is more efficient in the removal of ^{14}C respect to the organic solvents. NaOH increases the production of carbonate (highly soluble in water) confirming that the next experiments have to be designed following this evidence, focusing on efforts to develop a "total green" procedure.

6   During three years of CAST project FZJ participated in the Tasks 5.1-5.3 and 5.5 of WP5, providing contributions to a number of reports and deliverables. Within the first year FZJ contributed to the "Review of CARBOWASTE and other relevant R&D activities to establish the current understanding of inventory and release of ^{14}C from i-graphites" (D5.5) and "Characterisation of the ^{14}C inventory in i-graphites" (D5.6). The relevant to the project information on different German i-graphite (FRJ-1, FRJ-2, AVR, HTHR-300, RFR) was summarized and provided to the CAST-community. Within the Task 5.3 FZJ comprehensively characterized RFR i-graphite and investigated the leaching behaviour of RFR i-graphite, providing for contributions to the "Definition of the scientific scope of leaching experiments" (D5.4), Annual Progress Reports (D 5.6 and D5.9), as well as to the "Final evaluation of leach rates of treated and untreated i-graphite from the Rossendorf Research reactor" (D5.12). The outcome of the Task 5.5 is the current "Final report on results from WP5" (D5.19).
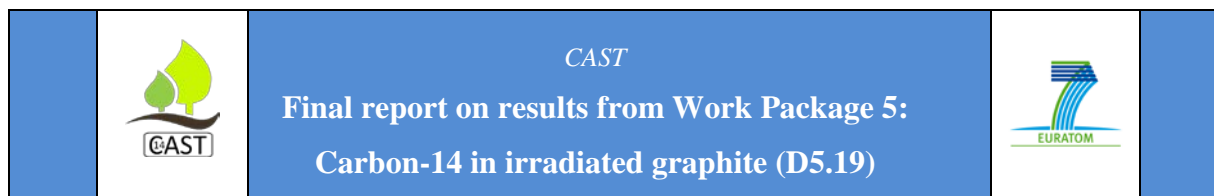
7   Throughout the CAST project CIEMAT has been involved in four of the five main tasks of the WP5: Graphite. These tasks are Task 5.1 "Review of CARBOWASTE and other relevant R&D activities to establish the current understanding of inventory and release of ^{14}C from i-graphites", Task 5.3 "Measurement of release of ^{14}C inventory from i-graphites", Task 5.4 "New waste forms and ^{14}C decontamination techniques for i-graphites" and Task 5.5 "Data interpretation and synthesis – final report".

Regarding the Tasks 5.1 and 5.5, CIEMAT provided its contribution to the deliverables D5.4 "Definition of a recommended scientific scope of leaching experiments and harmonized leaching parameters", D5.5 "WP5 Review of Current Understanding of Inventory and Release of ^{14}C from Irradiated Graphite" and the current report (D5.19), all generated as an output of these tasks.

For the Task 5.3, CIEMAT developed both analytical methods and protocols to measure the release of ^{14}C from irradiated graphite samples and the speciation in the aqueous and gaseous phase. The conclusions of these works were depicted in the report D5.15 "WP5 CIEMAT Final Report on ^{14}C Leaching from Vandellós I Graphite".

Finally, for Task 5.4, CIEMAT manufactured a new impermeable graphite matrix denominated (IGM), and investigated the behaviour of this material (corrosion progress and leaching rates of radionuclides) in contact with two types of aqueous media, deionized water and granitic - bentonite water. An additional research line consisted on the validation of the ^{14}C decontamination procedure based on the thermal treatment of the Vandellós I NPP graphite. The outcome of these works was reported in the document D5.13 "Vandellós I graphite compilation report: thermal decontamination and IGM waste form results".

8   During the first four years of the CAST Project, the activities carried out by IFIN-HH were focused on three directions: Task 5.1 – "Review of CARBOWASTE and other relevant R&D activities to establish the current understanding of inventory and release of C-14 from i-graphite", Task 5.2 – "Characterization of the C-14 inventory in i-graphites" and Task 5.3 "Measurement of release of C-14 inventory from i-graphites". For the Task 5.1, IFIN-HH reviewed the outcome of CARBOWASTE Project in the national context and based on that, provided input for deliverable D5.2 "Review of current understanding of inventory and release of C-14 from irradiated graphites". For the Task 5.2, IFIN-HH explored the use of accelerator mass spectrometry to measure C-14 distributions in i-graphite and beta imaging to determine the distribution of C-14 and H-3 on graphite surfaces and prepared deliverable D5.7 "Report on C-14 distribution in irradiated graphite from research reactor VVR-S using accelerator mass spectrometry and beta imaging". In the Task 5.3 "Measurement of release of C-14 inventory from i-graphites" IFIN-HH developed

CAST
Final report on results from Work Package 5:
Carbon-14 in irradiated graphite (D5.19)

a separation technique, based on silica gel columns and oxidation at high temperature over a CuO catalyst be decoupled with LCS device (TRICARB 2800 TR PerkinElmer) in order to measure the release rate of C-14 into gas and solution phase from irradiated graphite (intact and crushed samples from VVR-S reactor and prepared deliverable D5.14 "Release of C-14 from irradiated VVR-S graphite to solution and gas phase (Task 5.3)". IFIN-HH also contributed to the last Task of WP5 (Task 5.5) that summarizes and synthesises in a final report the work undertaken in the previous Tasks by all participants. The outcome of this Task is this deliverable D5.19 "Final report on results from WP5".

9   Work reported by Radioactive Waste Management (RWM) considers the release of gaseous carbon-14 from irradiated graphite samples from Oldbury Magnox power station. Key conclusions from the study are that under baseline conditions, the predominant carbon-14 release was to the solution phase, with about 0.07% of the carbon-14 inventory being released into solution in one year and with about 1% of the released carbon-14 being released to the gas phase. An initial rapid release of ~3 Bq of carbon-14 to the gas phase was observed in the first week, and subsequently the rates of release decreased with time but detectable quantities of carbon-14 were found in all gas samples. For the final cumulative sampling period, a release of ~2 Bq was measured. Gaseous carbon-14 was predominantly in the form of hydrocarbons and other volatile organic compounds and CO, and less than 2% of the gas-phase release was in the form of $^{14}CO_2$. The differences between the fractional releases of carbon-14 from Oldbury graphite and that released from BEP0 graphite – a subject of previous study - are likely to be due to differences between the original graphites, their irradiation histories, operating temperatures and coolant gases; the results of this study do not allow determination of whether any one of these differences is a dominant effect although a wider comparison of irradiated graphites might.

Over the course of the EC CAST project, RWM undertook its role as Work Package 5 leader.

10   For Ukraine, the main radiocarbon source is irradiated graphite from the Chernobyl Nuclear Power Plant. The ChNPP is a decommissioned nuclear power station about 14 km northwest of the city of Chernobyl, and 110 km north of Kyiv (Kiev). The ChNPP had four RBMK reactor units. The commissioning of the first reactor in 1977 was followed by

CAST
Final report on results from Work Package 5:
Carbon-14 in irradiated graphite (D5.19)

reactor No. 2 (1978), No. 3 (1981), and No.4 (1983). Reactors No.3 and 4 were second generation units, whereas Nos.1 and 2 were first-generation units. RBMK is an acronym for "High Power Channel-type Reactor" of a class of graphite-moderated nuclear power reactor with individual fuel channels that uses ordinary water as its coolant and graphite as its moderator. The combination of graphite moderator and water coolant is found in no other type of nuclear reactor.

The approved «ChNPP Decommissioning Program» establishes a preferred decommissioning strategy.

Work undertaken by IEG NASU in CAST presented information on graphite characterisation as is being undertaken as part of the ChNPP Decommissioning Program. Work considering chemical decontamination of graphite is reported, as is the overall graphite waste management approach.

Work of IEG NASU in the EC CAST project targeted provision of input on the use of graphite in the RBMK reactor, particularly the decommissioning of each category, classification, volume, weight and activity (the inventory of i-graphite in Ukraine is not finished: in compliance with the requirements of the regulatory documents, the composition and activities of radionuclides accumulated in structural materials and structures during the operation of the NPP power unit must be evaluated before its removal from service.). IEG NASU reviewed characterisation data on the speciation of ^{14}C in RBMK reactor, i-graphites and relevant information from decommissioning projects in Ukraine. IEG NASU is also involved in the review of the outcome of the IAEA project investigating conversion of i-graphite from decommissioning of Chernobyl NPP into a stable waste form.

Contents

1 Introduction

Work Package 5 of the EC CAST project considers irradiated (i-) graphite and related ^{14}C behaviour and is led by Radioactive Waste Management (RWM) from the UK. The objective of this Work Package is to understand the factors determining release of ^{14}C from irradiated graphite under disposal conditions (to include surface disposal facilities and geological disposal facilities). This is to be achieved by:

• Determining the ^{14}C inventory and concentration distribution in i-graphites, and factors that may control these;

• Measuring the rate and speciation of ^{14}C release to solution and gas from i-graphites in contact with aqueous solutions; and

• Determining the impact of selected waste treatment options on ^{14}C releases and relating this to the nature of ^{14}C in i-graphite.

To achieve these objectives, five tasks have been undertaken

• Task 5.1 – Review of CARBOWASTE and other relevant R&D activities to establish the current understanding of inventory and release of ^{14}C from i-graphites;

• Task 5.2 – Characterisation of the ^{14}C inventory in i-graphites;

• Task 5.3 – Measurement of release of ^{14}C inventory from i-graphites;

• Task 5.4 – New wasteforms and ^{14}C decontamination techniques for i-graphites;

• Task 5.5 – Data interpretation and synthesis – final report.

This is the final report of Work Package 5 and details, on an organisation by organisation basis, progress in the Work Package over its total duration.

CAST
Final report on results from Work Package 5:
Carbon-14 in irradiated graphite (D5.19)

2   Organisation Reports

2.1   Centre National de la Recherche Scientifique (CNRS/IN2P3) laboratory: Institute of Nuclear Physics of Lyon (IPNL)

Objectives

The aim of the work undertaken by IPNL is to simulate the behaviour of ^{14}C during reactor operation. Indeed, the knowledge of the location and speciation of ^{14}C in irradiated graphite at reactor shutdown is important, to understand and foresee its behaviour during dismantling, to optimize an eventual decontamination process and to evaluate its migration behaviour during disposal.

^{14}C is formed through the activation of ^{13}C and is also generated through the activation of ^{14}N. Previous laboratory studies had been carried out at IPNL on ^{13}C or ^{14}N implanted virgin nuclear graphites of the UNGG Saint Laurent A2 reactor [Silbermann 2013], [Silbermann 2014], [Moncoffre 2016]. ^{13}C and ^{14}N was used to simulate respectively the presence of ^{14}C displaced from its original structural site through recoil and its precursor ^{14}N. These studies have shown that, extrapolating to reactor conditions, irradiation and thermal annealing promotes both ^{14}C and ^{14}N migration towards the free surfaces under the effect of temperature. Thus, most of ^{14}C formed by activation of the remaining ^{14}N might be located close to free surfaces (open pores). The sole influence of heat at reactor temperatures (200-500°C) did not promote ^{14}C release. However, both ^{14}N and ^{14}C should have been released through radiolytic corrosion when located close to free surfaces. The results thus strengthen the conclusion of Poncet et al. [Poncet 2013] that the ^{14}C inventory remaining in French UNGG irradiated graphites has been mainly produced through the activation of ^{13}C.

Thus, the objective of IPNL contribution to CAST is to get more insight into the behaviour of ^{14}C formed by neutron activation of ^{13}C and to evaluate the independent or synergistic effects of temperature and irradiation on ^{14}C behaviour. For that purpose, ion irradiation (simulating neutrons) was carried out on ^{13}C (simulating ^{14}C) implanted model Highly Ordered Pyrolitic Graphite samples (representing the coke grains which build around 80% of nuclear graphite).

CAST
Final report on results from Work Package 5:
Carbon-14 in irradiated graphite (D5.19)

Experimental

Implantation

[13]C was implanted at different fluences. This allows the induction of a high or a low disorder into the graphite matrix which is representative of the multiplicity of the structure states present in irradiated nuclear graphite. For example, it allows simulating structural differences resulting from early neutron irradiation in high or low flux regions of the reactor. Then, the samples were ion-irradiated to simulate neutron irradiation using ions of different types and energies. We have studied the irradiation and temperature effects on the migration of ^{13}C and followed also the evolution of the HOPG structure. In certain cases, we did experiments in a configuration enabling the evolution of the structure to be followed by in situ Raman microspectrometry. [13]C was implanted into HOPG samples parallel to c axis at two fluences: 6×10^{16} at.cm^{-2} on one hand and 4×10^{14} at.cm^{-2} on the other hand (at room temperature). The highest fluence allows implanting around 5 at.% at the maximum projected range (Rp). This value is five times higher than the natural abundance of 1.07 at.% and is necessary to enable the analyses of ^{13}C by Secondary ion Mass Spectrometry (SIMS). It induces a great disordering of the structure (around 7.4 dpa at the maximum projected defect range (Rd) which is located close to the Rp). This value of the disordering is high but it is in the same order of magnitude than that reached in UNGG reactors after 11.3 years of full power operation at a neutron fluence of 3.4×10^{21} n.cm^2 (around 2.6 displacements per atom ((dpa) [Bonal 2006]. The lowest fluence allows obtaining a less disordered structure (around 0.05 dpa at the Rd) but the maximum ^{13}C concentration is of 0.039 at/% and is therefore not measurable by SIMS. It allows creating around 0.02 dpa at the Rd. Thus, the disorder induced by the low fluence implantation might reflect the early operation stage while the one induced by the high fluence implantation might reflect the graphite structure at the reactor operation breakdown. Moreover, and because the behaviour of [37]Cl was also studied in our laboratory (to simulate [36]Cl), we used in some cases samples implanted with [37]Cl to induce a low disorder level into the graphite structure. In this case the implantation energy was of 250 keV and the Rp around 200 nm. An implantation fluence of 5×10^{13} at.cm^{-2} allows simulating a disorder level close to that induced by the implantation of ^{13}C at 4×10^{14} at.cm^{-2}. The number of dpa was evaluated at 0,024 dpa at the Rd [Vaudey 2010].

Irradiation

During neutron irradiation, the neutrons interact with the matter both by collision i.e. with the atom nuclei (i.e. ballistic damage) and by nuclear reactions. The first atoms hit by neutrons are caused to move, thus starting a cascade of atomic collisions leading to electronic excitation as they go through the matter and on the path of the atoms they displace (recoil atoms). The ballistic damage can be evaluated using the nuclear stopping power and can be denoted by the number of displacements per atom (dpa). The effect of electronic excitation can be quantified using the electronic stopping power.

The experimental simulation of neutron irradiation in a reactor is done by irradiation of the graphite samples with different ions of different energy. The choice of the latter enables the study of the effects with or without electron excitation or ballistic damage. It is possible to cover a wide range of the electronic and nuclear stopping powers by working with different particle accelerators. For example, we used the 4 MV Van de Graaff accelerator belonging to the IPNL, the 15 MV Tandem in the IPN in Orsay, and the Cyclotron of the CEMHTI in Orléans. From the beams available on the Van de Graaff (proton, deuteron, helium, carbon and argon), we chose to use the carbon and argon ones because, within the energy range of the accelerator, these ions would allow us to preferentially simulate ballistic damage. In the Tandem in Orsay, we used high energy sulphur and iodine beams with the objective of preferentially simulating the electronic excitation effects. Finally, we worked on the cyclotron in Orléans with helium ions (with a higher energy than that produced at the IPNL) in order to realise irradiation in the conditions closest to those in a reactor. By simulation using the SRIM-2013 software [Ziegler 1985, Ziegler 2010], the nature and energy of the ions were selected. These calculations were done for graphite with a density of 2.2 g/cm^3, very close to that of the HOPG which is highly-crystalline and non-porous. Table 2.1.1 summarizes the irradiation parameters.

CAST
Final report on results from Work Package 5:
**Carbon-14 in irradiated graphite (D5.19)**

Table 2.1.1: Irradiation parameters and their associated characteristics notably in the implanted zone, determined by SRIM calculations for a graphite with a density of 2.2g/cm^3

Ion used	Energy (MeV)	Irradiation fluence (ion.cm^{-2})	Rp (nm)	Rd (nm)	S_e (keV/µm)	S_n (keV/µm)	Number of dpa
					In the implanted zone (≈ 315 nm)		
C$^+$	0.4	5 x 10^{16}	675	640	585	15	1.3
C$^+$	0.6	6 x 10^{16}	890	850	730	10	0.9
Ar$^+$	0.8	2 x 10^{16}	630	545	980	175	4.4
He$^+$	15.7	1 to 2 x 10^{16}	121 500	121 500	75	0.003	0.0001 to 0.0002
S^{9+}	100	2 x 10^{15}	24 000	24 000	3 700	1	0.002
I^{19+}	200	2 x 10^{15}	19 100	18 900	16 700	30	0.038

In an UNGG reactor, the energy input by electronic excitation is between 0 and 700 keV/µm and may even go up to 1600 keV/µm. However, we also investigated the domains above the track creation threshold estimated in HOPG by certain authors [Liu 2006, Lehtinen 2011] as about 7300 ± 1500 keV/µm. The track creation is a process which occurs in about 10^{-11} s. It can be interpreted with the help of the thermal spike model which can explain certain structural modifications caused by irradiation with high energy ions. Since its application to metals in 1956 [Seitz 1956], this model has been revised by Toulemonde [Toulemonde 1993, Toulemonde 2012]. The model is based on the theory that the energy of the incident particle, passed on to the atoms in the matter network *via* an electron-phonon interaction, is converted into thermal energy i.e. heat. In the cylindrical region that the ion passes through,

CAST
Final report on results from Work Package 5:
Carbon-14 in irradiated graphite (D5.19)

if the energy passed on is sufficiently high for the temperature of the ion network to reach the matter fusion temperature, then melting of this region is observed. The melted zone cools rapidly, there is a tempering phenomenon which could lead to recrystallization. The track corresponds to this cylindrical zone which recrystallizes. The radius of these tracks depends on the volume which reaches the melting point.

Figure 2.1.1 summarises the simulation results for the ions in our study (using the software SRIM-2013 [Ziegler 1985, Ziegler 2010]) at a depth of about 300 nm in a graphite with a density of 2.2 g/cm^3 and for the irradiation fluences chosen for these the experiments (summarised in Table 1).
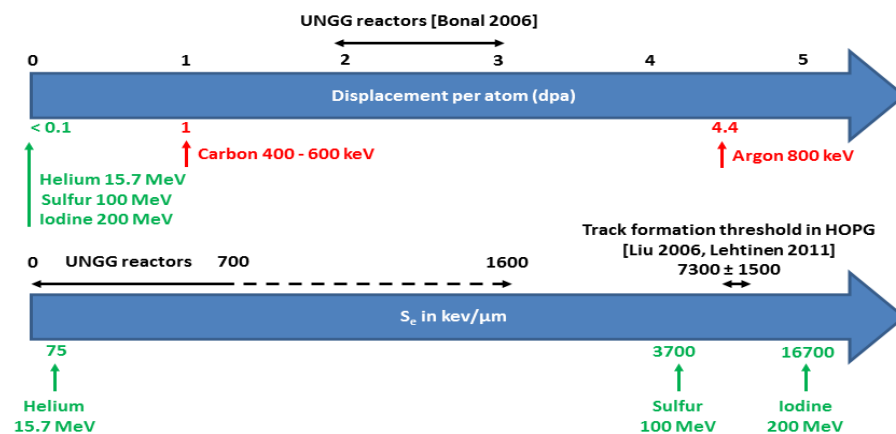
Figure 2.1.1: Number of dpa and electronic stopping power S_e calculated in the implanted zone ($\approx$ 315 nm) in graphite with a density of 2.2 g/cm^3 using the SRIM-2013 software for irradiation with the chosen ions, energy and fluence. The number of dpa were calculated for a fluence of 5×10^{16} at.cm^{-2}

As can be seen on the above Figure, the ions used to predominantly cause ballistic effects are given in red and those used for electronic excitation are in green. We can therefore conclude that, in order to work in a ballistic regime, it is better to use carbon ions with energies between 400 and 600 keV. It is also possible to induce a greater number of dpa in the graphite by irradiating with low energy argon ions. For the electronic regime, we chose to work with 15.7 MeV helium ions. However, it is still interesting to use 100 MeV sulphur ions in order to work outside the range of electronic stopping power of UNGG reactors or

above that with 200 MeV iodine ions in order to obtain an extremely large electronic stopping power which is well above the track creation threshold in HOPG.

Characterization

The samples were analyzed by Secondary Ion Mass Spectrometry (SIMS) in order to measure the ^{13}C concentrations (for the high fluence implanted samples). The analyses were carried out with an IONTOF ToF-SIMS V facility at the Science et Surface laboratory, Ecully, France.

The structure evolution was followed systematically using Raman spectrometry analyses. Raman microspectrometry allows obtaining local information on the structure disorder. It was carried out using a Renishaw INVIA Reflex spectrometers equipped with an Ar laser source (514.5 nm wavelength, i.e., 2.41 eV), focused through a Leica microscope. The spectra were collected under microscope (x50 objective). A very low incident power (<1 mW) was used to avoid heating effect and possible subsequent structural modifications.

Microscopic techniques such as scanning electron microscopy (SEM) in the secondary electron mode were also used systematically for preliminary observation of sample surfaces. In some cases, High Resolution Transmission Electron Microscopy (HRTEM) was also carried out on some selected samples because the high resolution mode (HRTEM) allows the imaging of graphene layer profiles.

The microscope resolution is of 1.8 Å.

Results

Effect of temperature alone

Before looking closely at the irradiation effects, we wanted to verify the effects of temperature alone. In order to do that, we heated the samples in the same conditions as the irradiation i.e. each was put in the heated sample holder in the irradiation cell under a secondary vacuum during periods of 5 hours (average irradiation period) at different temperatures. In this section, we present the results obtained.

	CAST	
	Final report on results from Work Package 5:	
	Carbon-14 in irradiated graphite (D5.19)	

For graphite samples initially very disordered

Structural behaviour of graphite

Figure 2.1.2 shows the Raman spectra for the as-implanted samples (TQI) (^{13}C - ϕ = 6 x 10^{16} at.cm^{-2} – 7.4 dpa) and heated for 5 hours at 400, 600 and 1000 °C.
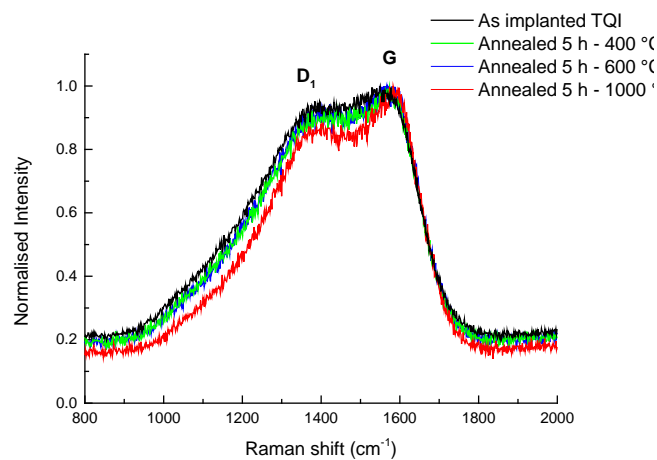

Figure 2.1.2: Raman spectra obtained from the samples implanted with ^{13}C and heated for 5 h at 400, 600 and 1000 °C compared to the Raman spectra of an as-implanted sample (TQI)

On Figure 2.1.2, we observe that the spectrum for the TQI sample that both band G and band D_1 are high intensity and broad, which is synonymous with very disordered graphite. This therefore shows that the graphite does not seem to reorder even at a temperature of 1000 °C. In fact, the spectra of the heated samples are very similar to those of the TQI sample even though we observe a slight decrease in the intensity and the width of band D_1 for the sample heated at 1000 °C.

We can thus conclude that temperature has a negligible effect on the reordering of graphite during periods of heating of 5 hours.

Migration behaviour of ^{13}C in graphite

We also studied the effect of temperature on the mobility of the implanted ^{13}C. Figure 2.1.3 shows the ^{13}C concentration curves obtained by SIMS analysis on a TQI sample, as well as on samples heated for 5 hours at 400, 600 and 1000 °C.
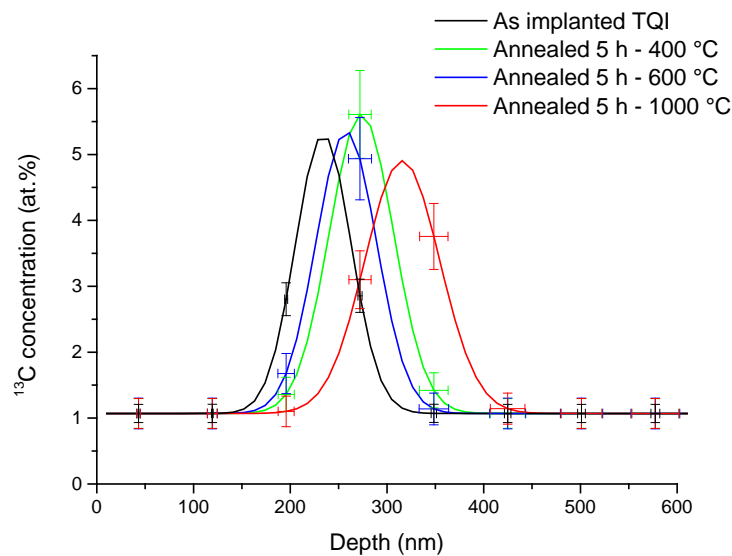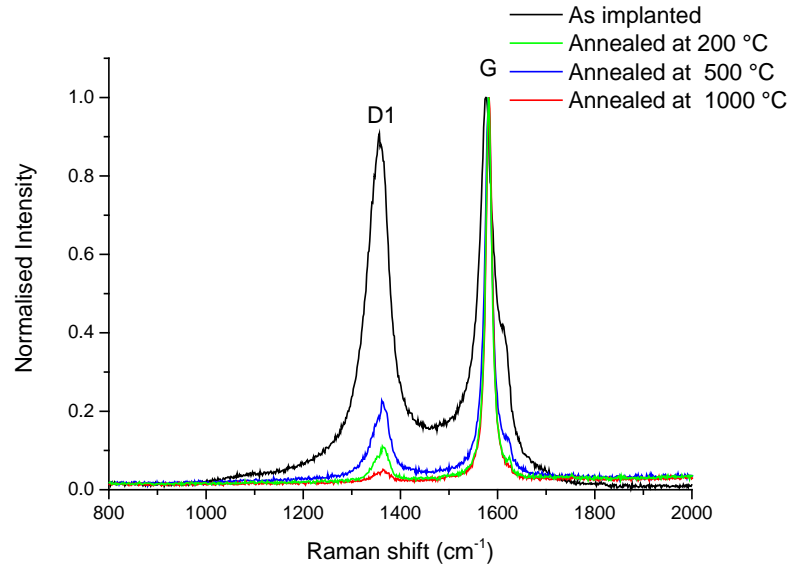

Figure 2.1.3: ^{13}C concentration curves obtained by SIMS analysis on a TQI sample as well as on samples heated for 5h at 400, 600 and 1000 °C

The above Figure shows that the curves for the heated samples are very similar to those of the TQI sample except for the sample heated at 1000 °C which has slightly shifted. During heating, the areas under the curves and the FWHM values are similar, taking into account the uncertainties. There is therefore no release of ^{13}C. We can thus conclude that temperature has a negligible effect on the mobility of implanted ^{13}C in graphite.

For initially slightly disordered graphite samples

We have also studied the behaviour of samples which were initially slightly disordered by the implanting of ^{37}Cl. Figure 2.1.4 shows the state of the structure of the implanted graphite (^{37}Cl - ϕ = 5 x 10^{13} at.cm^{-2} – 0.02 dpa) studied by Raman microspectrometry at different temperatures.

CAST
Final report on results from Work Package 5:
Carbon-14 in irradiated graphite (D5.19)

Figure 2.1.4: Raman spectra obtained for the TQI ^{37}Cl sample as well as samples implant and heated at 200, 500 and 1000 °C

The above Figure shows that the Raman spectra for the TQI sample consist of two very distinct bands, G and D_1 and both are high intensity, sharp peaks. When the implanted sample is heated, the intensity of the band indicating the structural defects (band D_1) greatly decreases. We can therefore say that the structure of the graphite is progressively reordered from 200 °C. Note that this behaviour is observed whatever the nature of the implanted ion (^{37}Cl or ^{13}C).

Effect of irradiation in a mainly ballistic regime

-   For initially very disordered graphite samples
Study of the structure of graphite by Raman microspectrometry

We will now compare the Raman spectra obtained from the samples irradiated with either a carbon or argon ion beam at different temperatures. Irradiation with C^+ ions with energies of 400 or 600 keV are done at fluences allowing us to reach about 1 dpa in the implanted zone, whereas irradiation with 800 keV Ar^+ ions allow us to reach 4.4 dpa. The Raman microspectrometry spectra of the irradiated samples in these conditions are presented in

	CAST	
	Final report on results from Work Package 5:	
	Carbon-14 in irradiated graphite (D5.19)	

Figures 2.15 *a* and 2.1.5 *b*, respectively, and compared with the spectrum from the TQI sample.
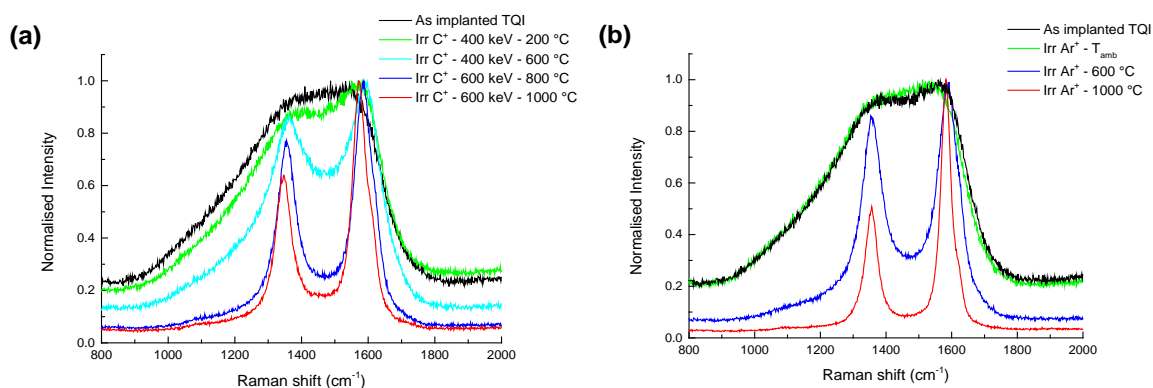
Figure 2.1.5: Comparison of the Raman spectra for a As implanted TQI sample with those of samples irradiated with (a) carbon or (b) argon ions at different temperatures

Figure 2.1.5 (a) shows that for irradiation with carbon ions, the G and D_1 bands are clearly separated and become narrower with the increase in temperature, which signifies a dynamic heating of the defects resulting from the implanting process. There is also a decrease of the I_{D1}/I_G ratio with temperature indicating a progressive reordering of the graphite. In fact, in well-structured graphite, the majority of C-C bonds are aromatic sp^2. However, during the implanting process, the disordering leads to the presence of isolated defects (vacancies, interstitials) but also more significant defects such as fractured graphene planes. Thus, the Raman signal defect band i.e. D_1 broadens and its intensity increases [Ammar 2015]. During irradiation at a higher temperature, the isolated defects combine and so may form new well-ordered graphene planes. The increase in the number of C-C sp^2 bonds leads to a structural rearrangement which is revealed in the spectra as a narrowing of band D_1 and a decrease in its intensity. The comparison of these results with those obtained in the study of the effect of heating show that temperature and irradiation in a ballistic regime seem to have a synergistic effect with respect to the restructuring of graphite. In fact, when the sample is only heated at 1000°C, the structure reorganises significantly less than under irradiation at 1000 °C. Figure 2.1.5 (b) shows the synergy effect between ballistic irradiation and temperature on reordering which is even clearer when irradiating with argon ions. For

CAST
Final report on results from Work Package 5:
Carbon-14 in irradiated graphite (D5.19)

example, the spectrum obtained with the sample irradiated at 600°C is in a better structural state than that corresponding to the sample irradiated with carbon ions at 600°C. In fact, the D_1 and G bands are broader for irradiation with carbon ions compared to those observed for irradiation with argon ions and the intensity between these two bands, attributed to band D_3 by certain authors [Couzi 2016], increases.

In conclusion, the combined effects of temperature and irradiation in a mainly ballistic regime favour a reordering of the graphite structure which was initially highly disordered. The interstitials are mobile from ambient temperature whereas the mobility of the vacancies increases progressively above 250 °C. The local defect structure stores Wigner energy that can be released by defect rearrangement to configurations with lower energy. The process of recombination of interstitials and vacancies is expected to be the primary step in Wigner energy release observed at 200-250°C [Ewels 2003, Telling 2003]. It would therefore seem that this disordering regime at higher temperature favours the mobilisation and recombination of the defects initially present as well as those caused by irradiation and so enables a progressive reordering of the graphite structure.

Microstructural study of graphite by HRTEM

We observed the evolution of the inter-layer distances and the angular distributions. The inter-layer distance for virgin graphite is 3.35 Å. However, the larger this value becomes, the more the structure is disordered. The graphs in Figure 2.1.6 show the results obtained for graphite samples initially implanted with ^{13}C at 6 x 10^{16} at.cm^{-2} then irradiated with 600 keV C$^+$ ions at 1000°C. The points corresponding to the virgin graphite and the TQI sample also appear on these graphs. The shaded zone covers the Rp value for the implanted ^{13}C and the dashed lines have been added to guide the eye. These lines allow the trends in the evolution of the values as a function of depth to be more clearly seen.
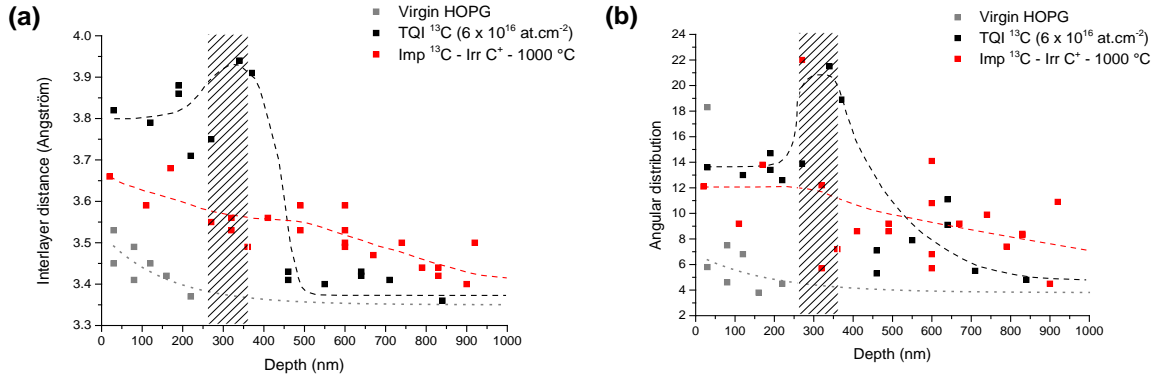
Figure 2.1.6: Inter-layer distance and angular distribution measured on the TEM images at different depths for the samples implanted with ^{13}C at high fluence then irradiated. The shaded zone covers the Rp value for implanted ^{13}C and the dashed lines enable the trend in the evolution of these values as a function of depth to be more clearly seen

From these graphs we observe that the values of the inter-layer distance and the angular distribution are greater in the implanted zone of the TQI sample and decrease notably with depth outside this zone down to values close to those for a virgin sample. However, the values of the sample irradiated at 1000 °C are a little higher on the surface than below but globally more homogenous and lower than those of the TQI sample. These results indicate a better-ordered structure in the irradiated sample compared to the TQI sample, which is in agreement with the results obtained previously by Raman microspectrometry.

Migratory behaviour of ^{13}C in graphite

Irradiation with argon ions

Irradiation with argon ions slightly disordered the sample surface so that the topographic measurements could not be exploited. We have therefore chosen to represent the ^{13}C concentration profiles measured by SIMS as a function of abrasion time and not as a function of depth. The ^{13}C concentration profiles in the samples irradiated with argon ions at different temperatures are compared in Figure 2.1.7 with those of the TQI sample.

	CAST		
	Final report on results from Work Package 5:		
	Carbon-14 in irradiated graphite (D5.19)		
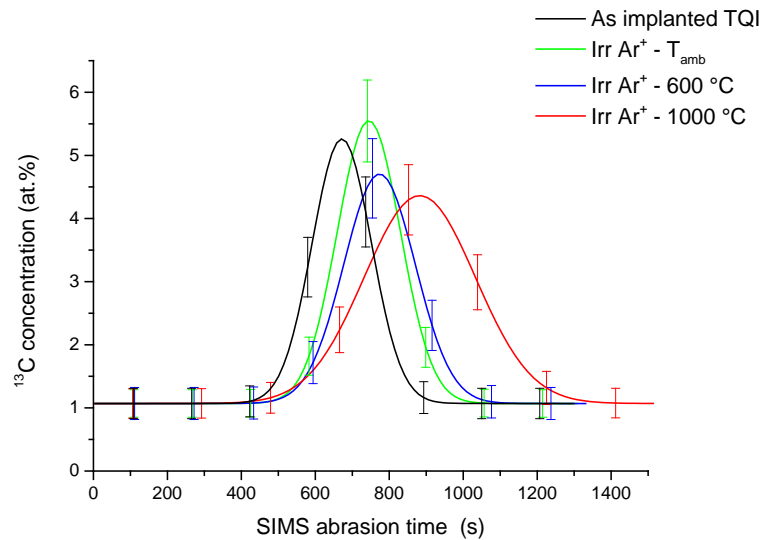
Figure 2.1.7: Comparison of the ^{13}C concentration profiles of the TQI sample and the samples irradiated with 800 keV Ar ions $^+$ at ambient temperature (T_{amb}), 600 °C and 1000 °C as a function of abrasion time during SIMS analysis

The Figure shows that ^{13}C does not migrate, with the exception of the profile for the sample irradiated at 1000 °C which broadens, suggesting a possible diffusion of ^{13}C but which we could not quantify

Irradiation with carbon ions

In Figure 2.1.8, the ^{13}C concentration profiles of the samples irradiated with carbon ions at different temperatures are compared with those of the TQI sample. In order to directly compare these results with those of irradiation with argon ions, we have presented, as previously, the ^{13}C concentration profiles measured by SIMS as a function of abrasion time.

CAST
Final report on results from Work Package 5:
Carbon-14 in irradiated graphite (D5.19)
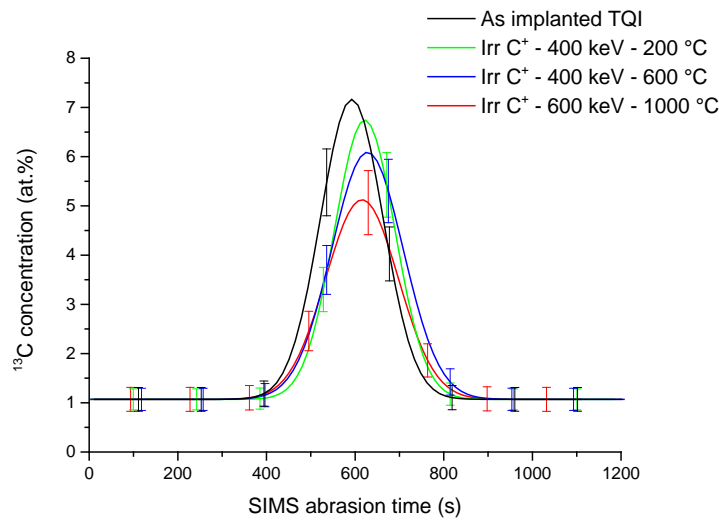
Figure 2.1.8: Comparison of the ^{13}C concentration profiles for the TQI sample and the samples irradiated with C $^{+}$ ions of 400 or 600 keV at 200 °C, 600 °C and 1000 °C

This Figure indicates that within the uncertainties ^{13}C does not migrate.

In conclusion, the results of irradiation with argon or carbon ions show that the ballistic damage does not favour release of ^{13}C for the initially highly disordered samples. Therefore, from the Raman microspectrometry results obtained previously, it seems that ^{13}C is stabilised in sp^2- and sp^3-type structures where the proportion varies according to the irradiation temperature of the graphite.

- *For initially slightly disordered graphite samples*

In this section, initial disordering of graphite was realised by implanting ^{37}Cl at a fluence of 5×10^{13} at.cm^{-2}. This fluence led to about 0.024 dpa of the Rp, i.e. damage of about two orders of magnitude smaller than that generated by implanting with ^{13}C in the previous section.

Study of the graphite structure by Raman microspectrometry

Irradiation with C$^+$ ions at an energy of 400 or 600 keV realised at a fluence varying between 5 and 6 x 10^{16} at.cm^{-2} enables about 1 dpa to be obtained in the implanted zone whereas, irradiation with 800 keV Ar$^+$ ions at a fluence of 2 x 10^{16} at.cm^{-2} enables 4.4 dpa to be reached. On Figure 26, we present the Raman spectra obtained for irradiation with carbon ions (Figure 2.1.9 *a*) and argon ions (Figure 2.1.9 *b*).

16
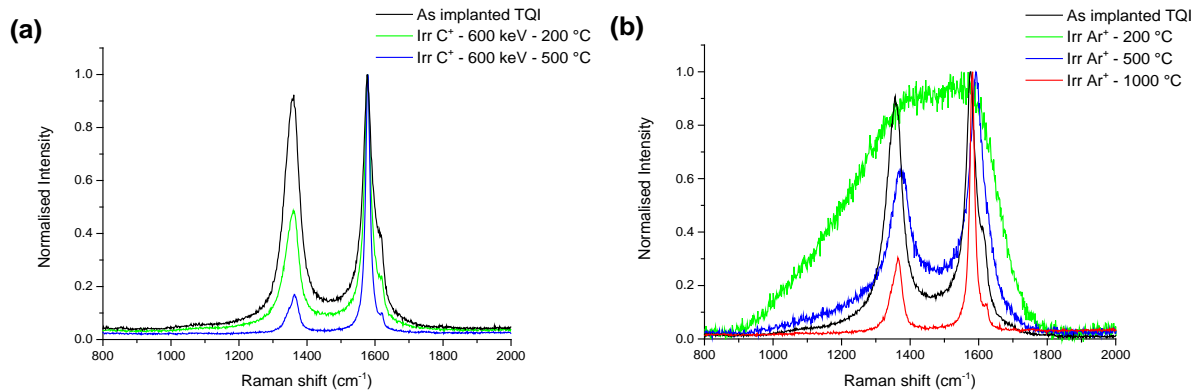
Figure 2.1.9: Comparison of the Raman spectrum of a TQI sample with those of samples irradiated with carbon ions (a) or argon ions (b) at different temperatures

For irradiation with carbon ions, the Raman spectra in Figure 2.1.9 *a* show that the intensity of the defect band D_1 decreases with temperature. In addition, the bands become narrower indicating a reordering of the graphite. For irradiation with argon ions (Figure 2.1.9 b), irradiation realised at 200 °C disordered the graphite and we observed that the D_1 and G bands broaden considerably and so overlap. The shape of the spectrum shows that the structure tends towards amorphization. However, at 500 °C, the bands become narrower, indicating that the disordering effect of irradiation is completely balanced by the reordering effects of temperature. This phenomenon is even clearer at 1000 °C.

In conclusion, in the case of samples which are initially slightly disordered, irradiation and temperature have antagonistic effects. There therefore seems to be a critical damage value between 1 and 4.4 dpa, above which the temperature (between 200 and 500 °C) is less efficient in reordering the graphite.

Study of the microstructure of graphite by HRTEM

The graphs in Figure 2.1.10 show the values of the inter-layer distances and the angular distributions as a function of depth obtained for a graphite sample previously implanted with [37]Cl then irradiated with 600 keV ions C[+] in a mainly ballistic regime at 500 °C.

17

CAST
Final report on results from Work Package 5:
Carbon-14 in irradiated graphite (D5.19)
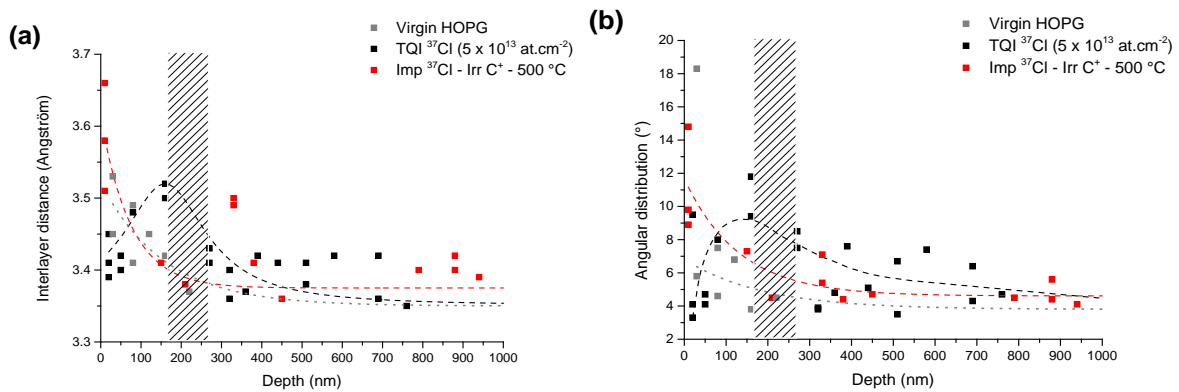
Figure 2.1.10: Inter-layer distance (a) and angular distribution (b) measured on the TEM images at different depths for samples implanted with [37]Cl then irradiated. The shaded zone covers the Rp value of the implanted [37]Cl and the dashed lines enable the evolution of the values as a function of depth to be followed more clearly

In comparison to a TQI sample, the values corresponding to a sample irradiated at 500 °C indicate reordering of the graphite where even in the implanted zone they are lower (except on the outer surface). These results corroborate those previously obtained by Raman microspectrometry.

- *Conclusions concerning irradiation effects in a mainly ballistic regime*

For all the irradiation experiments, we observed that the effects of irradiation in a mainly ballistic regime are greatly dependent on the initial structure of the graphite. For example, in **very disordered graphite** (about 7 dpa), the combined effects of **temperature and irradiation act in synergy** favouring reordering. Above 250 °C (temperature above which the vacancies and interstitials are mobile), irradiation at an elevated temperature favours the mobilisation and recombination of the pre-existing defects and of those introduced by irradiation thus enabling a progressive reordering of the structure. However, in **graphite which is only slightly disordered** (<< 0.1 dpa), **irradiation and temperature have an antagonistic effect**. The possibility of reordering the graphite is in this case strongly dependent on the temperature and the degree of damage. All in all, if there is a high degree of damage (about 4 dpa) and a low temperature (less than 200 °C), there will only be a poor reordering of the graphite. There is therefore a competitive effect between the irradiation and temperature with a critical damage value of between 1 and 4.4 dpa, above which the temperature (between 200 and 500 °C) is less efficient in reordering the graphite. In both the

above cases, **the ^{13}C is stabilised** in the sp^2- and sp^3-type structures where the proportion varies according to the irradiation temperature of the graphite.

Effect of irradiation in a mainly electronic regime

The present part of the study concerned the effects of irradiation in a mainly electronic regime using the same procedure as above. The irradiation was done with 15.7 MeV helium ions, 100 MeV sulphur ions and 200 MeV iodine ions which enabled the electronic stopping power of 75, 3700 and 16700 keV/µm to be reached, respectively.

-   For the initially very disordered graphite samples

<u>*S_e lower than the track creation threshold (S_e = 3700 keV/µm)*</u>

The irradiation for this study was done with 100 MeV sulphur ions at ambient temperature and at 500 and 1000 °C. In these conditions, the electronic stopping power is 3700 keV/µm in the implanted zone. This value is higher than those encountered in a working UNGG reactor but it is lower than the theoretical threshold of track creation in HOPG graphite.

Study of the graphite structure by Raman microspectrometry

Figure 2.1.11 shows the Raman spectra obtained for the samples irradiated with 100 MeV sulphur ions at different temperatures.
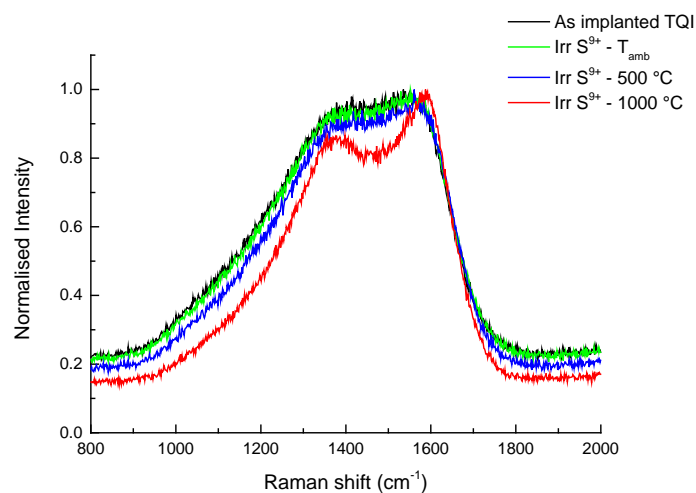

Figure 2.1.11: Comparison of the Raman spectrum of the TQI sample with the spectra of samples irradiated with sulphur ions at different temperatures

Figure 2.1.11 shows that for this irradiation, there is almost no reordering of the graphite at 500 °C and only slightly at 1000 °C. In fact, the D_1 and G bands only begin to separate at 1000 °C. Contrary to the results obtained in a ballistic regime, the combined effects of irradiation and temperature in an electronic regime only lead to a slight reordering of the graphite, even at 1000 °C. On the atomic scale, the larger proportion of sp^3 carbons produced at the time of implantation decreases very slightly or not at all.

Microstructural study of graphite by HRTEM

To study the disordering of the graphite, we used HRTEM. The graphs in Figure 2.1.12 show the values for the inter-layer distances and the angular distribution measured on the graphite samples initially implanted with ^{13}C at 6 x 10^{16} at.cm^{-2} then irradiated with S^{9+} ions at 1000 °C. These values are compared with those for the TQI graphite. In these conditions, the sulphur ions stop at a depth of about 24 µm but the probed depths were limited to 1 µm.
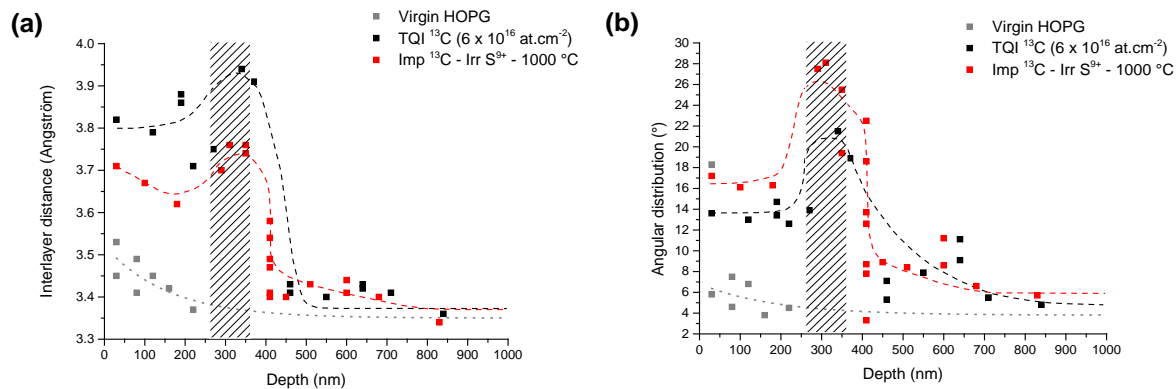

Figure 12: (a) inter-layer distance and (b) angular distribution measured on the TEM images at different depths for the samples implanted with ^{13}C at high fluence then irradiated with 100 MeV sulphur ions. The shaded zone covers the Rp value of the implanted ^{13}C and the dashed lines enable the trends in the evolution of these values as a function of depth to be seen more clearly

Figure 2.1.12*a* shows that the inter-layer distances measured for the samples irradiated at 1000°C are less than the TQI sample in the implanted zone. This indicates restructuring of the graphite the same as that observed by Raman microspectrometry. However, the angular distribution values for the layers do not indicate reordering in the implanted zone.

CAST
Final report on results from Work Package 5:
Carbon-14 in irradiated graphite (D5.19)

Therefore, the reordering process could be similar to the model suggested by Rouzaud et al. [Rouzaud 1983]. In this article, the authors show that the graphitisation process occurs in successive steps. Below 1200 °C, the basic structural units (BSU's) associate to form deformed columns then, above 1200 °C, these columns coalesce to form planes, which are wrinkled/ridged and deformed. In our case, at 1000 °C, it is likely that the layers associate to form stacks which remain disordered with respect to each other.

Migration behaviour of ^{13}C in graphite

Figure 2.1.13 shows the ^{13}C concentration profiles as a function of irradiation temperature compared to the ^{13}C profile for the TQI sample.
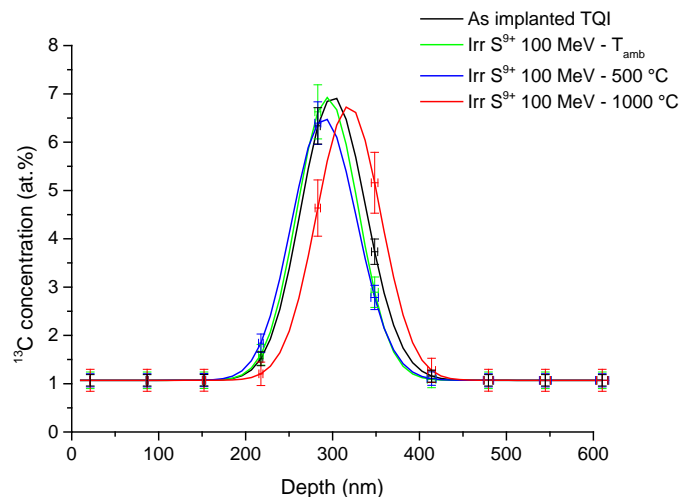
Figure 2.1.13: Comparison of the ^{13}C concentration profiles for the TQI sample and the samples irradiated with 100 MeV S^{9+} ions at different temperatures

The profiles show that, whatever the irradiation temperature, ^{13}C does not migrate.

S_e greater than the track creation threshold ($S_e = 16700$ keV/µm)

We also used 200 MeV iodine ions. In these conditions, the electronic stopping power is 16700 keV/µm in the implanted zone. This S_e is much higher than that calculated for the working UNGG reactors and it is also higher than the threshold estimated for track formation in HOPG graphite. Irradiation was done at two temperatures, i.e. ambient temperature and 1000 °C.

	CAST		
	Final report on results from Work Package 5:		
	Carbon-14 in irradiated graphite (D5.19)		

Study of the graphite structure by Raman microspectrometry

Figure 2.1.14 shows the Raman spectra obtained for the samples irradiated with 200 MeV iodine ions at different temperatures compared to the spectrum for the TQI sample.
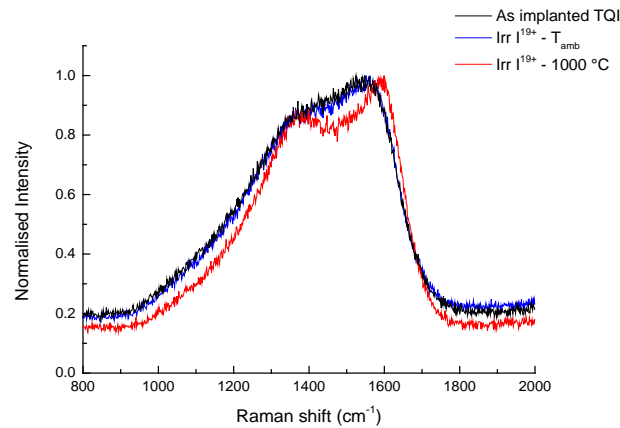

Figure 2.1.14: Comparison of the Raman spectrum for a TQI sample with the spectra for samples irradiated with iodine ions at different temperatures

The above Figure shows that for irradiation at a high electronic stopping power (16700 keV/µm), which is above the track creation threshold in HOPG graphite for 200 MeV iodine ions, the reordering of the graphite is very slight, even at 1000 °C. In fact, the D_1 and G bands are only just beginning to separate. The reordering of graphite is of the same order as that previously observed for a sample only heated at 1000 °C.

Migration behaviour of ^{13}C in graphite

Figure 2.1.15 shows the ^{13}C concentration profiles as a function of irradiation temperature compared to the ^{13}C profiles in a TQI sample.

	CAST	
	Final report on results from Work Package 5:	
	Carbon-14 in irradiated graphite (D5.19)	
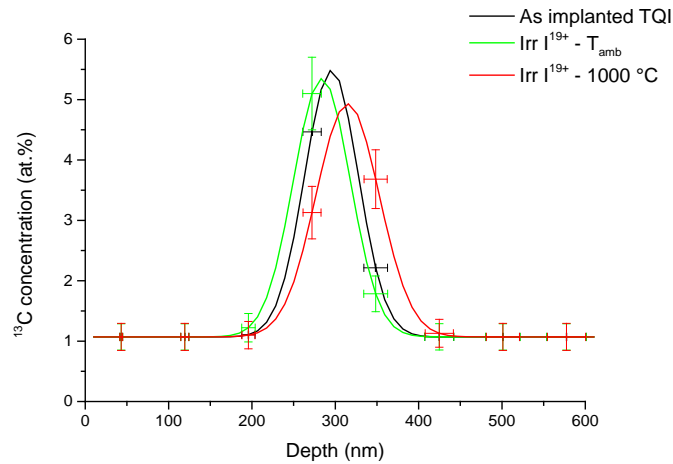
Figure 2.1.15: Comparison of the ^{13}C concentration profiles of the TQI sample and the samples irradiated with 200 MeV I^{19+} ions at ambient temperature and 1000 °C

In the above case, we also observe that the Figure reveals that the ^{13}C concentration profiles in irradiated graphite remain unchanged (within the precision limits of the analysis) and this therefore shows structural stabilisation.

In conclusion, with irradiation in a mainly electronic regime done at high S$_e$ values, greater than those encountered in UNGG reactors, the graphite reorders only very slightly, even at 1000 °C, contrary to our observations for irradiation in a ballistic regime. The implanted ^{13}C is stabilised in the graphite but mostly in sp^3-type structures.

- *For initially slightly disordered graphite samples*

<u>*S$_e$ less than the track creation threshold*</u>
Study of the graphite structure by Raman microspectrometry

The spectra obtained by Raman microspectrometry for the samples irradiated with 100 MeV sulphur ions at different temperatures are given in Figure 2.1.16.

23
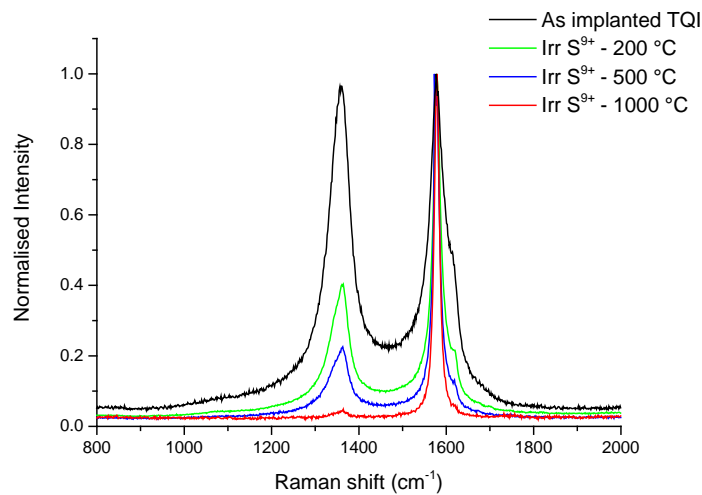
Figure 2.1.16: Comparison of the Raman spectrum of a TQI sample with the spectra of samples irradiated with sulphur ions at different temperatures

As can be seen from the above results for irradiation at higher temperatures, the intensity of band D_1 decreases and bands D_1 and G become narrower indicating the progressive reordering of the graphite. However, at 200 °C, the reordering is less than the effect of temperature (heating) alone (cf Figure 4). This is not the case at 1000 °C as the reordering is the same for both the irradiated sample and the one which was only heated.

Microstructural study of graphite by TEM

We also observed samples irradiated with 100 MeV sulphur ions at 500 °C by TEM. As previously, the graphs in Figure 2.1.17 show the values of the inter-layer distance and angular distribution compared to those of a TQI sample. Comparison of these values indicate a reordering of the implanted zone, and are thus in agreement with the measurements realised by Raman microspectrometry.

	CAST	
	Final report on results from Work Package 5:	
	Carbon-14 in irradiated graphite (D5.19)	

(a)

(b)
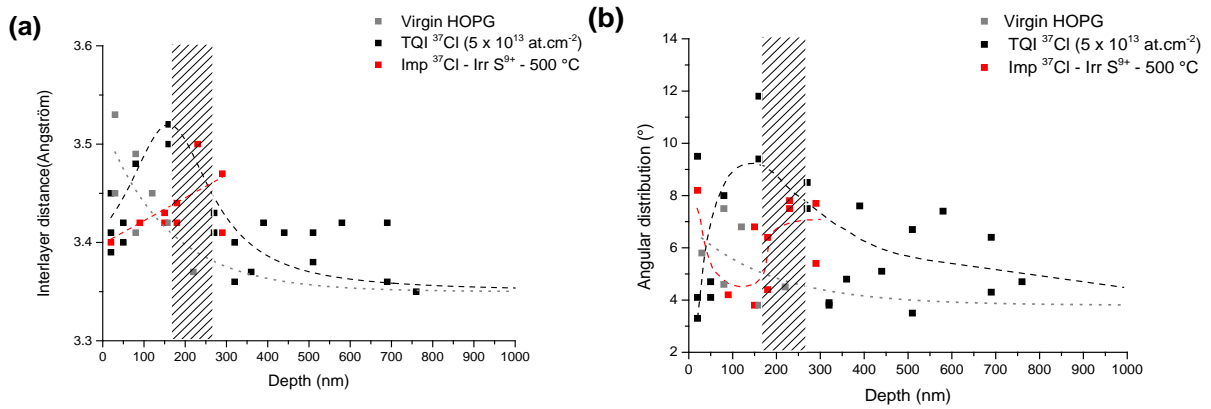
Figure 2.1.17: Inter-layer distance and angular distribution measured on the TEM images at different depths for samples implanted with ^{37}Cl then irradiated. The shaded zone covers the Rp value of the implanted ^{37}Cl and the dashed lines enable the trends in the evolution of these values as a function of depth to be seen more clearly.

<u>*S_e greater than the track creation threshold (S_e = 16700 keV/µm)*</u>

Study of the graphite structure by Raman microspectrometry

The spectra obtained by Raman microspectrometry for the samples irradiated with 200 MeV iodine ions at different temperatures (200 and 1000 °C) are given in Figure 2.1.18.
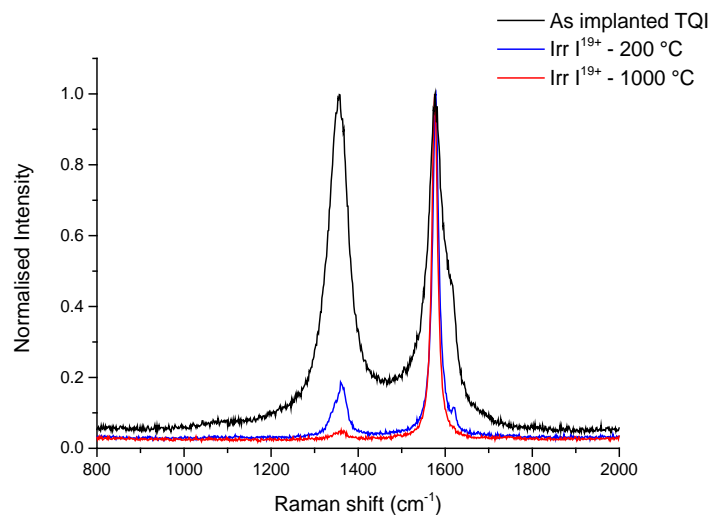
Figure 2.1.18: Comparison of the Raman spectrum for a TQI sample with the spectra of samples irradiated with iodine ions at different temperatures

As for the findings obtained above, these results show that during irradiation at higher temperatures, the intensity of band D_1 decreases and bands D_1 and G narrow indicating

progressive reordering of the graphite. At 1000 °C, the reordering is again the same as that for the only heated sample.

In conclusion, for irradiation in a mainly electronic regime done at a high Se, greater than the values observed in UNGG reactors, there is a progressive reordering in the samples irradiated at higher temperatures but which is less efficient than when the sample is only heated. This indicates an antagonistic effect between irradiation and temperature.

*S_e in the same order of magnitude as in a reactor ($S_e = 75$ keV/µm)*

In the previous sections concerning irradiation with sulphur and iodine ions, we have seen that in a mainly electronic regime the structure of the graphite could be damaged. However, we must not ignore the hypothesis that part of the damage may also be linked to the ballistic effect even if the latter is relatively small. Consequently, irradiation with helium ions should allow us to better understand the effect of electronic damage within the limits where the S_n/S_e ratio in the implanted zone for irradiation with helium ions is 1 to 3 orders of magnitude lower than those for irradiation with sulphur and iodine ions, respectively. Therefore, in the following sections, we will study in more depth the effects of irradiation with helium ions on virgin or slightly disordered samples (implanted with ^{13}C at a fluence of 4×10^{14} at.cm^{-2}).

Irradiation was done with 15.7 MeV He$^+$ ions. The electronic stopping power is 75 keV/µm in the implanted zone. The irradiation was mostly done at a current of 40 nA, corresponding to a flux of 1×10^{12} ions.cm^{-2}.s^{-1}, with a fluence of 1×10^{16} ions.cm^{-2}. With the objective of testing the influence of flux and fluence, some irradiation was done with a current of 80 nA, corresponding to a flux of 2×10^{12} ions.cm^{-2}.s^{-1}, with a fluence of 2×10^{16} ions.cm^{-2}. The samples, put in contact with a gas simulating the coolant gas of the UNGG reactors, were irradiated at ambient temperature or 250 °C or 500 °C and were studied using *in situ* **Raman microspectrometry**. In addition, in order to understand the effects of the structural modifications associated with the variations in temperature alone, the Raman signal was recorded in certain cases before starting the irradiation, during the rise in temperature of the sample and at the end of the irradiation during the drop in temperature. The heating and

cooling temperature ramps were about 10°C/min (i.e. a time of 50 minutes for irradiation at 500 °C).

A | Virgin HOPG graphite

We began by irradiating a virgin HOPG sample (non-implanted) which had no structural defects before irradiation. Figure 2.1.19 gives the spectra obtained by Raman microspectrometry on a sample irradiated at 500 °C at a fluence of 1×10^{16} at.cm^{-2}. The analysis was done after irradiation, i.e. no presence of gas and with a longer measurement time.
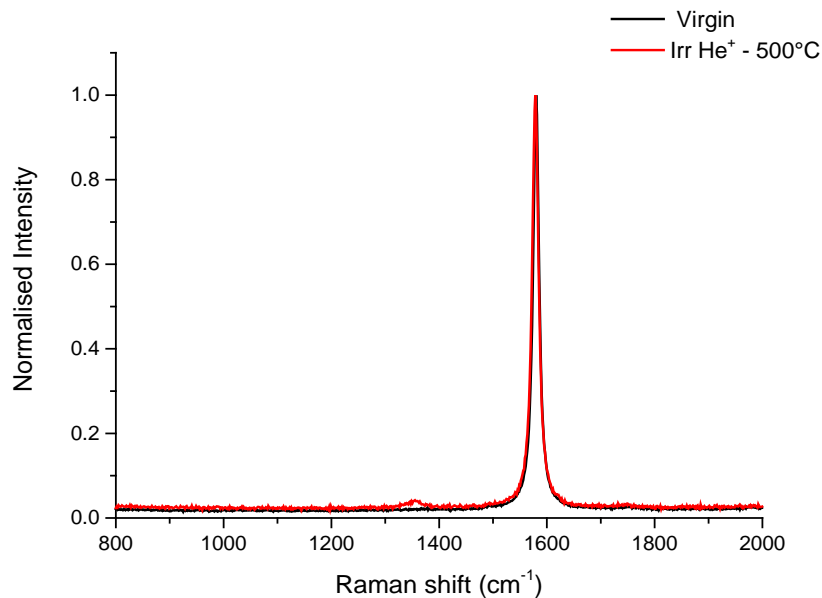
**Figure 2.1.19:** Raman spectra of the virgin and irradiated HOPG samples with He$^+$ ions

In conclusion, it seems that irradiation with helium ions at a low electronic stopping power can lead to slight disordering as much at ambient temperature as at 500 °C.

B | Initially slightly disordered graphite

Role of temperature

The irradiation was done at 500 °C. The results obtained are given in Figures 2.1.20 (***a***) is for the spectra that were recorded at different stages of the experiment; (***b***) is the evolution of the position of band G; (***c***) is the I_{D1}/I_G intensity ratio as the temperature is increased; (***d***)

and (*e*) are the evolution of the position of band G and the I_{D1}/I_G intensity ratio during irradiation, respectively.
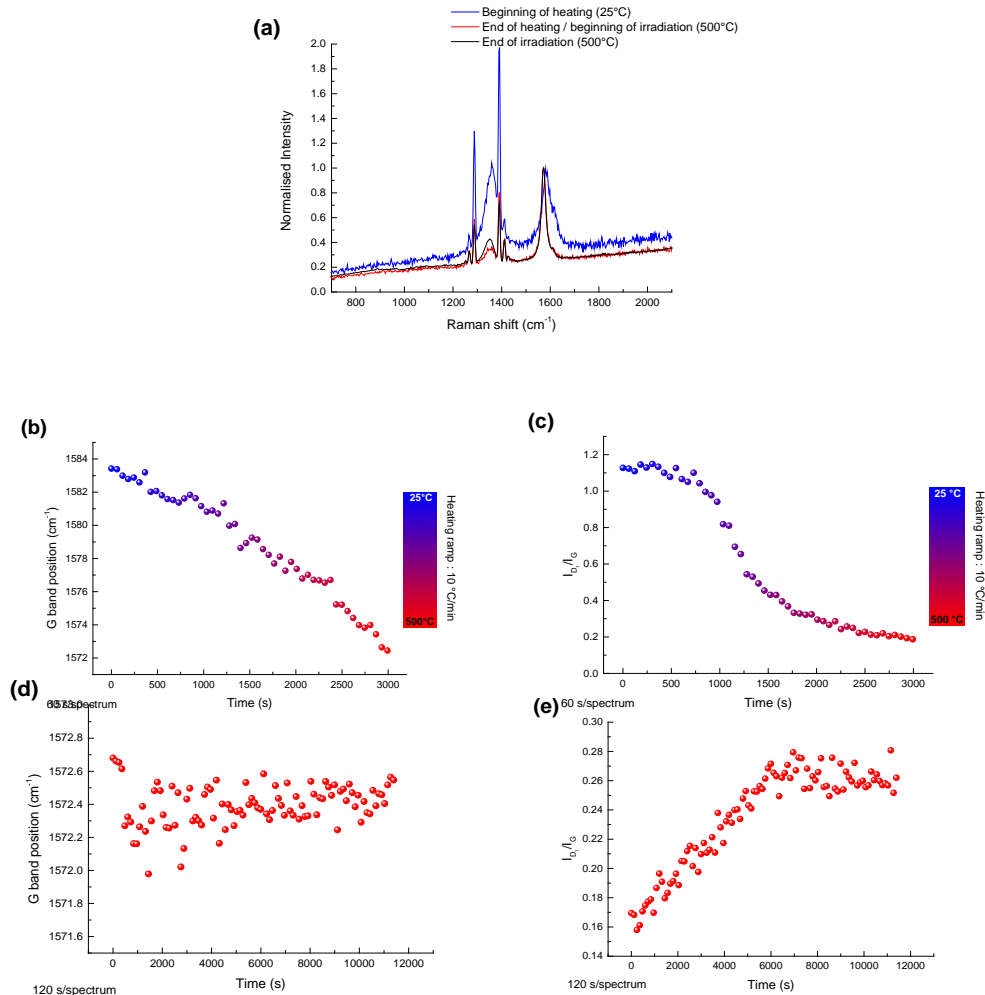
Figure 2.1.20: (a) Spectra recorded by Raman microspectrometry at different stages of the experiment (b and c) how the position of band G and the I_{D1}/I_G intensity ratio change as the temperature is increased to 500 °C and (d and e) how the position of band G and the I_{D1}/I_G intensity ratio change during irradiation with 15.7 MeV He$^+$ ions at 250 °C and a fluence of 1×10^{16} at.cm^{-2}

Figures 2.1.20 *b* shows a variation in the position of band G from 1583cm^{-1} to about at 1572cm^{-1} at 500°C which could be related to an expansion in the matter network as the temperature rises. The shift in band G as a function of temperature has already been described in the literature [Calizo 2007, Ferrari 2007, Reich 2004]. However, our experiments enable these changes to be followed in real time. Figures 2.1.20 *c* shows that

CAST
Final report on results from Work Package 5:
Carbon-14 in irradiated graphite (D5.19)

the I_{D1}/I_G ratio decreases over the time taken for the temperature to increase (from 250 to 500°C) from 1.1 to 0.4 at 250°C to 0.2 at 500 °C. This drop can be attributed to reordering due to temperature increase. We also point out that there is a clear acceleration in the restructuring process between 200 and 250 °C. This effect is probably due to the relative mobility of the vacancies and interstitials which can recombine [Gauthron 1986].

The I_{D1}/I_G ratio, increases linearly and stabilises at 500 °C where it reaches a threshold value of about 0.26 when the fluence reaches 5 x 10^{15} at.cm^{-2} at about 6000 s of irradiation. This plateau indicates the competitive effect of temperature which tends to reorder the graphite. In other terms, before this plateau, the effects of irradiation are dominant whereas later the effects of temperature and irradiation balance out.

In conclusion, in a mainly electronic regime, these results again indicate the antagonistic effects of temperature and irradiation on the evolution of the graphite structure. Furthermore, they clearly show the existence of a critical damage value above which the effects of irradiation and temperature balance out. This threshold value is reached more quickly when the temperature is higher.

Furthermore, we repeated the experiment by irradiating a virgin nuclear graphite from G2 reactor (results not shown here). We put in evidence that the dynamic annealing of the graphite structure is extremely dependent, not only on the initial state, in particular the degree of disorder, but also on the nature of the graphite. In fact, the threshold value for which an equilibrium is reached between the disordering effects of irradiation and the reordering effects of temperature for the implanted HOPG samples is reached at higher fluences compared to the G2 graphite for the same temperature and irradiation conditions.

*Conclusion concerning the effects of irradiation in a mainly electronic regime*
The effect of irradiation in a mainly electronic regime is greatly dependent on the initial structural state of the graphite. For **initially very disordered graphite** which is then irradiated at a high electronic stopping power S_e (greater than in the range of UNGG reactors), **its structure only slightly reorders**, even at 1000 °C, contrary to that observed

	CAST	
	Final report on results from Work Package 5:	
	Carbon-14 in irradiated graphite (D5.19)	

for irradiation in a mainly ballistic regime. Furthermore, the implanted ^{13}C is stabilised in the graphite mainly in sp^3-type structures.

In **initially slightly disordered graphite**, whatever the value of S_e, there is **competition between disordering caused by irradiation and temperature which clearly have antagonistic effects**. Even at very low S_e values, found in the lower range of those in UNGG reactors, irradiation induces **slight disordering** of the graphite as much at ambient temperature as at 500 °C. In addition, **the ability of irradiation to cause disordering depends not only on the flux, temperature and initial structural state, but also on the nature of the graphite itself.**

Summary and general conclusion

Ion irradiation of Highly Oriented Pyrolitic Graphite (HOPG) samples was carried out on ^{13}C pre-implanted samples. ^{13}C implantation was used to simulate ^{14}C displaced from its original structural site through recoil. In order to simulate neutron irradiation, the irradiations were carried out under temperature. Moreover, in order to monitor the ballistic and electronic effects independently, ion irradiation was carried out by varying the ion nature and energy. We gathered the results obtained for the different irradiations on the initially very disordered (Figure 2.1.21 a) samples and only slightly disordered samples (Figure 2.1.21 b).
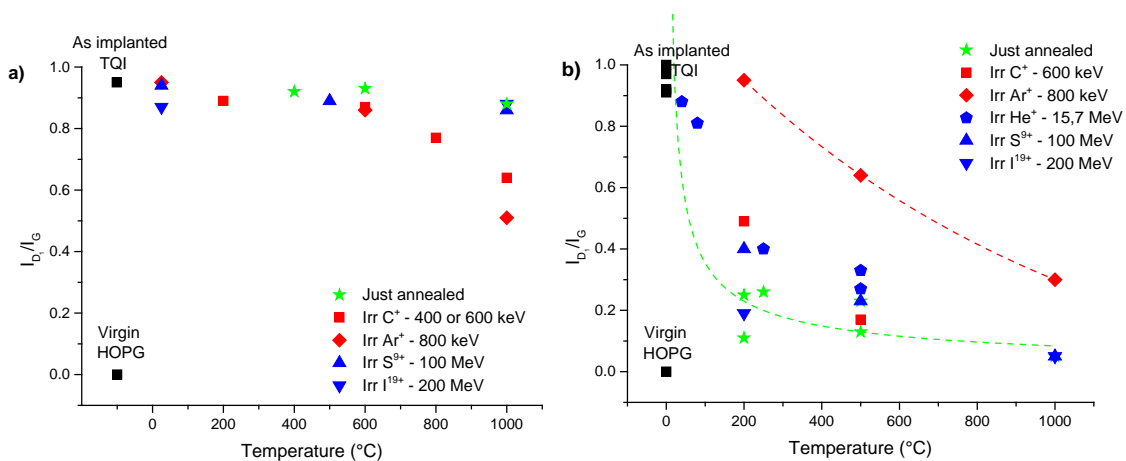
Figure 2.1.21: Evolution of the I_{D1}/I_G intensity ratio as a function of temperature and the type of irradiation for initially very disordered (a) and slightly disordered samples (b). The dashed lines enable the trends of these values as a function of temperature to be clearly seen.

CAST
Final report on results from Work Package 5:
**Carbon-14 in irradiated graphite (D5.19)**

When the initial disorder of the structure is important, there is a difference in behaviour depending on whether the samples are irradiated in a ballistic or electronic regime. **Irradiation in a ballistic regime, at higher than ambient temperature, favours the reordering of the graphite and the stabilisation of the ^{13}C in the sp^2 structures** (Figure 2.1.21 **a**). This effect is even clearer when the sample is irradiated at a high damage rate. In fact, the Figure shows that the value of the I_{D1}/I_G intensity ratio for the sample irradiated with argon ions at 1000 °C at a high dpa rate (4.4 dpa) is lower than for the sample irradiated with carbon ions (1 dpa). This Figure also shows that irradiation in an electronic regime, even at 1000 °C, leads to almost no reordering of the graphite. There is a synergy between temperature and irradiation i.e. when working at higher than ambient temperature and during irradiation in a ballistic regime the reordering of initially very disordered graphite is favoured. This effect is particularly visible above 600 °C, most certainly due to the greater relative mobility of the vacancies and interstitials. **Up to 600 °C, the irradiation regime has only a small impact on the structural state of the graphite.**

When the initial disorder is low, **whatever the regime, irradiation and temperature have antagonistic effects.** However, the possibility of the reordering of the graphite is in this case greatly dependent on the temperature and the rate of damage. If the latter is high (about 4 dpa for irradiation with argon ions) and at a low temperature (below 200 °C), the graphite cannot reorganise due to the reduced mobility of the defects. However, with a smaller damage rate (i.e. for irradiation with carbon ions) there is some reordering of the graphite, even at 200 °C. Between these two damage rates, there is probably a threshold value below which the effect of temperature cannot counterbalance the effects of irradiation. For a given temperature and irradiation flux, the value of this threshold is decided by the type of graphite and its initial amount of damage (structural state).

Extrapolation of the results to UNGG reactors and consequences for the subsequent management options (purification, disposal)

We can now try to extrapolate these results to the structural modifications induced in graphite by irradiation in a reactor and also to the behaviour of the ^{14}C in the irradiated graphite. In order to do this, we can use Figure 2.1.22 which shows schematically the

neutron flux conditions and the temperatures the graphite was subjected to as a function of its position in the SLA2-type graphite stack.
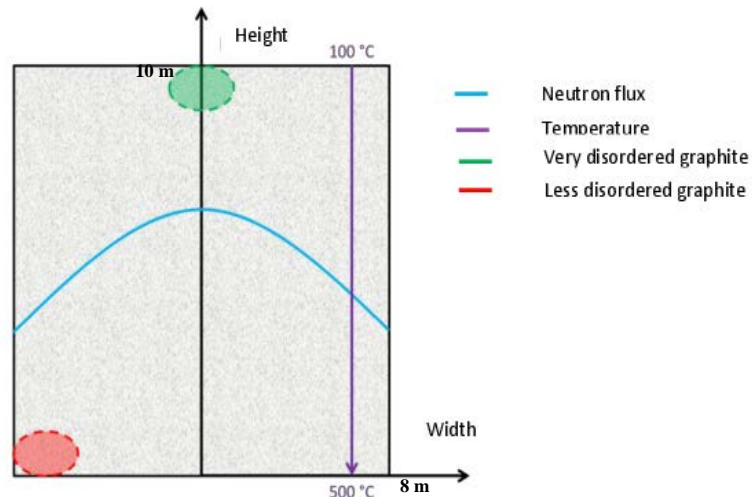
Figure 2.1.22: Structural behaviour of the graphite depending on its location in the SLA2-type stack

The main structural modifications that the graphite undergoes in the reactor are linked to the ballistic damage; the low values of the electronic stopping power probably lead to little damage.

For a very damaged graphite structure (for example, coke grains which have remained in a reactor for several years in a high neutron flux zone), the irradiation will have little impact on the evolution of its structure. This is because the temperatures at which the UNGG reactors function, i.e. between 200 and 500 °C at the most, are insufficient in annealing the defects. However, the evolution of an initially slightly disordered graphite structure (in the case of coke grains irradiated with a low neutron flux), will be greatly affected by the irradiation flux and temperature. The result could therefore lead to very different structural states as a function of the position of the graphite in the reactor. Consequently, graphite irradiated with a low neutron flux and situated in a hot zone (500 °C), such as the red zone in Figure 2.1.22, would probably be characterised by a structure similar to that of well-ordered graphite. However, graphite irradiated with a high neutron flux situated in a cold zone (200°C), such as the green zone in Figure 2.1.22, would keep its damaged/disordered

structure. Thus, both the nature and initial structural state of the graphite, as well as the irradiation conditions in the reactor, are likely to generate significant structural heterogeneity in the graphite moderator in the UNGG reactors. These results could explain, or at least be in agreement with, the significant structural contrasts observed by J. Pageot [Pageot 2014] for graphites irradiated with neutrons.

Concerning ^{14}C, apart from the ^{14}C formed by activation of ^{14}N located close to free surfaces for which a great part has probably been removed through radiolytic corrosion, both temperature and irradiation would tend to be stabilise it in the irradiated graphite structure: in planar sp^2 structures (in both aromatic cycles and chains) or three dimensional sp^3 structures (allowing interstitials carbon atoms to bond between the basal layers) [Ammar 2015, Eapen 2014]. The proportion of these structures would be variable and linked with the irradiation history. Thus, in case of disposal, the ^{14}C stabilisation, especially into sp^2 aromatic structures, should lead to reduced leaching rates in comparison to ^{14}C present in degraded and porous graphite. Furthermore, in case of prior purification, ^{14}C stabilised into the "hot" parts of the irradiated graphite should be more difficult to extract in comparison to ^{14}C present in "cold" and disordered zones. Moreover, as the majority of the ^{14}C would have been produced in zones submitted to high neutron flux and greatly disordered, these ^{14}C enriched zones would then be easier to decontaminate using CO_2 gasification based or steam reforming processes as shown by Pageot [Pageot 2015] and Galy [Galy 2016] due to the selective gasification of the most degraded areas. Thus, keeping a reduced mass loss of around 5%, Pageot showed that around 20% of the total ^{14}C could be gasified in SLA2 or G2 graphites.

	CAST	
	Final report on results from Work Package 5:	
	Carbon-14 in irradiated graphite (D5.19)	

REFERENCES

[Ammar 2015] M. R. Ammar, N. Galy, J.-N. Rouzaud, N. Toulhoat, C.-E. Vaudey, P. Simon, N. Moncoffre, Characterizing various types of defects in nuclear graphite using Raman scattering: Heat treatment, ion irradiation and polishing, Carbon 95 (2015) 364-373

[Bonal 2006] BONAL, J.-P. et ROBIN, J.-C. (2006). *Les réacteurs nucléaires à caloporteur gaz*, pages 27–32. CEA/DEN.

[Calizo 2007] I. Calizo, A.A. Balandin, W. Bao, F. Miao, C.N. Lau, Temperature dependence of the Raman spectra of graphene and graphene multilayers, Nano Letters, 2007, Vol. 7, No.9, 2645-2649

[Couzi 2016] M. Couzi, J.-L. Bruneel, D. Talaga, L. Bokobza, A multi wavelength Raman scattering study of defective graphitic carbon materials: The first order Raman spectra revisited, Carbon 107 (2016) 388-394

[Eapen 2014] J. Eapen, R. Krishna, T.D. Burchell, K.L. Murty (2014), Early damage mechanisms in nuclear grade graphite under irradiation, Materials Research Letters 2:1, 43-50

[Ewels 2003] C.P. Ewels, R.H Telling, A.A. El-Barbary, M.I. Heggie, Metastable Frenkel Pair Defect in Graphite: Source for Wigner Energy?, Physical Review Letter, Vol 91, 2 (2003)

[Ferrari 2007] A.C. Ferrari, Raman spectroscopy of graphene and graphite: Disorder, electron-phonon coupling, doping and nonadiabatic effects, Solid State Communications 143 (2007) 47-57

[Galy 2016] N. Galy, (2016) *Comportement du ^{14}C dans le graphite nucléaire: Effets de l'irradiation et décontamination par vaporéformage*, Thèse de Doctorat, Université Claude Bernard Lyon 1, LYCEN – T 2016-12

[Gauthron 1986] GAUTHRON, M. (1986). *Introduction au génie nucléaire Tome 1 : Neutronique et matériaux*. INSTN/CEA.

[Lehtinen 2011] O. Lehtinen and T. Nikitin (2011). "Characterization of ion-irradiation-induced defects in multi-walled carbon nanotubes." New Journal of Physics 13.

[Liu 2006] J. Liu, H.-J. Yao, et al. (2006). "Temperature annealing of tracks induced by ion irradiation of graphite." Nuclear Instruments and Methods in Physics Research Section B: Beam Interactions with Materials and Atoms 245(1): 126-129.

[Moncoffre 2016] N. Moncoffre et al., Impact of radiolysis and radiolytic corrosion on the release of ^{13}C and ^{37}Cl implanted into nuclear graphite: Consequences for the behaviour of ^{14}C and ^{36}Cl in gas cooled graphite moderated reactors, Journal of Nuclear Materials 472 (2016) 252-258

[Pageot 2014] J. Pageot, Etude d'un procédé de décontamination du ^{14}C par carboxy-gazéification des déchets de graphite nucléaire, thèse de doctorat de l'Université Paris-Sud, Andra, 2014.

[Pageot 2015] J. Pageot, J.-N. Rouzaud, M. Ali Ahmad, D. Deldicque, R. Gadiou, J. Dentzer, L. Gosmain, Milled graphite as a pertinent analogue of French UNGG reactor graphite waste for a CO_2 gasification-based treatment, Carbon 86 (2015) 174-187

[Poncet 2013] B. Poncet, L. Petit, Method to assess the radionuclide inventory of irradiated graphite waste from gas-cooled reactors, J. Radioanal. Nucl. Chem. 298, 941-953, 2013

[Reich 2004] S. Reich, C. Thomsen, Raman spectroscopy of graphite, The Royal Society, Phil. Trans. R. Soc. Lond. A (2004) 362, 2271-2288

[Rouzaud 1983] Rouzaud, J.-N., Oberlin, A. & Beny-Bassez, C., 1983. Carbon films: Structure and microtexture (optical and electron microscopy, Raman spectroscopy). Thin Solid Films, 105(1), pp.75–96.

[Seitz 1956] F. Seitz, J.S. Koehler, Solide state physics 2, 305, 1956

[Silbermann 2013] SILBERMANN, G. (2013). *Effets de la température et de l'irradiation sur le comportement du ^{14}C et de son précurseur ^{14}N dans le graphite nucléaire. Etude de la décontamination thermique du graphite en présence de vapeur d'eau.* Thèse de doctorat, Université Claude Bernard Lyon 1, IPNL & EDF/CIDEN, LYCEN T 2013-12

[Silbermann 2014] G. Silbermann, N. Moncoffre, N. Toulhoat, N. Bérerd, A. Perrat-Mabilon, G. Laurent, L. Raimbault, P. Sainsot, J.-N. Rouzaud, D. Deldicque, Temperature effects on the behavior of carbon 14 in nuclear graphite, Nuclear Instruments and Methods in Physics Research B 332, 106–110, 2014.

[Telling 2003] R.H Telling, C.P. Ewels, A.A. El-Barbary, M.I. Heggie, Wigner defects bridge the graphite gap, Nature Materials, Vol 2 May 2003 doi:10.1038/nmat876

[Toulemonde 1993] M. Toulemonde, E. Paumier, C. Dufour, Thermal spike model in the electronic stopping power regime, Radiation Effects and Defects in solide 126 (1993) 201-206
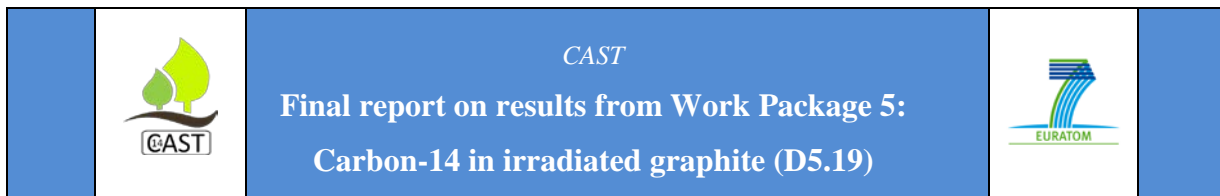
[Toulemonde 2012] M. Toulemonde, W.Assmann, C.Dufour, A. Meftah, C. Trautmann Nanometric transformation of the matter by short and intense electronic excitation: Experimental data versus inelastic thermal spike model, Nuc. Ins. Meth. B 277 (2012) 28-39

[Vaudey 2010 a] C.E.Vaudey, N.Toulhoat, N.Moncoffre, N.Bérerd, Chlorine speciation in nuclear graphite: consequences on temperature release and on leaching, Radiochim. Acta 98, 1–7 (2010) / DOI 10.1524/ract.2010.1767

[Vaudey 2010 b] Vaudey, C.-E. (2010). *Effets de la température et de la corrosion radiolytique sur le comportement du chlore dans le graphite nucléaire : conséquences pour le stockage des graphites irradiés des réacteurs UNGG.* Thèse de doctorat, Université Claude Bernard Lyon 1, IPNL. LYCEN T 2010-12

[Ziegler 1985] J-F.Ziegler et al., (1985) « The Stopping and Range of Ion in Solids », Pergamon Press, New York.

[Ziegler 2010] J.F. Ziegler et al., 2010. Srim – the stopping and range of ions in matter (2010). Nuclear Instruments and Methods in Physics Research Section B: Beam Interactions with Materials and Atoms, 268(11–12): 1818-1823.

2.2   Lithuanian Energy Institute (LEI) summary

LEI participated in Tasks 5.1, 5.2 and 5.5 within Work Package 5 (WP5) of the CAST Project.

During the first three years of the CAST Project, LEI concentrated on the performance of the Task 5.1 – "Review of CARBOWASTE and other relevant R&D activities to establish the current understanding of inventory and release of ^{14}C from i-graphites" and Task 5.2 – "Characterisation of the ^{14}C inventory in i-graphites". Task 5.5 "Data interpretation and synthesis – final report" is a final project year activity. For Task 5.1, LEI reviewed the outcome of CARBOWASTE Project in the national context and based on that, provided input for deliverable D5.5 "Review of current understanding of inventory and release of ^{14}C from irradiated graphites". For the Task 5.2, LEI modelled the ^{14}C inventory in a RBMK-1500 reactor core using new developed models and experimental data and prepared deliverable D5.17 "Report on modelling of ^{14}C inventory in RBMK reactor core". The Task 5.5 "Data interpretation and synthesis – final report" is the last Task of WP5 that summarises and syntheses in a final report the work undertaken in the previous Tasks by all participants. The outcome of this Task is this deliverable D5.19 "Final report on results from WP5".

For the Task 5.1, LEI activities are completed. The outcomes from the CARBOWASTE Project were reviewed and summarised for the RBMK-1500 reactor. Based on that, the draft input for deliverable D5.5 "Review of current understanding of inventory and release of ^{14}C from irradiated graphites" was produced and sent to the RWM for the incorporation into the draft deliverable in the end of the first Project year. Some comments regarding LEI input were received during the second Project year. The LEI input then was updated based on the comments, and revised input for deliverable D5.5 was produced and sent to the RWM for the incorporation into the final deliverable. The final version of deliverable D5.5 [Toulhoat et al., 2015] was issued on 2015-07-15 and is available from CAST Project public website.

For the Task 5.2, LEI activities are completed also. Following the knowledge gained in the CARBOWASTE Project, IAEA CRP, etc., new models for numerical estimation of

CAST
Final report on results from Work Package 5:
Carbon-14 in irradiated graphite (D5.19)

RBMK-1500 graphite activation were developed (SCALE and MCNP software). Combining numerical modelling results obtained using these new models and experimental data for the induced activity of ^{14}C, the inventory of ^{14}C in i-graphite of the whole core of Ignalina NPP Unit 1 reactor was estimated. It should be noted, that sampling of the Ignalina NPP Unit 1 RBMK-1500 reactor graphite stack has been already done by the Ignalina NPP staff and it was expected that radiological characterisation of the taken samples (activity of ^{14}C is of most importance for CAST project) will be made in the course of the CAST project. However, to the date of issue of the report D5.17, no results of ^{14}C activity measurements in GR-280 grade graphite were made publically available, except in a paper [Mazeika et al., 2013]. This paper presented ^{14}C activity measurements in one sample of the graphite bushing from the temperature channel of the reactor. Consequently, the exhaustive combination of the modelled and measured ^{14}C activities for the more detailed and more confident estimation of ^{14}C inventory in the whole RBMK-1500 reactor graphite stack has not been achieved to date, as the only ^{14}C activity measurement data that were used for the inventory estimation was that from a paper [Mazeika et al., 2013]. The draft version of the deliverable D5.17 was produced and sent to RWM for review and comments. Some comments regarding this LEI report were received and were taken into account preparing the final version of that report. The final version of deliverable D5.17 [Narkunas & Poskas, 2017] was issued on 2017-07-12 and is available from CAST Project public website.

For the Task 5.5 "Data interpretation and synthesis – final report" LEI prepared the input to the deliverable D5.19 "Final report on results from WP5", addressing the work performed in the WP5, and sent it to the NDA. It is the last deliverable of WP5, i.e. this report, and it summarises and synthesises the work undertaken in the previous WP5 Tasks by all participants.

MAIN RESULTS OF PROJECT CAST WP5

The main scientific task for LEI in the WP5 of the CAST project was to perform the neutron activation modelling of Ignalina Nuclear Power Plant (Ignalina NPP) Unit 1 reactor RBMK-1500 graphite stack and determine the C-14 inventory. In order to fulfil this task, the new numerical models for neutron activation modelling were developed and activity distribution

CAST
Final report on results from Work Package 5:
Carbon-14 in irradiated graphite (D5.19)

of C-14 within the whole reactor graphite stack was obtained. Then, combining this data with the available C-14 activity measurement results, estimation of the total C-14 inventory in the graphite stack was made. The text below presents only the summary of the work performed, whereas the full details are available in the CAST project deliverable D5.17 [Narkunas & Poskas, 2017].

Description of the RBMK-1500 reactor

Ignalina NPP contains two power Units with RBMK-1500 reactor in each. While in operation, these reactors were the most powerful and most advanced versions of all RBMK reactors. Since the end of 2004 y, Unit 1 is permanently shut-down (its start-up dates back to the end of 1983 y). After being more than 10 years in a decommissioning stage, a number of systems and equipment of Unit 1 were radiologically characterised and dismantled. However, these works were performed for relatively low contamination systems, while the reactor itself is intact (although defueled) and not radiologically characterised. The highest volume of reactor structures is attributed to the graphite core, so radiological characterisation of it still is an open issue, affecting dismantling and temporal storage strategies as well as final disposal routes (especially C-14 inventory).

A general view of the RBMK reactor is presented in Figure 2.2.1. The RBMK-1500 is a graphite-moderated, water-cooled, channel-type boiling water reactor having a thermal power generation capacity of 4800 MW, which was decreased to 4200 MW after the Chernobyl accident. The reactor is housed in a 25 m deep, 21x21 m wide concrete vault. The core volume is dominated by a large cylindrical graphite stack. The graphite stack is located in a hermetically sealed cavity, consisting of cylindrical wall and top and bottom metal plates, which is filled with a helium-nitrogen mixture (nitrogen ~60 % by mass) preventing graphite oxidation and improving heat transfer from the graphite to the fuel channels. This also excludes the radiolytic corrosion of graphite, thus the mass loss of graphite is not specific for the RBMK reactors.
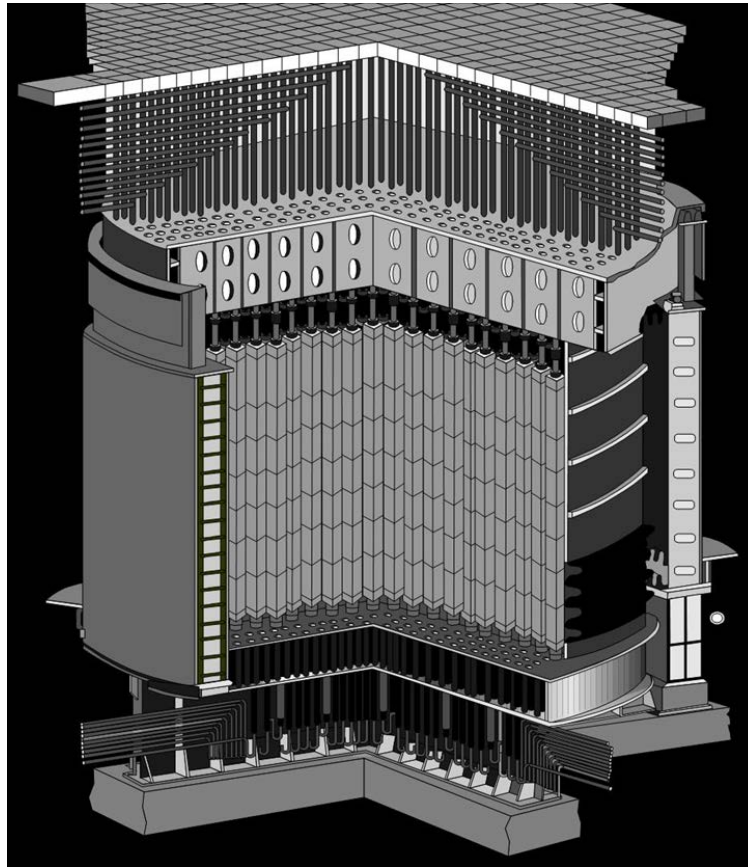
Figure 2.2.1: General view of the RBMK reactor [http://www.atomic-energy.ru**]**

The stack can be visualized as a vertical cylinder of 8 m height and 14 m diameter, made up of 2488 graphite columns arranged next to each other without keying. The outer four rows of columns of the stack make up the radial reflector (RR), and a 0.5 m thick layer at the top and bottom make up the top and the bottom reflectors, respectively. The total mass of graphite blocks in a whole graphite stack is about 1700 tonnes.

Every graphite column is constructed from graphite blocks of different height, see Figure 2.2.2. The blocks are rectangular parallelepipeds, with a base of 0.25 x 0.25 m, and heights of 0.2, 0.3, 0.5 and 0.6 m of which the 0.6 m blocks are most common. The short blocks are used only in the top and bottom ends of the column.
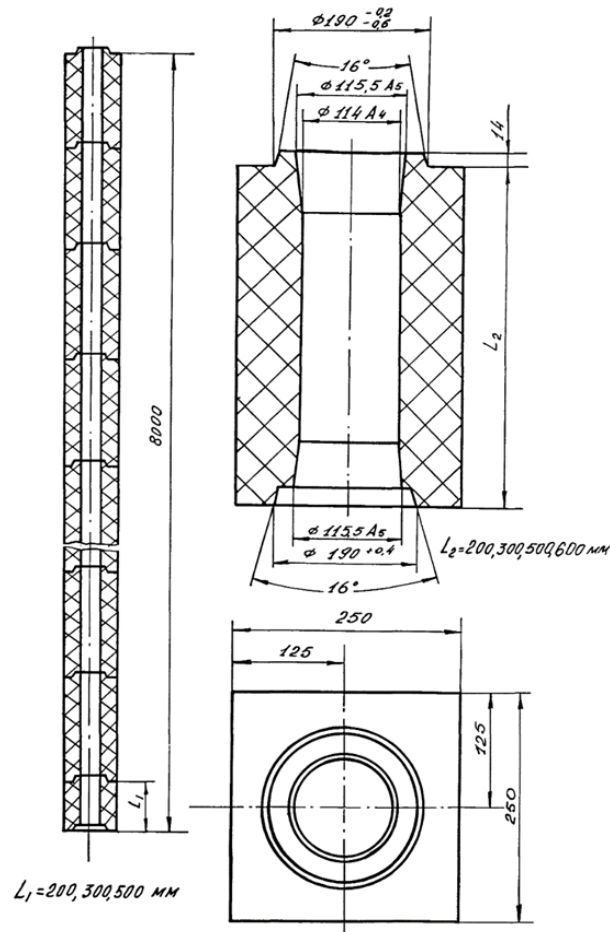
Figure 2.2.2: Schematic view of graphite column and block of RBMK-1500 reactor [Ignalina Nuclear Power Plant, 1985]

The blocks possess a 0.114 m diameter bore opening through the vertical axis. This provides a space for a total of 2052 channels which are used for placing Fuel Assemblies (FA) (so called Fuel Channels – FC), reactivity regulating control rods and several types of other instrumentation (so called Control and Protection System channels – CPS channels) into the core and cooling of radial reflector (so called Radial Reflector Cooling channels – RRC channels). The blocks of the remaining 436 columns located within the radial reflector have the central bore openings of 0.089 m diameter and this space is filled by graphite rods providing keying of the blocks within the column, increasing the density and neutron reflecting effectiveness of this part of the graphite stack. Graphite rods are manufactured from the different grade graphite compared to the blocks (GRP-1-280 is the grade of

CAST
Final report on results from Work Package 5:
Carbon-14 in irradiated graphite (D5.19)

graphite used for rods while GR-280 is the grade used for blocks), however the total mass of the graphite rods in a whole graphite stack is much lower, i.e. ~60 tonnes.

Within the reactor core, FC and CPS channels are positioned by the help of special graphite rings and sleeves. In order to improve heat transfer from the graphite stack, the central segment of FC is surrounded by the 0.02 m height and 0.0115 m thickness split rings of GRP-2-125 grade graphite. These rings are arranged next to one another in such a manner that one is in contact with the channel, and the other with the graphite stack block. Above and below graphite rings section, there are also GRP-2-125 grade graphite sleeves of different shape and size placed. The arrangement of graphite rings and sleeves for CPS channels is somewhat different. The total mass of the graphite rings and sleeves of FC and CPS channels is ~120 tonnes in the reactor.

CPS channels could be equipped with control rods of 4 different types. Manual Control Rods of type 1 (MCR1) are control rods of initial design used to control the radial field of energy distribution. Later part of the MCR1 rods were replaced by the modified control rods (MCR2). Fast Acting Scram Rods (FASR) are used to rapidly cease the nuclear chain reaction. Shortened Absorber Rods (SAR) are used to control the axial field of energy distribution. Additionally, some of CPS channels are equipped with the Axial Power Density Monitoring System sensors (PDMS-A) and Fission Chambers for monitoring purposes.

Although reactor graphite columns could be separated into different groups according to the various criteria, by considering the equipment placed inside the columns all 2488 pieces (pcs.) of reactor RBMK-1500 columns can be grouped in a structure as follows:
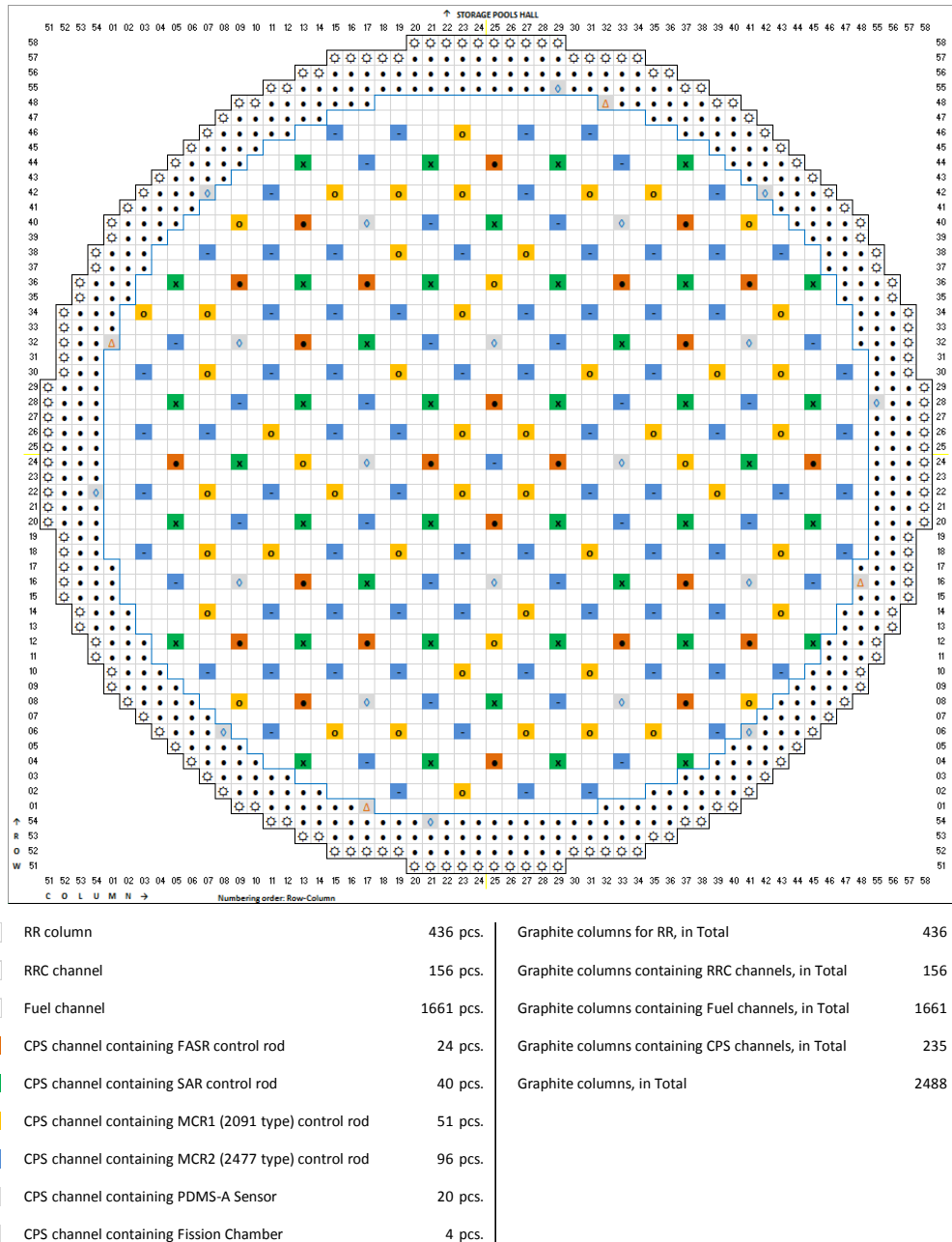
- Graphite columns with channel tubes (2052 pcs.), of which:
  - Fuel channel (1661 pcs.);
  - RRC channel (156 pcs.);
  - CPS channel (235 pcs.), of which:
    - containing MCR1 control rod (51 pcs.);
    - containing MCR2 control rod (96 pcs.);

- containing FASR control rod (24 pcs.);
- containing SAR control rod (40 pcs.);
- containing PDMS-A sensor (20 pcs.);
- containing Fission Chamber (4 pcs.);
- Graphite columns without channel tubes (436 pcs.), of which:
  - RR column containing graphite rods (436 pcs.).

The layout of the graphite columns in the RBMK-1500 reactor at Ignalina NPP Unit 1, based on the above-presented grouping structure, is shown in Figure 2.2.3.

CAST
Final report on results from Work Package 5:
Carbon-14 in irradiated graphite (D5.19)

•	RR column	436 pcs.	Graphite columns for RR, in Total	436 pcs.
✿	RRC channel	156 pcs.	Graphite columns containing RRC channels, in Total	156 pcs.
☐	Fuel channel	1661 pcs.	Graphite columns containing Fuel channels, in Total	1661 pcs.
●	CPS channel containing FASR control rod	24 pcs.	Graphite columns containing CPS channels, in Total	235 pcs.
✕	CPS channel containing SAR control rod	40 pcs.	Graphite columns, in Total	2488 pcs.
o	CPS channel containing MCR1 (2091 type) control rod	51 pcs.		
-	CPS channel containing MCR2 (2477 type) control rod	96 pcs.		
◇	CPS channel containing PDMS-A Sensor	20 pcs.		
△	CPS channel containing Fission Chamber	4 pcs.		

Figure 2.2.3: Layout of graphite columns in RBMK-1500 reactor at Ignalina NPP Unit 1

C-14 inventory modelling and results

The methodology for modelling of C-14 inventory in the irradiated RBMK-1500 graphite for the CAST project, in principle, is the same as used for EC 7th FP CARBOWASTE project [Narkunas et al., 2013a; Narkunas et al., 2013b], i.e. initially, the energy and spatial

distribution of neutron flux is modelled in the analysed system and later, the results of this modelling are used for neutron activation modelling. However, the modelling approach, developed models and computer codes used in the current study differ a lot compared to those of the CARBOWASTE project.

For the CAST project, modelling of the neutron flux was performed using MCNP 5 ver. 1.6 code [Los Alamos National Laboratory, 2003]. The newly developed model envelopes the whole reactor core with the graphite stack consisting of 2488 graphite columns and surrounding structures, in the space region of 21x21x15 m (21x21 m is the length and the width of a concrete reactor vault while 15 m is the height of the modelled reactor core including surrounding structures). The modelled neutron flux was grouped into 238 energy groups (the most detailed neutron energy group structure used in SCALE codes system). The modelled neutron flux in these 238 groups structure then was used by COUPLE code from SCALE 6.1 codes system [Oak Ridge National Laboratory, 2011] for automated preparation of problem-specific cross-section data for ORIGEN-S code (also from SCALE 6.1 codes system). Having problem-specific cross-section data and using total neutron flux, the neutron activation modelling of the reactor RBMK-1500 graphite stack was performed.

Neutron flux and neutron activation modelling results here are presented only for the graphite columns containing fuel channels in RBMK-1500 reactor central part of the reactor at Ignalina NPP Unit 1. Results for the remaining graphite columns could be found in the CAST deliverable D5.17 [Narkunas & Poskas, 2017].

Although modelled neutron flux is only an intermediate result used for the estimation of induced C-14 activity in the irradiated graphite, presenting it gives an idea of the correlation between modelled flux and respective C-14 activity. The modelled flux represents reactor operation at 4200 MW thermal power. Furthermore, the neutron flux presented here was collapsed to the 3 energy groups (Thermal, Resonance and Fast) from the 238 energy group structure, as initially modelled with MCNP.

The results of the neutron flux and C-14 specific activity modelling in the graphite columns with FC located in the central part of the reactor (see Figure 2.2.4), are presented respectively in Figure 2.2.5 and Figure 2.2.6.

H	Fuel channel	580 pcs.
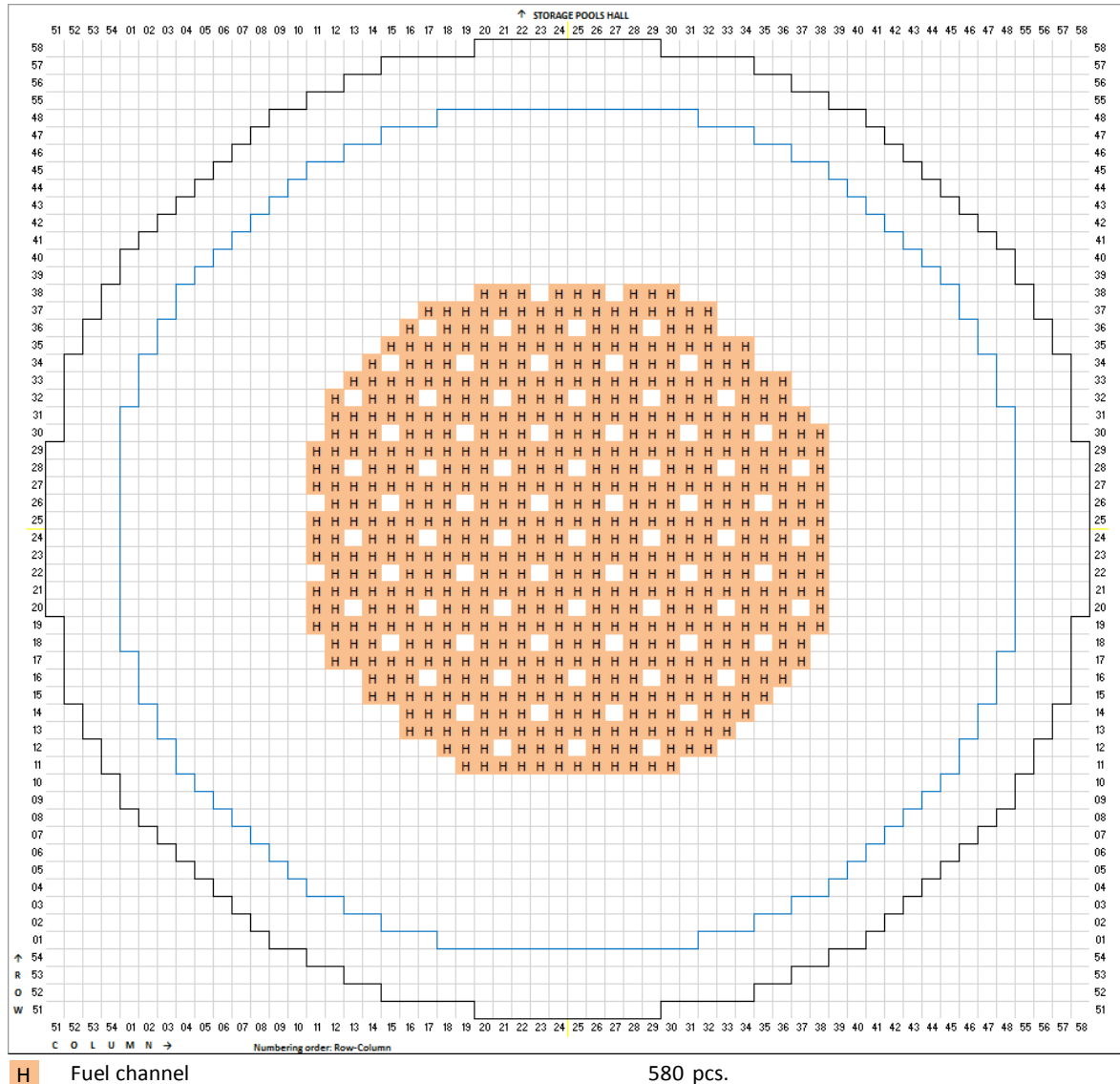
Figure 2.2.4: Layout of graphite columns containing fuel channels in RBMK-1500 reactor central part at Ignalina NPP Unit 1

The graphite columns with FC are regularly distributed over the whole cross-section of the central part of the active core of the reactor, as given in Figure 2.2.4. These FC contain a fuel assembly that consists of two fuel bundles. The fuel assemblies were explicitly

described in the MCNP model, so this accordingly affected the neutron flux distribution, see Figure 2.2.5.

The results of the neutron flux modelling show that the thermal and resonance neutron flux are dominant in the graphite column (blocks) with FC in the central reactor part; however, the thermal neutron flux is more intensive than the resonance neutron flux (though very insignificantly in a certain regions), see Figure 2.2.5 (Figure 2.2.5 a) shows the modelled neutron flux distribution in the absolute values, whereas Figure 2.2.5 b) shows the modelled neutron flux distribution in the relative units, i.e. normalized to the maximal value of the total modelled neutron flux).

The fast neutron flux is about 10 times lower than the resonance neutron flux and its distribution along the axial direction is almost the same as that of the resonance neutron flux (see Figure 2.2.5). There are two maximums in the distribution profiles of the fast and resonance neutron flux and one minimum in the area of the reactor core axial centre, which corresponds to the place of the fuel bundles connection in the fuel assembly. In the edges of graphite column (i.e. top and bottom reflector blocks) the fast neutron flux is ~150 (top reflector) and ~40 (bottom reflector) times lower than the maximal value of the fast neutron flux in the region of the active core (i.e. in the 700 cm height central part of the graphite blocks column). For the resonance neutron flux the differences are lower; the resonance neutron flux is ~100 (top reflector) and ~30 (bottom reflector) times lower than the maximal value of the resonance neutron flux in the region of the active core.

In the case of the thermal neutron flux, there is only one maximum in the neutron flux distribution profile and it is located in the central (lower) part of the reactor core (see Figure 2.2.5). Going further from that location the thermal flux decreases monotonically and in the edges of the graphite column i.e. top and bottom reflectors is ~24 and ~7 times lower than the maximal flux, respectively. The average (averaged over the 700 cm long central part of the graphite column) thermal neutron flux in the graphite column is ~1.2×10^{14} n/cm^2·s while the maximal value of the thermal flux is nearly 2×10^{14} n/cm^2·s.
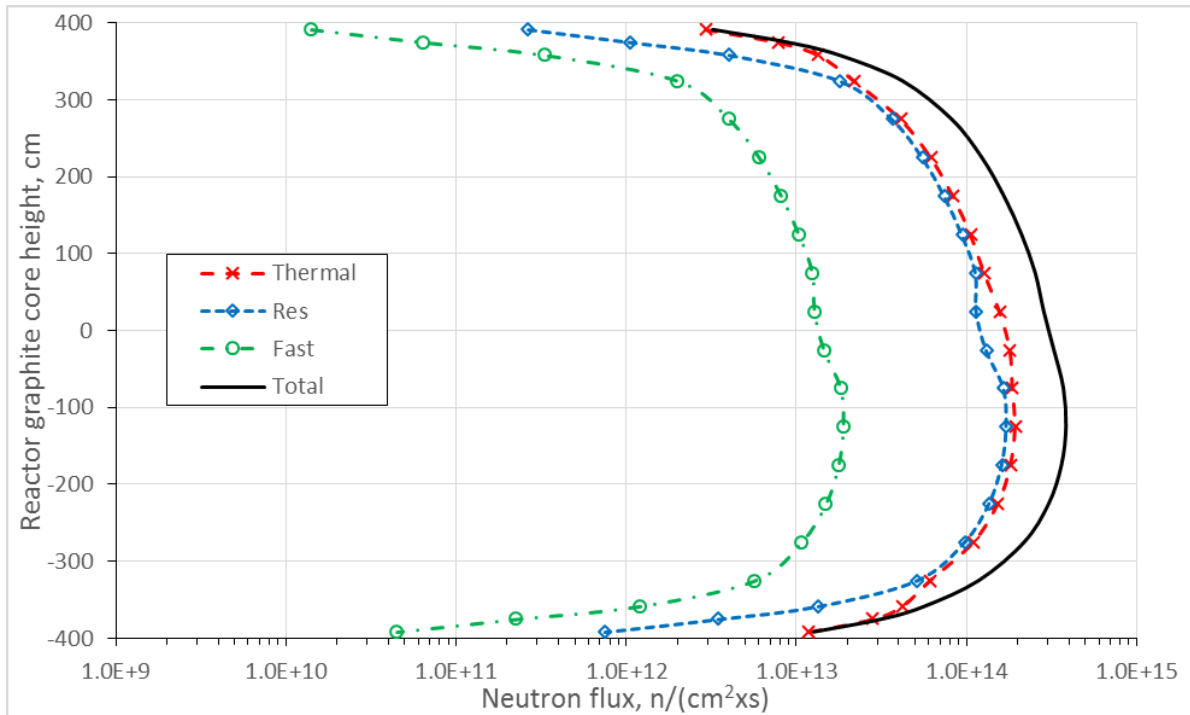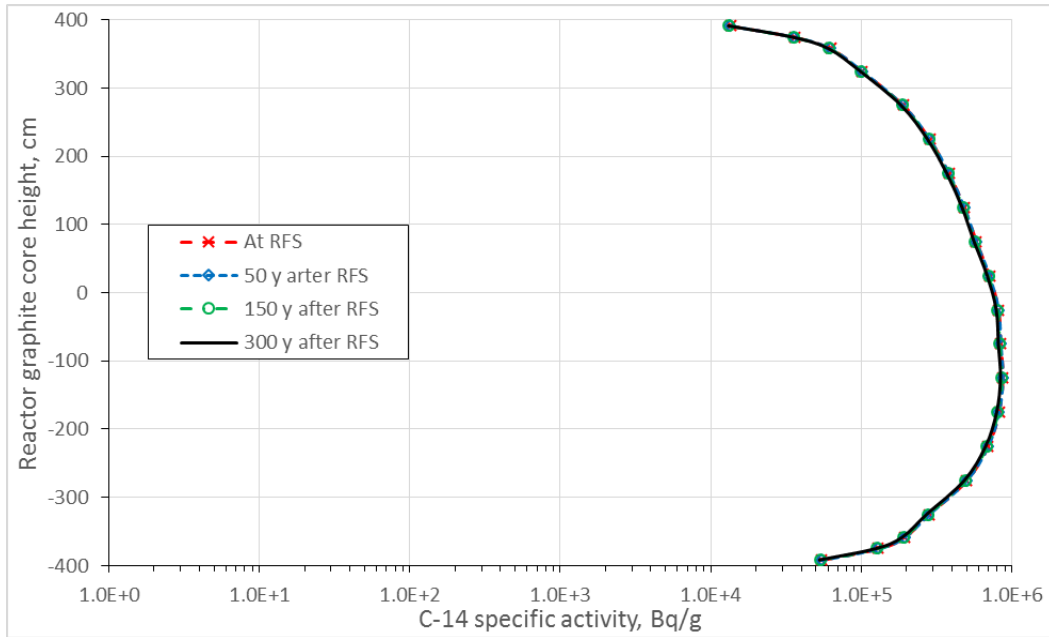
a)
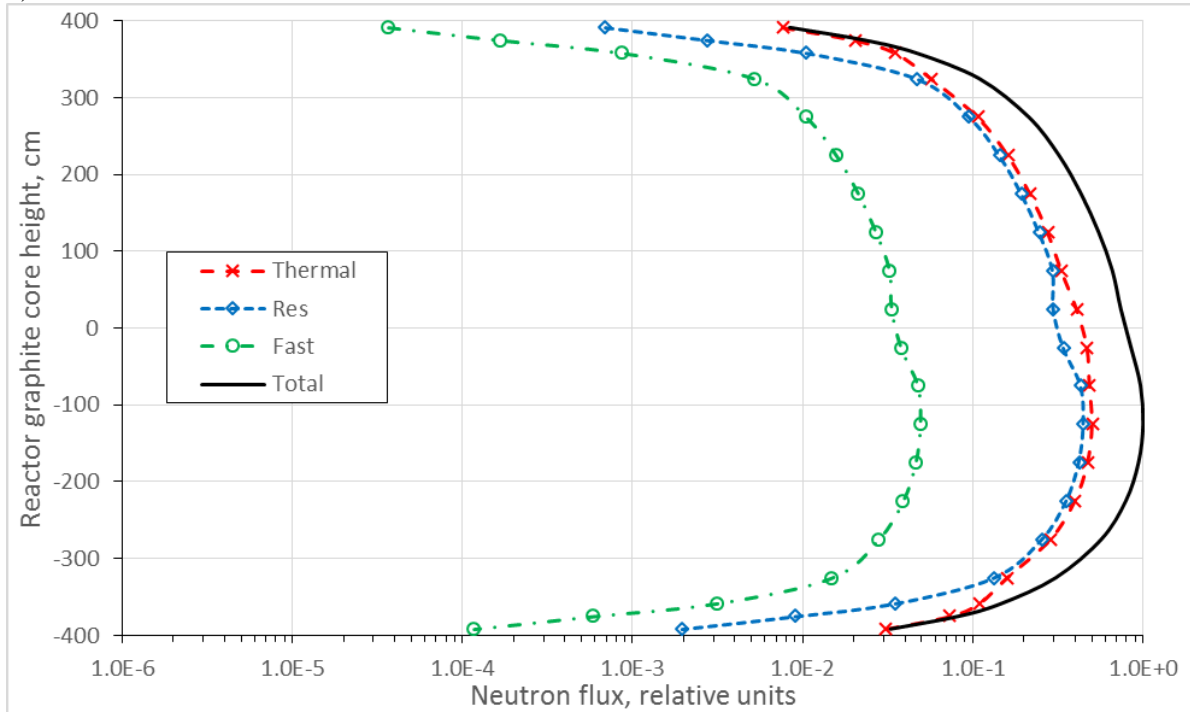
b)

Figure 2.2.5: Distribution of absolute a) and normalised b) neutron flux in graphite columns containing fuel channels in RBMK-1500 reactor central part at Ignalina NPP Unit 1

C-14 specific activity modelling results are presented in Figure 2.2.6 (Figure 2.2.6 a) shows the modelled C-14 specific activity distribution in the absolute values, whereas Figure 2.2.6 b) shows the modelled C-14 specific activity distribution in the relative units, i.e. normalized to the maximal value of the modelled C-14 specific activity). The modelling results show that C-14 specific activity distribution along the axial direction in the graphite columns containing fuel channels corresponds to the thermal neutron flux distribution (see Figure 2.2.5 and Figure 2.2.6). The average C-14 activity in the active core graphite blocks (i.e. average in the 700 cm height central part of the graphite blocks column) is ~5.4×10^5 Bq/g. The maximal C-14 activity (~8.7×10^5 Bq/g) position coincides with the maximal thermal neutron flux position, which is at mark "–125", and (analogous to the thermal flux) the C-14 specific activity in the top and bottom reflector parts is respectively ~24 and ~7 times lower than the maximal. This confirms the fact that production of C-14 from carbon activation, as well as from impurities activation, is determined mainly by the thermal neutron flux.

The influence of the radioactive decay to the induced activity of C-14 during the analysed 300 y period after RFS in insignificant. As C-14 is a long-lived radionuclide having the half-life of ~5.7×10^3 y, during the 300 y period its activity decreases less than 4 percent.

Comparing C-14 specific activity modelling results of the current study with the ones obtained previously in EC 7th FP CARBOWASTE project [Narkunas et al., 2013a; Narkunas et al., 2013b] (max. impurities case), it could be noted that the results are somewhat different. The average activity of the active core graphite blocks obtained in [Narkunas et al., 2013a; Narkunas et al., 2013b] was ~3.6×10^5 Bq/g (~5.4×10^5 Bq/g here), the activity in the bottom reflector was just above 8×10^4 Bq/g (1.3×10^5 Bq/g here) and in the top reflector it was nearly 6×10^4 Bq/g (3.7×10^4 Bq/g here). This gives a clear indication that, on the whole, the results of the current study are higher, but in the upper region of graphite stack, the modelled activities are lower. This means that the distribution profiles of the modelled neutron flux and, consequently, C-14 activities have changed. The main reason for this is the full description of the RBMK-1500 reactor and its surrounding structures in this study (especially control rods in their withdrawn positions), thus representing their

influence on the modelled neutron flux. Additionally, activation modelling (with the use of COUPLE module for cross-sections preparation and updated data libraries) had an influence.


a)
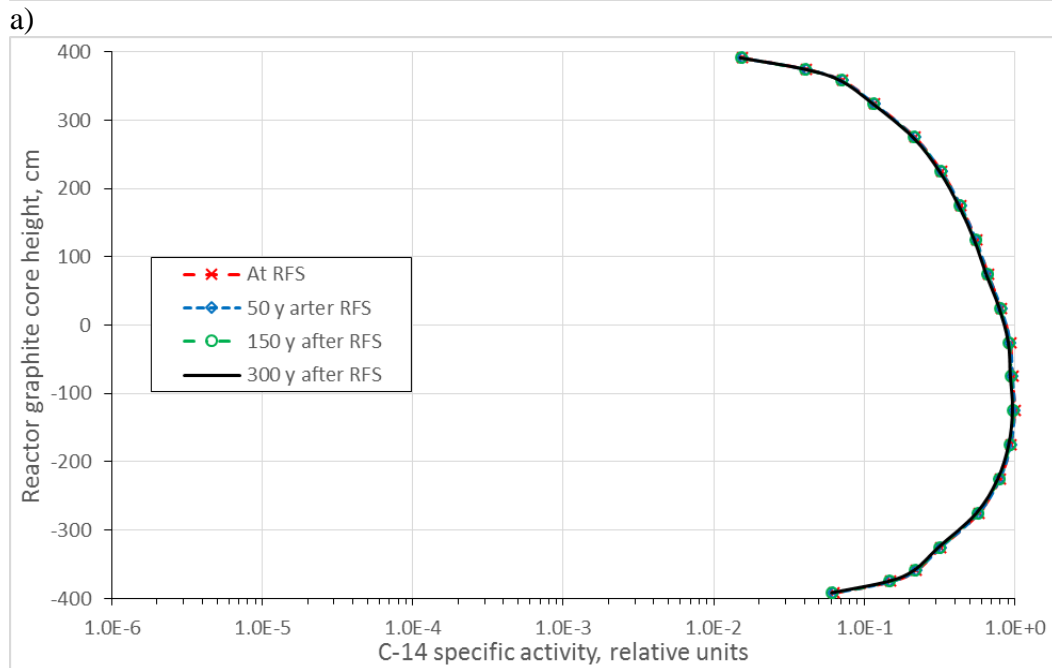
b)

Figure 2.2.6: Distribution of absolute a) and normalised b) C-14 specific activity in graphite columns containing fuel channels in RBMK-1500 reactor central part at Ignalina NPP Unit 1

Estimation of C-14 inventory

Sampling of the Ignalina NPP Unit 1 RBMK-1500 reactor graphite stack has been already done by the Ignalina NPP staff and it was expected that radiological characterisation of the taken samples (activity of C-14 is of most importance for CAST project) will be made in the course of the CAST project. However, to the issue date of deliverable D5.17 [Narkunas & Poskas, 2017], no results of C-14 activity measurements in GR-280 grade graphite were made publically available, except in a paper [Mazeika et al., 2013]. This paper presented C-14 activity measurements in one sample (see Figure 2.2.7 for location) of the graphite bushing from the temperature channel of the reactor.
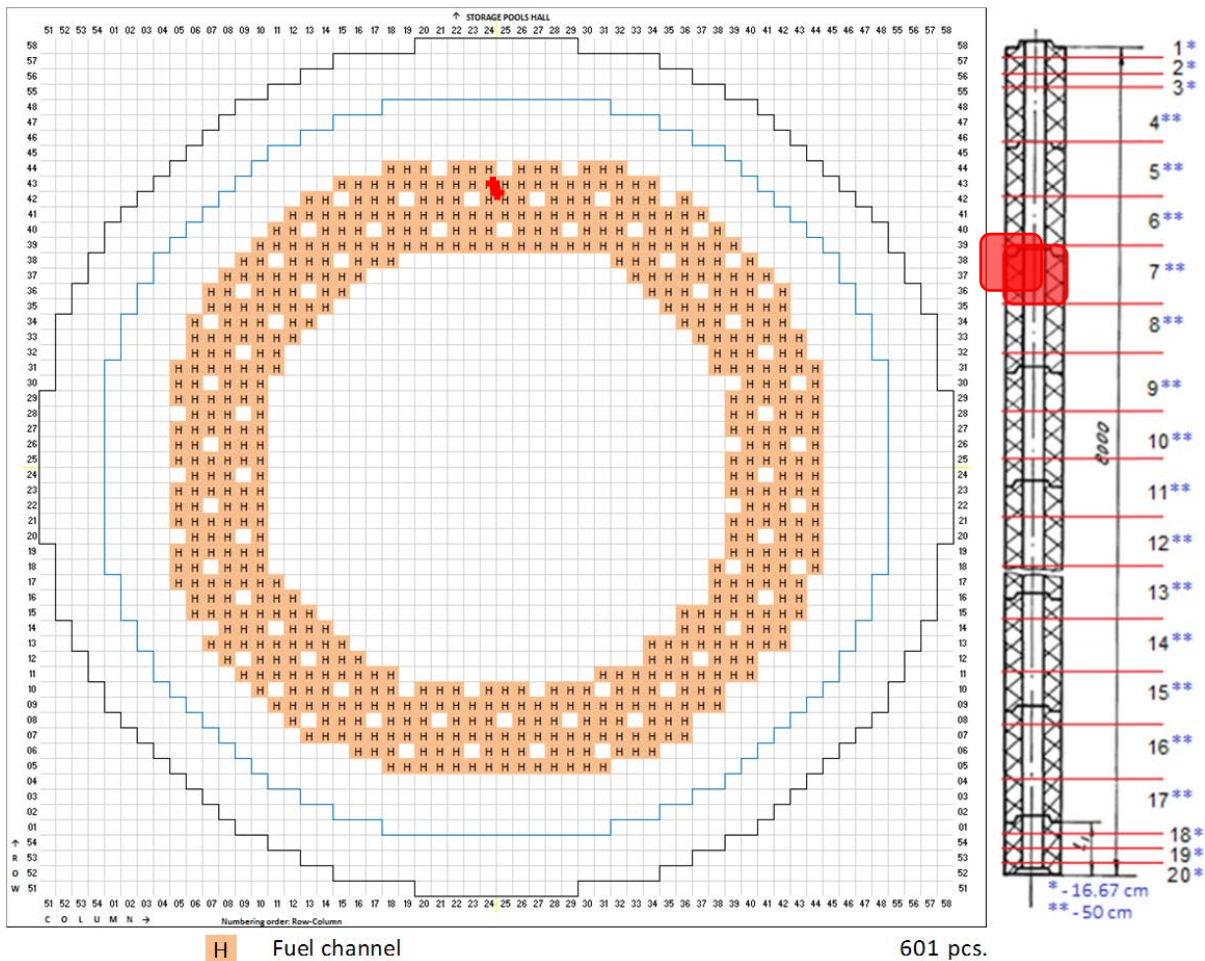
Figure 2.2.7: Position of graphite sample taken from the area of graphite columns in RBMK-1500 reactor first peripheral part at Ignalina NPP Unit 1

Consequently, the exhaustive combination of the modelled and measured C-14 activities for the more detailed and more confident estimation of C-14 inventory in the whole RBMK-1500 reactor graphite stack has not been achieved to date, as the only C-14 activity measurement data that could be used for the inventory estimation was that from a paper [Mazeika et al., 2013]. This paper presented preliminary studies of the experimental C-14 activity estimation in several graphite sub-samples, attributed to the same sample of the GR-280 grade graphite bushing from the temperature channel of the Ignalina NPP Unit 1 RBMK-1500 reactor. Based on the statistical analysis of the sub-samples activity, the average value of the C-14 specific activity in this graphite sample was 1.67×10^5 Bq/g [Mazeika et al., 2013]. According to the information on the location of the analysed sample [Mazeika et al., 2013], the sample was taken from the area of graphite columns with fuel channels in the RBMK-1500 reactor first peripheral part (see Figure 2.2.7) and the measured specific activity of 1.67×10^5 Bq/g corresponds to the point at +175 cm elevation of the modelled specific activity distribution in the first peripheral part of the reactor, as marked in Figure 2.2.8. This gives that the modelled specific activity of C-14 (at +175 cm elevation in the first peripheral part of the reactor) is 0.258 relative units (see Figure 2.2.8) and corresponds to the measured specific activity of 1.67×10^5 Bq/g in that location.
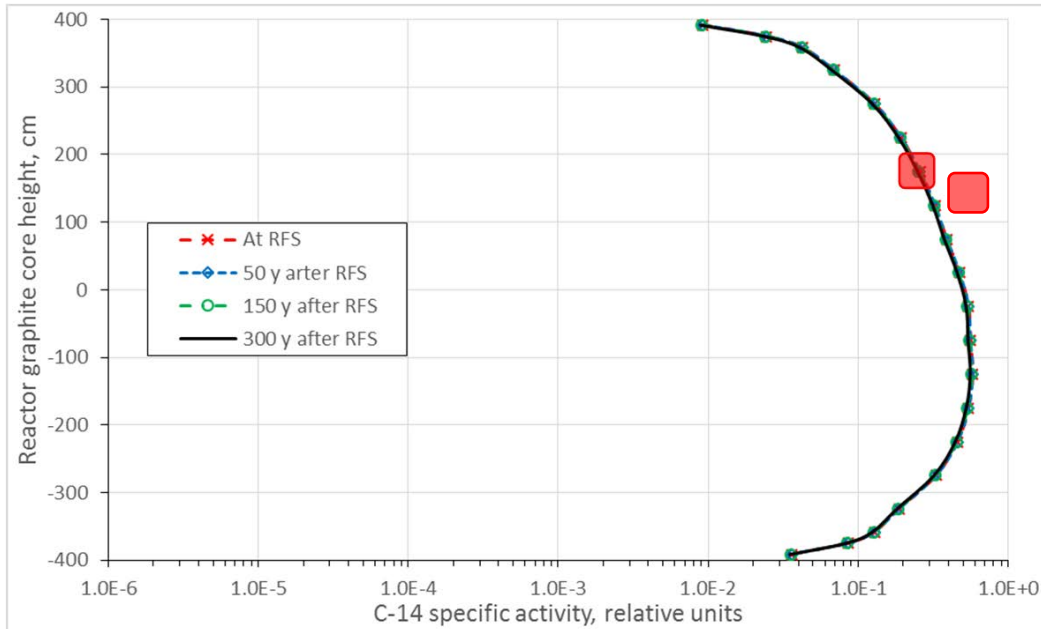
Figure 2.2.8: Indication of measured C-14 specific activity in the distribution of modelled C-14 specific activities

By having the modelled distributions of the specific C-14 activity in each group of the graphite columns in relative units (presented in deliverable D5.17 [Narkunas & Poskas, 2017]), by knowing the correspondence of the measured specific C-14 activity to the exact point (location) of the modelled specific activity distribution (see Figure 2.2.8), and by applying quantities and masses of the graphite columns in the respective group, the integral C-14 activity in the graphite stack was calculated.

As a final emphasis of this estimation it could be stated that, combining C-14 activity modelling and measurement results, the following numbers regarding C-14 inventory in the irradiated graphite stack of the Ignalina NPP Unit 1 RBMK-1500 reactor at the time of RFS were obtained:

- Total C-14 activity in the graphite stack: 3.222×10^{14} Bq;
- Total mass of the graphite stack: 1.700×10^{9} g (1700 t);
- Average C-14 activity in the graphite stack: 1.895×10^{5} Bq/g.

CAST
Final report on results from Work Package 5:
Carbon-14 in irradiated graphite (D5.19)

However, it should be also noted that the above numbers are only for the reactor RBMK-1500 graphite stack consisting of GR-280 grade graphite blocks. The remaining graphite components in the reactor (graphite rings, sleeves, rods and other graphite parts in minor quantities) are not taken into account. For these parts, as a first attempt, the same average specific activity could be applied, which together with the mass of ~200 t results in 3.790×10^{13} Bq of C-14. Finally, this sums to 3.601×10^{14} Bq of C-14 in ~1900 t of the irradiated graphite of all types in one RBMK-1500 reactor.

Additional caution should be paid to the above presented estimation of the total and the average specific activity of C-14 in Ignalina NPP Unit 1 reactor RBMK-1500 graphite, as the estimation performed relies only on the preliminary measurements of only one graphite sample. It could not be totally excluded that the measurements of the sample are somehow misleading, or the sample is not representative, etc. Anyhow, these are the only officially-published experimental measurement results of C-14 activity in the GR-280 grade graphite of Ignalina NPP Unit 1 reactor to date, and they were used in the presented study.

	CAST	
	Final report on results from Work Package 5:	
	Carbon-14 in irradiated graphite (D5.19)	

References

1 TOULHOAT, N., NARKUNAS, E., ZLOBENKO, B., DIACONU, D., PETIT, L., SCHUMACHER, S., CATHERIN, S., CAPONE, M., VON LENSA, W., PINA, G., WILLIAMS, S., FACHINGER, J., NORRIS, S. Report D5.5. 2015. WP5 Review of Current Understanding of Inventory and Release of C-14 from Irradiated Graphite. CAST Project.

2 MAZEIKA, J., LUJANIENE, G., PETROSIUS, R., ORYSAKA, N., OVCINIKOV, S. 2015. Preliminary Evaluation of ^{14}C and ^{36}Cl in Nuclear Waste from Ignalina Nuclear Power Plant Decommissioning. *Open Chemistry*, Vol. 13(1), 177–186.

3 NARKUNAS, E., POSKAS, P. Report D5.17. 2017. Report on Modelling of C-14 Inventory in RBMK Reactor Core. CAST Project.

4 http://www.atomic-energy.ru

5 Technical description of RBMK-1500 reactor. Ignalina Nuclear Power Plant, 1985 (In Russian).

6 NARKUNAS, E., SMAIZYS, A., POSKAS, P., DRUTEIKIENE, R., DUSKESAS, G., GARBARAS, A., GUDELIS, A., GVOZDAITE, R., LUJANIENE, G., PLUKIENE, R., PLUKIS, A., PUZAS, A. Technical Report T-3.4.2. 2013. Assessment of Isotope-Accumulation Data from RBMK-1500 Reactor. CARBOWASTE Project.

7 NARKUNAS, E., POSKAS, P., BLACK, G., JONES, A., IORGULIS, C., DIACONU, D., PETIT, L., PONCET, B. Technical Report T-3.4.3. 2013. Modelling of Isotope Release Mechanism Based on Fission Product Transport Codes. CARBOWASTE Project.

8 MCNP – A General Monte Carlo N-Particle Transport Code, Version 5, (Vol. I-III.) Reports LA-UR-03-1987, LA-CP-03-0245, LA-CP-03-0284. Los Alamos National Laboratory. Los Alamos, New Mexico, 2003.

9 SCALE: A Comprehensive Modeling and Simulation Suite for Nuclear Safety Analysis and Design. ORNL/TM-2005/39, Version 6.1, Oak Ridge National Laboratory, Oak ridge, Tennessee, 2011.

	CAST
	Final report on results from Work Package 5:
	Carbon-14 in irradiated graphite (D5.19)

2.3   Regia Autonoma pentru Activitati Nucleare – Institute for Nuclear Research (RATEN ICN)

Introduction

The thermal column of the TRIGA Reactor is a graphite block (1716x1144x710 mm) made up of 98 rectangular graphite cells (12 rows x 8 bricks) in Aluminium cladding and it is placed into the reactor pool on the North side of the steady-state core. It was built up in 1985, using sintered graphite blocks with a density of 1.72 g/cm^3 and various geometries. The graphite was imported in the '50s from a UK producer but documents of its origin were lost. No information on its characteristics and on the impurity content could be found.

First experiments to measure the radionuclide inventory in TRIGA i-graphite were carried out under CARBOWASTE project. The measured data were complemented with data obtained by modeling, based on impurity content of the virgin graphite and the irradiation history [Toulhoat *et al.*, 2016].

In CAST WP5, RATEN ICN proposed to update the ^{14}C inventory in the irradiated graphite from thermal column of the TRIGA 14MW reactor and to evaluate the ^{14}C release in alkaline conditions (relevant to disposal in cementitious environment), both in terms of total ^{14}C as well as inorganic and organic fractions.

Materials and Methods
Irradiated graphite used in the leaching tests

Two cylindrical bars (Figure 2.3.1) originating from a brick extracted and dismantled in 2000 from the thermal column of TRIGA reactor were available for the experimental programme carried out in RATEN ICN under CAST WP5: one cylinder with a diameter of 50 mm and length of 200 mm (noted B1), and the second one with diameter of 60 mm (noted B2) and length of 250 mm. From the extraction from the column thermal until their usage in the experimental programme, the irradiated graphite bars were stored in the air. No information regarding their position in the thermal column was found.

	CAST		
	Final report on results from Work Package 5:		
	Carbon-14 in irradiated graphite (D5.19)		

By mechanical cutting, four cylindrical samples were obtained: two with 50 mm diameter and 50 mm height (from B1 bar) and two with 60 mm diameter and 50 mm height (from B2 bar).

Figure 2.3.1. The irradiated graphite cylindrical bars used to cut intact samples for leaching experiments and powder samples to measure the radionuclide content

The two intact specimens obtained from B 1 bar (Figure 2.3.2) were used for the leaching tests carried out in aerobic conditions, while those obtained from B2 bar were used in the leaching tests performed in anaerobic conditions [Toulhoat *et al.*, 2016].
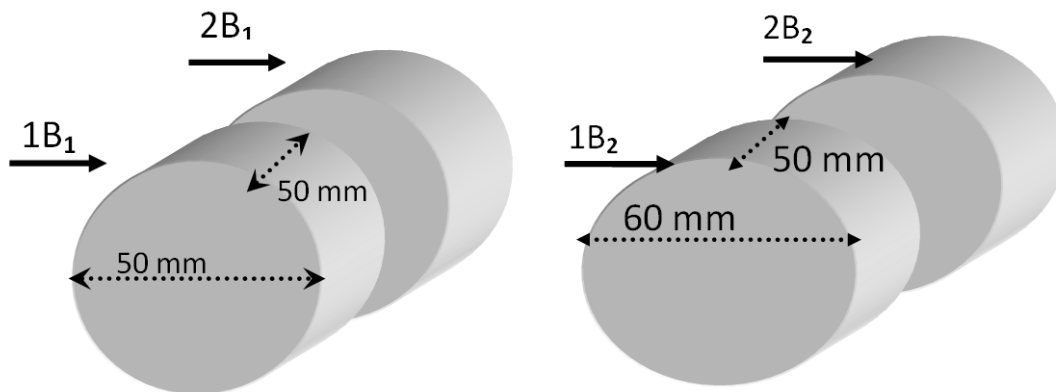
Figure 2.3.2. Intact specimens obtained from B 1 and B2 bars

The physical characteristics of the four irradiated graphite samples used in the leaching tests are reported in Table 2.3.1.

The powder graphite resulted during cutting was sampled both from the ends of the cylindrical bars and from their middle and the resuling powder samples were used to measure the radionuclide content (^{14}C and gamma emitters). Four powder samples were taken from the B1 bar (two from the end of the bar and two from the middle).

Table 2.3.1. Characteristics of the irradiated graphite samples used for leaching tests

Sample ID	Type of leaching test	Mass, g	Geometric volume, cm^3	Volumetric density, g/cm^2	Surface area, cm^2
1B1	aerobic	172.72	98.13	1.76	117.75
2B1		168.24	98.12	1.72	117.75
1B2	anaerobic	250.10	141.30	1.77	150.72
2B2		249.70	141.30	1.76	150.72

To get more information on the ^{14}C distribution inside the irradiated graphite bar, powder samples were taken from different position from the B2 bar, by cutting one cylinder of 60x50 mm in half and then in quarters (Figure 2.3.3).
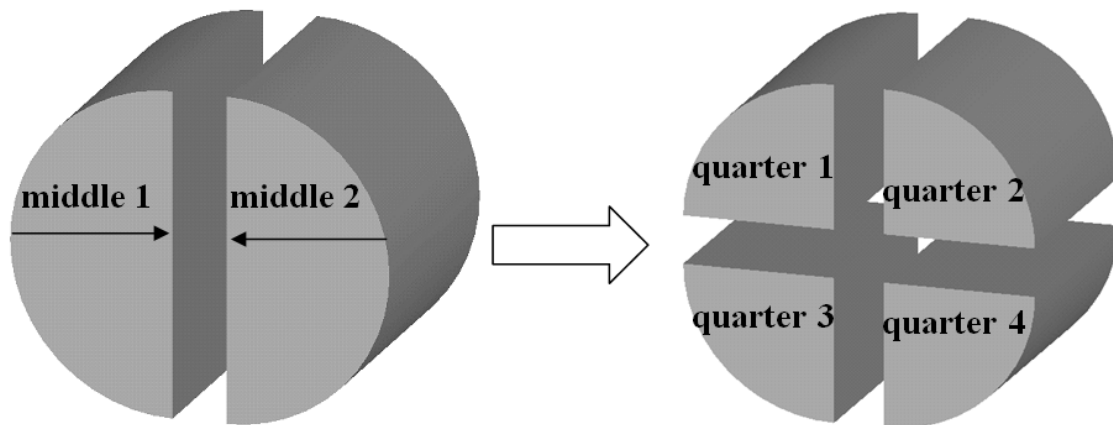
Figure 2.3.3. Cutting of one cylindrical piece of B2 bar for powder sampling

By this supplementary cutting of one cylindrical piece obtained from B2 bar, 12 powder samples were taken: 3 samples from the first half, 3 from the second half, 3 samples taken during first half cutting in quarters and 3 more samples taken during the second half cutting in quarters.

CAST
Final report on results from Work Package 5:
Carbon-14 in irradiated graphite (D5.19)

Experimental conditions for leaching tests

To evaluate the ^{14}C release from TRIGA irradiated graphite in chemical conditions relevant to geological disposal (cementitious environment) leaching tests in aerobic and anaerobic conditions were performed.

The leaching tests were carried out in 0.1 M NaOH solution (pH ~ 13) and room temperature (25±3°C), in Pyrex glass vessels.

All leaching tests were performed in semi-dynamic conditions, with a precise time scale for leachate sampling/replacement, until equilibrium was reached. The ratio of leachate volume to exposed surface area of the cylindrical samples was held constant (it does not exceed 0.1 m) by replacing the volume of leachate sampled at each sampling time with the same volume of fresh 0.1 M NaOH solution.

The volume of leachate solution was 1118 cm^3 in the aerobic leaching tests and 1500 cm^3 in the anaerobic ones.

The anaerobic leaching tests were carried out in N_2 atmosphere, in closed Pyrex glass vessels placed on a magnetic stirrer. The lids of the glass bottles were adapted to allow N_2 purging (Figure 2.3.4) before starting the leaching tests (to ensure the anaerobic conditions) and sampling the leachate solution without opening the vessels.

Figure 2.3.4. Photo of the leaching set-up for anaerobic conditions

According to D5.4 [Petrova et al., 2015], the leachate solution was sampled and renewed after 1, 3, 7, 10, 14 days, twice on week II, once on weeks III to VI and after that monthly until the equilibrium is reached.

Methods used for total ^{14}C measurement

For total ^{14}C measurement both in irradiated graphite and in leachate solutions sampled from the leaching tests, non-catalytic combustion by flame oxidation method was used.

For inorganic and organic ^{14}C measurement the analytical method adapted after the one developed by Magnusson [Magnusson et al., 2008] for ^{14}C measurement in spent ion exchange resins and process waters was used. This method distinguishes between $^{14}CO_2$ released during acid stripping and $^{14}CO_2$ released by wet oxidation of hydrocarbons allowing determination of the inorganic and organic fractions of ^{14}C in irradiated graphite and leachate solutions.

Method for total ^{14}C measurement

For total ^{14}C measurement in irradiated graphite, non-catalytic combustion by flame oxidation method was used. By his method, the graphite samples are combusted in an oxygen-enriched atmosphere with a continuous flow of oxygen using Sample Oxidizer, Model 307 PerkinElmer® (Figure 2.3.5). During the combustion process any hydrogen is oxidized to H_2O and any carbon is oxidized to CO_2.

Figure 2.3.5. The experimental device used for total ^{14}C measurements in liquid samples

The Sample Oxidizer consists of the following major functional areas: combustion system, tritium collection system, ^{14}C and ^{3}H collection systems, water injection system, nitrogen system and programmer.

Since the carbon dioxide readily reacts with compounds containing amines, the Carbo-Sorb® E was chosen to absorb the ^{14}CO$_2$ released during combustion process. The absorption reaction of carbon dioxide can be described as follows [Ahn at al., 2013]:

$$^{14}CO_2 + RNH_2 \rightarrow RNH_2^{+14}COO^-$$

(eq. 1)

$$RNH_2^{+14}COO^- + \begin{bmatrix} RNH_2 \rightarrow RNH^{14}COO^- + RNH_3^+ \\ H_2O \rightarrow RNH^{14}COO^- + H_3O^+ \\ OH^- \rightarrow RNH^{14}COO^- + H_2O \end{bmatrix}$$

(eq. 2)

$$RNH^{14}COO^- + H_2O \rightarrow RNH_2 + H^{14}CO_3^-$$

(eq. 3)
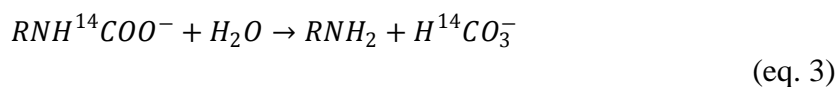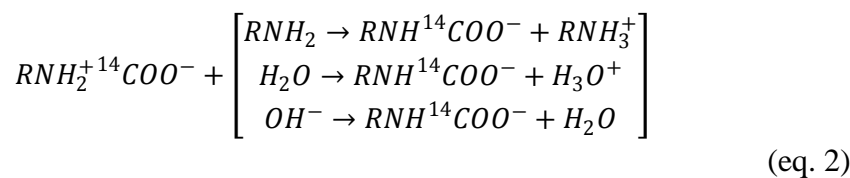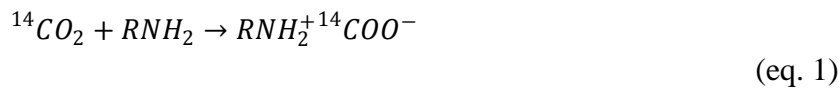
As shown in eq. 2, the amine contained by the Carbo-sorb E solution reacts with ^{14}C-labelled carbon dioxide to form a zwitterion[2], which reacts with H_2O to form a stable carbonate compound (eq. 3). This resulted carbonate compound is mixed with the LSC cocktail (Perma-fluor® E+) directly in the counting vial.

The ^3H_2O resulted in the combustion process is condensed in a cooled coil, washed into a counting vial where it is mixed with LSC cocktail (Monophase®S).

At the end of combustion process, two separate samples, one for ^{14}C measurement and one for ^3H measurement, are trapped at ambient temperature minimizing the cross-contamination.

The ^{14}C and ^3H radioactivity in the samples resulted from SIERs combustion was measured by liquid scintillation counting (LSC) using a Tri-Carb® analyser Model 3110 TR. This analyser allows for ultra-low level counting mode with typical count rate in the range of 1-20 CPM (counts per minute) above background.

Analytical method for inorganic and organic ^{14}C measurement

The analytical method used for inorganic and organic ^{14}C measurement in SIERs samples consists in a sequential extraction of inorganic ^{14}C and organic ^{14}C using acid stripping and wet oxidation, adapted after the method developed by Magnusson [Magnusson et al., 2008] for ^{14}C measurement in spent ion exchange resins and process waters.

The experimental set-up used to separate the inorganic and organic ^{14}C from the leachate solutions is schematically presented in Figure 2.3.6. It consists in a reaction vessel, a separatory funnel, a nitrogen supply and a vacuum pump, two gas washing lines with a catalytic furnace between them.

---

[2]   In chemistry, a zwitterion, formerly called a dipolar ion, is a molecule with two or more functional groups, of which at least one has a positive and one has a negative electrical charge and the net charge of the entire molecule is zero

An Erlenmayer flask (300 ml) with a three-hole rubber stopper (two for gas and separatory funnel inlets and one for gas outlet) was used as reaction vessel and a tap-water cooling loop, made of copper tubing that fit the outer side of the Erlenmeyer flask (Figure 2.3.6) ensured the vapour condensation. The reaction vessel was placed on a heater with magnetic stirring.

To ensure that no gases are released from the system all tests were carried out under vacuum (0.2 bar below atmospheric pressure) and the carrier gas (N_2) was introduced into the system with a flow rate around 50 ml/min (controlled by a flow meter).
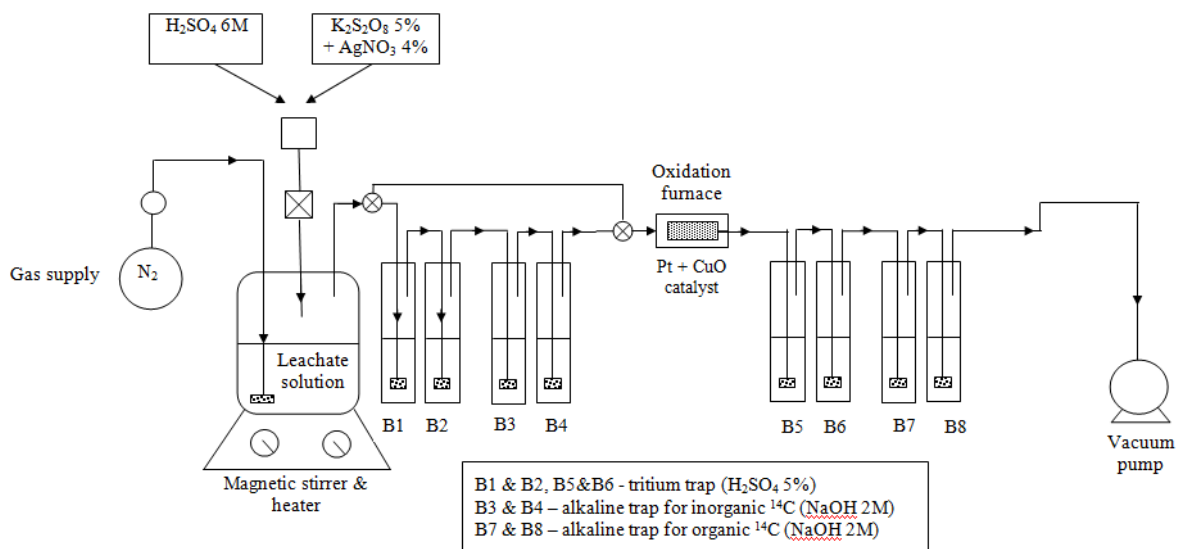
Figure 2.3.6. The experimental set-up for separation and purification of inorganic and organic ^{14}C from the solutions sampled from leaching tests

Since the irradiated graphite contains beside ^{14}C also tritium and other beta emitters that could be released during the leaching tests and interfere with ^{14}C measurement by LSC the gas washing lines contain slightly acidic traps with sulphuric acid (5% H_2SO_4) for absorption of the tritium and other potential interfering radionuclides (placed both before the catalytic furnace and after it) and four alkaline traps (two placed before the catalytic furnace and two after it) with 2M sodium hydroxide (NaOH).

Since the inorganic ^{14}C compounds (i.e. carbonates and bicarbonates) are easily decomposed by weak acids to carbon dioxide, the inorganic ^{14}C is released during acid

	CAST	
	Final report on results from Work Package 5:	
	Carbon-14 in irradiated graphite (D5.19)	

stripping step of the analytical method mainly as $^{14}CO_2$ and the gases released are carried by the carrier gas through the first gas washing line (Figure 2.3.6). If any ^{14}C is released during this step as CO or other organic molecules, it passes through the scrubbing bottles of the first gas washing line and is oxidized to CO_2 in the catalytic furnace and subsequently absorbed in the alkaline scrubbing bottles of the second gas washing line. After the acid stripping step is accomplished the first gas washing line is isolated from the system by means of three ways valves placed before the first scrubbing bottle and the forth one.

Because the organic compounds have high bounding energies between atoms they are decomposed by strong oxidants such as potassium persulphate ($K_2S_2O_8$). Presence of a catalyser such as silver nitrate ($AgNO_3$) enhances the decomposition of the organic compounds. During the wet oxidation step the temperature of the solution in the reaction vessel is slightly increased to 90°C.

The mechanism of ^{14}C-labelled organic compounds decomposition is based on the $OH^{(*)}$ radicals and can be expressed by the following equations [Ahn et al., 2013]:

$$K_2S_2O_8 \xrightarrow{H_2O} 2K^+ + S_2O_8^{2-}$$

(eq. 4)

$$S_2O_8^{2-} + 4H_2O \xrightarrow{Ag} 2SO_4^{2-} + 2H^+ + 2OH^*$$

(eq. 5)

$$^{14}C_nH_m + (4n + m)OH^* \rightarrow n^{14}CO_2 + (2n + m)H_2O$$

(eq. 6)
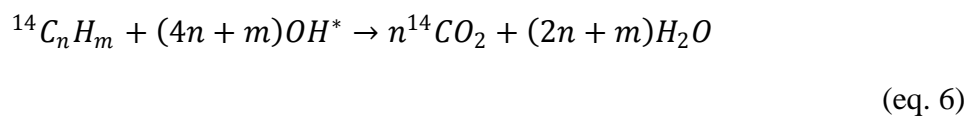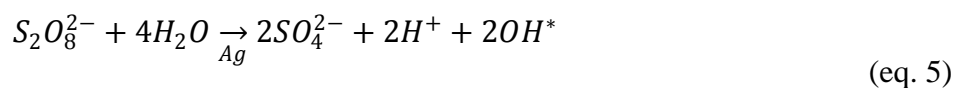
The ^{14}C released during wet oxidation step of the analytical procedure (both as CO_2, but also as CO or CH_4) is carried by the carrier gas through a catalytic furnace that ensures oxidation of any reduced compounds to CO_2 that is after that absorbed in the scrubbing bottles of the second gas washing line (Figure 2.3.6).

Two wet oxidation steps were carried out in order to ensure the complete decomposition of the organic ^{14}C-labelled compounds, and the carrier gas was purged into the system for one hour in each wet oxidation steps.

In order not to dilute too much the amount of $^{14}CO_2$ absorbed in the alkaline gas washing bottles, in the experimental set-up presented in Figure 2.3.6, scrubbers of small volume were used (15 ml).

The ^{14}C activity in the alkaline traps as well as and ^{3}H activity in solutions sampled from the acid scrubbing bottles were measured by liquid scintillation counting (LSC), using a Tri-Carb® analyser Model 3110 TR.

Hionic-Fluor liquid scintillation cocktail was used for ^{14}C measurement by LCS, and Ultima Gold AB liquid scintillation cocktail for tritium measurement. The ratio between sample and scintillation cocktail was 1 to 10. All samples were kept in darkness over night before counting.

Aliquots from the reaction vessel solution, as well as from all scrubbing bottles were sampled for gamma measurements. The system used for the gamma spectrometry comprises of the following components: HPGe ORTEC detector, digiDart analyser and GammaVision software. The spectrometer was calibrated in energy and efficiency using a standard liquid source containing ^{60}Co, ^{137}Cs, ^{241}Am, ^{152}Eu in 20 ml glass vials. The same geometry was used for gamma measurements on the sampled aliquots solutions from the acid stripping/wet oxidation experiments. The counting time was higher than 8 hours for each sample.

Results and discussion

Total ^{14}C content in the irradiated graphite samples used in leaching tests

Preliminary combustion tests were carried out using graphite samples spiked with the interest radionuclides (^{14}C – as Spec-Chec solution with known ^{14}C activity, ^{3}H, ^{60}Co, ^{137}Cs, ^{241}Am and ^{152}Eu) in order to optimize the combustion process and determine the recovery and memory effect of the combustion method.

The optimised experimental conditions for complete graphite oxidation were the following:

✓ 0.14 – 0.16 g of graphite powder

✓ 10 ml CarbosorbE (liquid scintillation cocktail for ^{14}C)

✓ 10 ml PermafluorE+ (liquid scintillation cocktail for ^{3}H)

The labelled graphite sample was placed into a combusto-cone that was further placed into platinum ignition basket. The average combustion recovery by this method was 97%. Virgin graphite samples were also combusted for background measurements.

The memory effect was less than 0.04% and no gamma emitters were identified either in the counting vial for ^{14}C measurement or in the ^{3}H one.

The experimental results obtained for ^{14}C content in the powder samples originating from the B1 graphite bar used for aerobic leaching tests are reported in Table 2.3.2, while those obtained for the powder samples taken from B2 bar are reported in Table 2.3.3.

Table 2.3.2. ^{14}C content in the powder graphite sampled from B1 bar

Sample ID	Graphite mass used in combustion tests, g	^{14}C specific activity, Bq/sample	^{14}C specific activity, Bq/g	Observations
virgin graphite_1	0.16	5.17E-01	3.23E+00	^{14}C background
end B1_1	0.13	6.18E+01	4.75E+02	Sampled from the end of B1 bar
end B1_2	0.14	6.18E+01	4.42E+02	
middle B1_1	0.14	6.16E+01	4.40E+02	Sampled from the middle of B1 bar
middle B1_2	0.16	7.14E+01	4.46E+02	
Average B1			**450.75±16.36**	

As it can be seen from data reported in Table 2.3.2, no notable difference in ^{14}C content in powder samples taken from the end and middle of B1 bar was observed.

For the total ^{14}C content in the irradiated graphite samples used for leaching tests carried out in aerobic conditions a value of 450.74 Bq/g was considered (the average of the 4 measurements presented in Table 2.3.2).

CAST
Final report on results from Work Package 5:
Carbon-14 in irradiated graphite (D5.19)

Table 2.3.3. ^{14}C content in the powder graphite sampled from B2 bar of irradiated graphite

Sample ID	Graphite mass used in combustion tests, g	^{14}C specific activity, Bq/sample	^{14}C specific activity, Bq/g	Observations
H1_1	0.14	1.38E+01	9.88E+01	
H1_2	0.16	1.37E+01	8.55E+01	Sampled from the first half
H1_3	0.14	1.73E+01	1.24E+02	
Average H1			102.77±19.55	
H2_1	0.13	1.67E+01	1.29E+02	
H2_2	0.16	1.24E+01	7.72E+01	Sampled from the second half
H2_3	0.15	1.03E+01	6.90E+01	
Average H2			91.73±32.53	
Q1_1	0.16	1.50E+01	9.36E+01	
Q1_2	0.12	1.45E+01	1.21E+02	Sampled from the first half cutting in quarters
Q1_3	0.12	1.39E+01	1.16E+02	
Average Q1			110.20±14.59	
Q2_1	0.14	1.31E+01	9.39E+01	
Q2_2	0.16	1.01E+01	6.28E+01	Sampled from the second half cutting in quarters
Q2_3	0.15	1.24E+01	8.25E+01	
Average Q2			79.73±15.73	
Average B2			**96.11±21.20**	

For the total ^{14}C content in the irradiated graphite samples used for leaching tests carried out in anaerobic conditions a value of 96.11 Bq/g was considered (the average of the 12 measurements presented in Table 2.3.3).

Recovery and memory effect of the acid stripping/wet oxidation method

Preliminary acid stripping/wet oxidation tests were carried out using aqueous solutions spiked with the radionuclides of interest: inorganic ^{14}C (in form of sodium carbonate / bicarbonate), organic ^{14}C (sodium acetate and lauric acid), ^{3}H, and gamma emitters (^{60}Co, ^{137}Cs, ^{241}Am and ^{152}Eu).

The ^{14}C recovery was between 94.79% and 98.32% [RIZZO *et al.*, 2017]. The average recovery was 96.97 % with a standard deviation of 1.46 %. No gamma emitters were

identified in any of the scrubbing bottles and entire activity of ^{60}Co, ^{137}Cs, ^{241}Am and ^{152}Eu were found in the solutions sampled from the reaction vessel (with average recovery higher than 96%). The solutions sampled from the alkaline gas washing bottles were also counted for tritium (using double labelled mode implemented on LCS counter), but no tritium was detected above the background in these samples. All tritium added in the reaction vessel was found in the acid scrubbing bottles.

An average memory effect of less than 1% was observed.

To account for the uncertainty associated to this analytical method, 6 identical tests were carried out using solutions spiked both with inorganic and organic ^{14}C, as well as with tritium and gamma emitters. The standard deviation of the results of these tests was less than 15%.

^{14}C release in alkaline solution

The leaching behaviour is represented by the ^{14}C cumulative release fraction (F_n) in time and also by leaching rate (R_n), computed using equations (eq. 7) and (eq. 8):

$$F_n = \frac{\sum a_n}{a_o} \qquad \text{(eq. 7)}$$

$$R_n = \frac{a_n \cdot V}{a_0 \cdot S \cdot t_n} = K \cdot \frac{a_n}{t_n} \qquad \text{(eq. 8)}$$

where: F_n is the cumulative release fraction at the moment n of the leaching test; R_n represents the release rate (cm/day) at the moment n of the test; a_0 is the initial ^{14}C content of the graphite sample (Bq); a_n represents the amount of ^{14}C released at the moment n of the test (Bq) in the leachate solution; t_n represent the time in the moment n of the test (days); V is the sample volume (cm^3); S is the geometric surface of the sample (cm^2); is a test constant (cm/Bq).

CAST
Final report on results from Work Package 5:
Carbon-14 in irradiated graphite (D5.19)

^{14}C release in alkaline solution under aerobic conditions

As presented in previous chapter, the leaching tests carried out in aerobic conditions were performed in 0.1 M NaOH solution, in semi-dynamic conditions. At the established leaching times, 30 ml of leachate were sampled and 30 ml of fresh NaOH solution were added in the leaching vessels. Two parallel tests were performed with the main parameters reported in Table 2.3.4.

Table 2.3.4. Tests parameters for aerobic leaching

Sample ID	Sample mass, g	Leachate volume, ml	Total ^{14}C content, Bq
1_B1	172.72	1118	7.79E+04
2_B1	168.24	1118	7.58E+04

The volume of NaOH solution was chosen to respect the ratio between the leachate volume to the sample surface not higher than 0.1 m.

To avoid kinetic effects at the graphite – leachate solution interface (e.g., heterogeneous distribution of ^{14}C in the solution), the leachate solution was stirred before sampling. At each sampling time, the leachate solutions were measured by gamma spectrometry and if no beta-gamma emitters were identified in solution sub-samples for LSC measurement were prepared. Both tritium and radiocarbon were measured by LSC using double-labelled method implemented on TRICARB 3100 TR.

20 ml from the leachate solution was used to evaluate the inorganic and organic ^{14}C content by means of acid stripping/wet oxidation method. This method also allows a good ^{14}C decontamination by other potential interfering radionuclides and the total ^{14}C measured directly by LSC was comparable with the sum of inorganic and organic ^{14}C measured by acid stripping/wet oxidation method.

The values of ^{14}C measured in leachate solution at each sampling times were used to compute the ^{14}C cumulative release fraction (F_n) and leaching rate (R_n). The measured ^{14}C activity in leachate solution were corrected for the dilution factor due to the leachate sampling/renewal and reported to the initial ^{14}C activity in the i-graphite subject to the

leaching test to get the cumulative release fraction. The results, both for the cumulative release fraction and for the leaching rate, are reported in Table 2.3.5.

The results obtained by the two parallel are very similar (see Figure 2.3.7) confirming the reproducibility of the leaching tests.
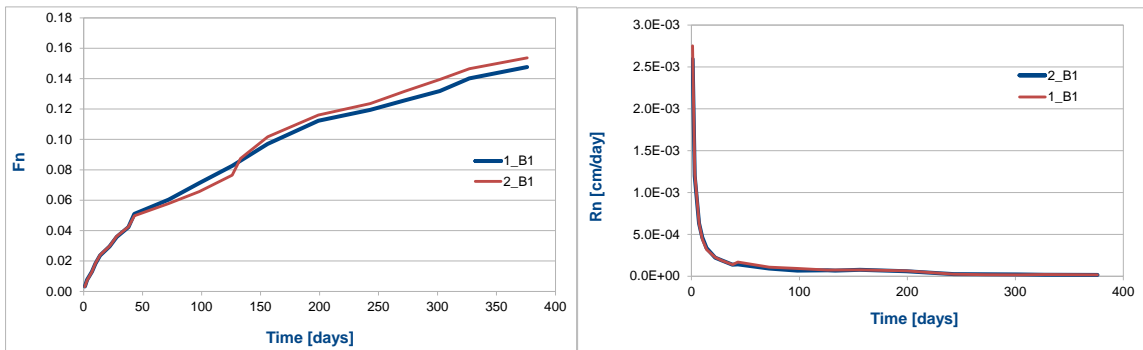
Figure 2.3.7. Evolution of the leaching rate (right) and ^{14}**C cumulative release fraction (left)**

Table 2.3.5. ^{14}C cumulative release fraction (F_n) and leaching rate (R_n) for the aerobic leaching tests

	Sample 1_B1		Sample 2_B1	
Time, days	Rn [cm/day]	Fn [%]	Rn [cm/day]	Fn [%]
1	2.75E-03	3.30E-03	2.59E-03	3.11E-03
3	1.22E-03	7.69E-03	1.20E-03	7.42E-03
7	6.29E-04	1.30E-02	6.32E-04	1.27E-02
10	4.42E-04	1.83E-02	4.66E-04	1.83E-02
14	3.17E-04	2.36E-02	3.36E-04	2.40E-02
22	2.24E-04	2.95E-02	2.22E-04	2.98E-02
28	1.89E-04	3.59E-02	1.90E-04	3.62E-02
38	1.39E-04	4.22E-02	1.38E-04	4.25E-02
43	1.14E-04	5.10E-02	1.42E-04	4.98E-02
72	1.07E-04	6.03E-02	9.25E-05	5.78E-02
98	9.36E-05	7.13E-02	6.70E-05	6.57E-02
126	7.47E-05	8.26E-02	7.16E-05	7.65E-02
156	7.68E-05	9.70E-02	6.83E-05	8.74E-02
199	6.40E-05	1.12E-01	7.62E-05	1.02E-01
243	2.47E-05	1.19E-01	5.99E-05	1.16E-01
272	1.90E-05	1.26E-01	2.59E-05	1.24E-01
302	1.71E-05	1.32E-01	2.45E-05	1.32E-01
327	2.13E-05	1.40E-01	2.17E-05	1.39E-01
376	1.65E-05	1.48E-01	1.82E-05	1.47E-01

The results of the aerobic leaching tests confirm the very low release rate of the ^{14}C. After 376 days of immersing in alkaline solution, around 1.33E3 Bq of ^{14}C was released as dissolved species, representing 1.75% from the initial ^{14}C activity of the i-graphite subject to the leaching test.

The leaching rate is higher in the first days of immersing and it decrease after that, indicating a two-stage process: an initial quick release with an average release rate of

CAST
Final report on results from Work Package 5:
Carbon-14 in irradiated graphite (D5.19)

5.48E-02 % of inventory/day[*] during the first 48 days, followed by a slower release of around 4.62E-3 % of inventory/day. These two stages of ^{14}C release could be associated with the initial release of the more labile species arising from the ^{14}N impurities or from the ^{13}C from different depositions, while the second stage is most probably linked to ^{14}C created in the matrix [Carlsson et al., 2014].

The acid stripping/wet oxidation tests carried out on the leachate solutions show that in all solutions more inorganic than organic ^{14}C was released. The ratio between inorganic and organic ^{14}C release during the leaching test is almost constant during the test. The inorganic fraction of ^{14}C measured on leachant solution sampled at different leaching intervals is ranging between 66% and 70% from the total ^{14}C released as dissolved species, with an average of 67.89% and a standard deviation of 1.84%. The organic ^{14}C on leachant solution sampled at different leaching intervals is ranging between 30% and 34% from the total ^{14}C released as dissolved species, with an average of 32.11%.

^{14}C release in alkaline solution under anaerobic conditions

The experimental conditions for anaerobic leaching tests were similar with those described at aerobic leaching tests, except for the volume of the leachate solution that was increased at 1500 cm^3 due to the larger diameter of the irradiated graphite available for these anaerobic leaching tests (Table 2.3.6).

Table 2.3.6. Tests parameters for anaerobic leaching

Sample ID	Sample mass, g	Leachate volume, ml	Total ^{14}C content, Bq
1_B2	250.10	1500	2.404E+04
2_B2	249.7	1500	2.400E+04

The volume of leachate solution sampled/renewed at each testing time was 50 ml. The values of ^{14}C measured in the sampled solutions at each sampling times were used to
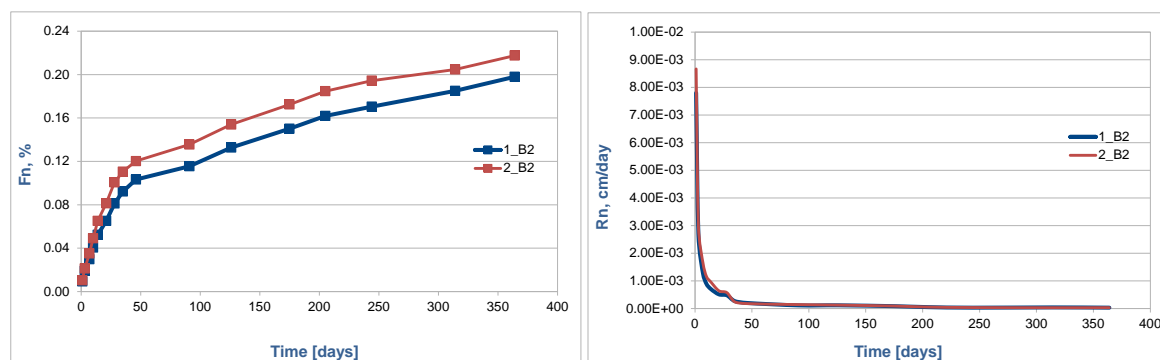
---

[*] % of inventory/day represent the ^{14}C activity release in each time interval divided by the initial inventory in irradiated graphite, divided by the leaching time and multiplied by 100.

	CAST	
	Final report on results from Work Package 5:	EURATOM
	Carbon-14 in irradiated graphite (D5.19)	

compute the ^{14}C cumulative release fraction (F_n) and leaching rate (R_n). The results are reported in Table 2.3.7.

Table 2.3.7. ^{14}C cumulative release fraction (F_n) and leaching rate (R_n) for the anaerobic leaching tests

	Sample 1_B1		Sample 2_B1	
Time, days	**Rn [cm/day]**	**Fn**	**Rn [cm/day]**	**Fn**
1	7.80E-03	9.36E-03	8.67E-03	1.04E-02
3	2.69E-03	1.90E-02	2.98E-03	2.12E-02
7	1.28E-03	2.97E-02	1.65E-03	3.51E-02
10	8.95E-04	4.05E-02	1.16E-03	4.91E-02
14	7.02E-04	5.23E-02	9.55E-04	6.51E-02
21	5.10E-04	6.51E-02	6.40E-04	8.13E-02
28	4.77E-04	8.11E-02	5.73E-04	1.01E-01
35	2.65E-04	9.23E-02	2.38E-04	1.11E-01
46	1.99E-04	1.03E-01	1.75E-04	1.20E-01
91	1.12E-04	1.15E-01	1.40E-04	1.36E-01
126	1.14E-04	1.33E-01	1.22E-04	1.54E-01
175	8.29E-05	1.50E-01	8.80E-05	1.72E-01
205	4.79E-05	1.62E-01	5.06E-05	1.85E-01
244	2.90E-05	1.70E-01	3.33E-05	1.94E-01
314	3.88E-05	1.85E-01	2.73E-05	2.05E-01
364	2.97E-05	1.98E-01	2.93E-05	2.18E-01

Similar to the aerobic leaching tests the experimental results indicate a good reproducibility of the tests (Figure 2.3.8).

Figure 2.3.8. Evolution of the ^{14}C cumulative release fraction (left) and leaching rate (right)

CAST
Final report on results from Work Package 5:
Carbon-14 in irradiated graphite (D5.19)

The results of the anaerobic leaching tests also show a low ^{14}C release. After 364 days of test, less than 450 Bq of ^{14}C was released as dissolved species, representing 1.85% from the initial ^{14}C activity of the i-graphite subject to the leaching test.

As it was also observed in the tests carried out in aerobic conditions, the leaching rate is high in the first days of immersing. The initial quick release takes place with an average rate of 9E-02 % of inventory/day during the first 48 days while the slower release has a rate of around 4E-3 % of inventory/day.

The acid stripping/wet oxidation tests carried out on the leachate solutions sampled at different leaching intervals show that under anaerobic conditions, more organic than inorganic ^{14}C was released, with an almost constant ratio between organic and inorganic ^{14}C. The organic ^{14}C released as dissolved species under anaerobic conditions was between 61% and 66%, with an average of 64.57% (and a standard deviation of 3.08%).

No ^{14}C was measured in gas phase, but it is expected for this high-pH conditions that any $^{14}CO_2$ released from the irradiated graphite to remain in solution as carbonate.

Conclusions

The results of the leaching tests confirm the very low release rate of the ^{14}C. At the end of the leaching tests (376 days), around 1.33E3 Bq of ^{14}C in aerobic conditions and 450 Bq in anaerobic condition was released as dissolved species, representing 1.75%, respectively 1.85% from the initial ^{14}C activity of the i-graphite subject to the leaching test.

Both for anaerobic and aerobic conditions, the leaching rates are high in the first days of immersing and it decrease after that, indicating a two-stage process: an initial quick release (less than 9E-02 % of inventory/day for the first 48 days) followed by a slower release rate (around 4E-3 % of inventory/day).

The ratio between inorganic and organic ^{14}C release during the leaching test is almost constant, with more organic than inorganic ^{14}C released under anaerobic conditions (with an average fraction of organic ^{14}C of around 65% from the total ^{14}C released) and more

inorganic than organic ^{14}C in aerobic conditions (with an average fraction of inorganic ^{14}C of around 68% from the total ^{14}C released).

No ^{14}C was measured in gas phase, but it is expected for this high-pH conditions that any $^{14}CO_2$ released from the irradiated graphite to remain in solution as carbonate.

	CAST	
	Final report on results from Work Package 5:	
	Carbon-14 in irradiated graphite (D5.19)	

REFERENCES

Ahn, H.J., Song, B.C., Sohn, S.C., Lee, M.H., Song, K., Jee, K.Y. Application of a wet oxidation method for the quantification of ^{3}H and ^{14}C in low-level radwastes. 2013. Appl. Radiat. Isot., 81:62-6, 2013.

Carlsson, T., Kotiluoto, P., Vilkamo, O., Kekki, T., Auterinen, I. And Rasilainen, K. 2014. Chemical aspects on the final disposal of irradiated graphite and aluminium - A literature survey, VTT Technology 156, ISBN 978-951-38-8095-8.

Magnusson, A., Stenstrom, K., Aronsson, P.O. 2008. ^{14}C in spent ion-exchange resins and process water from nuclear reactors – A method for quantitative determination of organic and inorganic fractions. Journal of Radioanalytical and Nuclaer Chemistry, Vol. 275, No. 2, 261-273, 2008.

Petrova, E., Shcherbina, N., Williams, S. 2015. Definition of the scientific scope of leaching experiments and definition of harmonized leaching parameters (D5.4). Carbon-14 Source Term (CAST) Project, N° 604779, CAST – D5.4.

RIZZO, A., BUCUR, C., COMTE, J., Källström, K, LEGAND, S., RIZZATO, C, Večerník, P. 2017. Final Report on the Estimation of the Source Term and Speciation (D4.5). Carbon-14 Source Term (CAST) Project, N° 604779, CAST - D4.5.

Toulhoat, N., Narkunas, E., Ichim, C., Petit, L., Schumacher, S., Capone, M., Shcherbina, N., Petrova, E., Rodríguez, M., Lozano, E.M., Fugaru, V. 2015. WP5 Review of Current Understanding of Inventory and Release of C14 from Irradiated Graphite (D5.5). Carbon-14 Source Term (CAST) Project, N° 604779, CAST – D5.5.

Toulhoat, N., Narkunas, E., Ichim, C., Petit, L., Schumacher, S., Capone, M., Shcherbina, N., Petrova, E., Rodríguez, M., Lozano, E.M., Fugaru, V. 2016. WP5 Annual Progress Report – Year 3 (D5.9). Carbon-14 Source Term (CAST) Project, N° 604779, CAST - D5.9.

2.4 Agence nationale pour la gestion des déchets radioactifs / EDF (Andra / EDF)

Andra and EDF were associated in the framework of Task 5.1 to review existing leaching data on carbon 14 in French i-graphite. This work led to the drafting of two technical deliverables. The first deliverable, D5.1, is devoted to the synthesis of the leaching rates of carbon 14 in French i-graphite. The second one, D5.8, concerns the speciation of the released carbon 14. Analysed data were collected among technical reports from the Carbowaste project with additional information coming from EDF and CEA internal reports since 1990 as shown below.

Graphite origin	Date of experiment	Duration	Leaching liquid	Gaseous phase	Graphite form	Operational conditions
G2 moderator	1990	90 days	Deionised pure water, 20°C	Hermetic vessel, air atmosphere	Solid (~630 g)	Dynamic
SLA2 sleeve	1999	455 days	Industrial water pH=7.2	Hermetic vessel, air atmosphere	Solid (<10g)	Dynamic
BUA1 moderator	2003	455 days	Lime water, 20°C	Hermetic vessel, inert gas purge (N_2)	Solid (~10g)	Semi-dynamic
BUA1 moderator	2003	455 days	Deionised water, 20°C	Hermetic vessel, inert gas purge (N_2)	Solid (~10g)	Semi-dynamic
BUA1 moderator	2003	144 days	Deionised water, 40 °C	Hermetic vessel, inert gas purge (N_2)	Solid (~10g)	Semi-dynamic
G2 moderator	2007	455 days	Deionised and lime water, 20°C	Hermetic vessel, inert gas purge (Ar)	Solid (~90g)	Dynamic
G2 moderator	2011….	548 days	NaOH water, 20°C, pH=13	Hermetic vessel, inert gas purge (Ar)	Powder (50 g)	Semi-dynamic
SLA2 moderator	2011….	551 days	NaOH water, 20°C, pH=13	Hermetic vessel, inert gas purge (N_2)	Powder (25 g)	Semi-dynamic

Concerning carbon 14 release rate during leaching experiments, the main result is that carbon 14 leaching rate is very slow for the graphite stack. In first leaching experiments on French i-graphite, operational conditions were mainly designed to study chlorine 36 leaching rate. As a consequence, most of the results on carbon 14 are below the quantification limits of the method used for carbon 14 measurement in the leaching liquor. To obtain significant results (above the quantification limit), it is needed to use more important masses of trepanned samples that are not always available, and also to use suitable methodologies for sampling of the leaching liquor and carbon 14 measurements.

In most cases, a quasi-steady state leaching rate is achieved after approx. 100 to 200 days. Over that period, the calculated mean radiocarbon leaching rate lies between 10^{-11} and 10^{-8} m.day^{-1} (meters per day). The reasons of the variability of this radiocarbon leaching rate

are still not clear. Similar results were obtained with studies carried out on graphite from different origins, with different operational histories.

Because of the low release rate of carbon 14 in graphite leaching tests, an experimental methodology was specifically designed to increase carbon 14 release so as to identify the organic and inorganic released species in the gas and liquid phases. Two powdered samples of two French reactors (graphite stack) were tested: Saint Laurent A2 and G2. The leaching experiments were carried out at pH 13 (NaOH 0.1M) under inert atmosphere.

As a result, these experiments showed that more than 95% of the released carbon 14 was found in the liquid phase mainly as inorganic species (carbonates). However, some carbon 14 is also released as organic species. After 100 to 200 days, the speciation of the released carbon 14 reaches a quasi-steady state to around 30% of the total carbon 14 released as organic species. In the gas phase, due to the pH of the solution no carbon dioxide is observed. The released carbon 14 in the gas phase samples is as a mixture of organic species and/or CO. Because of the analytical procedure, it is not possible to differentiate these forms.

Some parameters that can influence the release of carbon 14 were also studied. The water chemistry and the specific surface area seem to have an impact. Other parameters have not been studied yet (temperature, initial activity of the samples and location in the reactor).

The main consequence of these studies is that some additional work has to be done to clearly quantify the organic fraction of released carbon 14. Moreover, the experimental parameters of the leaching tests have to be chosen carefully, in accordance with the conditions of the future waste disposal facility.

Concerning the implications of these studies for other i-graphite, it seems important to remind that the results obtained on the radionuclide behavior might depend on the history and on the background behind i-graphite. The results obtained on the studied i-graphite can't be directly and simply extended to other i-graphite.

	CAST	
	Final report on results from Work Package 5:	
	Carbon-14 in irradiated graphite (D5.19)	EURATOM

2.5 Agenzia Nazionale per le Nuove Technologie, L'Energia e lo Sviluppo Economico Sostenibile (ENEA)

Principle of the Process

The i-graphite from Latina NPP, like all graphites coming from moderators exposed to a neutron flux (for Latina NPP is up to 5×10^{22} n/cm^2), presents a wide range and amount of activation products such as ^{3}H, ^{14}C, ^{36}Cl, ^{55}Fe, ^{60}Co, ^{63}Ni, ^{134}Cs, ^{154}Eu and ^{155}Eu.

This distribution of activated elements concerns the bulk of the samples, mainly in the closed porosity or between the typical graphite layers. Anyway, there are not usually involved chemical bonds. So that, in order to achieve an exhaustive and valid extraction for activation products, it is important to increase the surface area of the sample. This should allow to the solvent to reach the inner layers/areas (i.e. closed pores, crystallites, etc.) and extract contaminants in solution.

The main idea is to apply an exfoliation-like process on the graphite by organic solvents (liquid-phase exfoliation) to produce un-functionalized and non-oxidized graphene layers in a stable homogeneous dispersion (Khan et al. 2011, Choi et al. 2011, Hernandez et al. 2008 and Bourlinos et al. 2009). This process, helped by mild sonication, consists in separating the individual layers in a more or less regular manner. Such a separation, being sufficient to remove all the inter-planar interactions, thanks to the dipole-induced/dipole interactions between graphene layers and organic solvents, results in a dispersion of the graphite in a workable media. This facilitates processing, treatment and easy characterization for the contaminants recoveries (Figure 2.5.1).
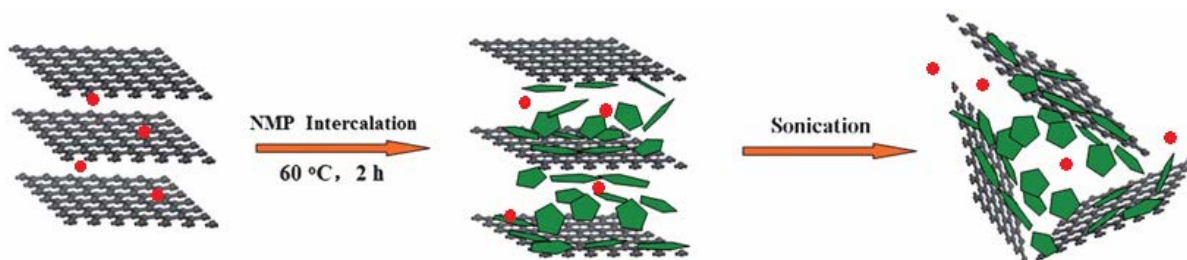
Figure 2.5.1: Representation of the main steps for the graphite exfoliation process promoted by organic solvents and ultrasound assisted

CAST
Final report on results from Work Package 5:
Carbon-14 in irradiated graphite (D5.19)

Moreover, neither oxidation process is performed for super-strong acid actions. This would lead to non-oxidized products so the graphite would be completely recovered as it is.

During this last year, the exfoliation-like process on the graphite by organic solvents (liquid-phase exfoliation) helped by mild sonication has been widely studied to establish the best process parameters so to obtain graphene layers in a stable homogeneous dispersion. This will result in a dispersion of the graphite in a workable media. In this way it should be allowed by the solvent to reach the inner layers/areas (i.e. closed pores, crystallites, etc.) and extract contaminants.

This facilitates processing, treatment and easy characterization for the contaminants recoveries when applied on i-graphite. As this purpose the overall process has been experimented on some samples of nuclear graphite from Latina NPP. The improvements to the process so as the results are here hence described.

Experimental Procedures: preliminary considerations

As it has been stated in the previous reports, the main steps in this process are:

1. Organic Solvents choice;
2. Low-power Sonication time
3. Centrifugation/Extraction
4. Removal Efficiency (as % of the recovered activities after treatment with respect to the original values before the treatment)

For the first point, in order to overcome the van der Waals-like forces between graphite layers to yield a good exfoliation and dispersing the resulted graphene sheets in a liquid media, highly polar organic solvents have to be used:

- N,N-Dimethylacetamide (DMA)
- N,N-Dimethylformamide (DMF)
- N-Methyl-2-pyrrolidone (NMP)

All of them are dipolar solvents, miscible with water, aqueous acid solution and most other solvents; they show good solvency properties, able to dissolve a wide range of chemicals.

CAST
Final report on results from Work Package 5:
Carbon-14 in irradiated graphite (D5.19)

For the second point a sonication power of 30W and a frequency of 37kHz has been assessed as it arises from the experiments made in the last year.

Although the right centrifugation rate should also be widely tested in order to remove all large aggregates to be reprocessed by following exfoliation step, in this work it has be chosen a low centrifugation rate (500rpm) followed by a filtration step, as in the all experiments already performed because the good results obtained. The supernatant liquid phases coming from the centrifugation are filtered on polyvinylidene fluoride (PVDF) filter membranes of 0.10 µm of pore size.

For the last point, the process has been applied on three samples of nuclear graphite coming from the decommissioning of the Italian NNP in Latina. Previously, on these i-graphite samples, a characterisation of ^{14}C contents has been performed. Then, the radiocarbon measurement by Liquid Scintillation Counting LSC on the extracting solutions has established the Removal Efficiency values.

Experimental Procedures: description of the process on irradiated graphite

Preliminary measurement of ^{14}C on i-graphite samples

Since all the works yet previously done during the last two years have been performed on virgin nuclear graphite for proving the validity of the overall process on the exfoliation of the nuclear graphite as well as for HOPG, from this point forward the work will be based on the trial to use the process for extracting radiocarbon from the irradiated nuclear graphite and after having assessed the best parameters in improving it.

First a characterisation on the i-graphite samples in term of ^{14}C content has been performed. For this purpose, 13 samples of the 15 available have been processed. For each of the 13 samples, 0.1 g of powder has been taken and added to 100mL of a mixture of H_2SO_4-HNO_3-$HClO_4$ 8:3:1 v/v/v for the determination of ^{14}C by Wet Oxidation Acid Digestion. The system for the graphite samples digestion consist in a hot acid digestion in a closed apparel under N_2 flow and a series of Drechsel bottles for trapping the ^{14}C as CO_2 in 3-MPA (3-methoxypropylamine). The system is shown in Figure 2.5.2.
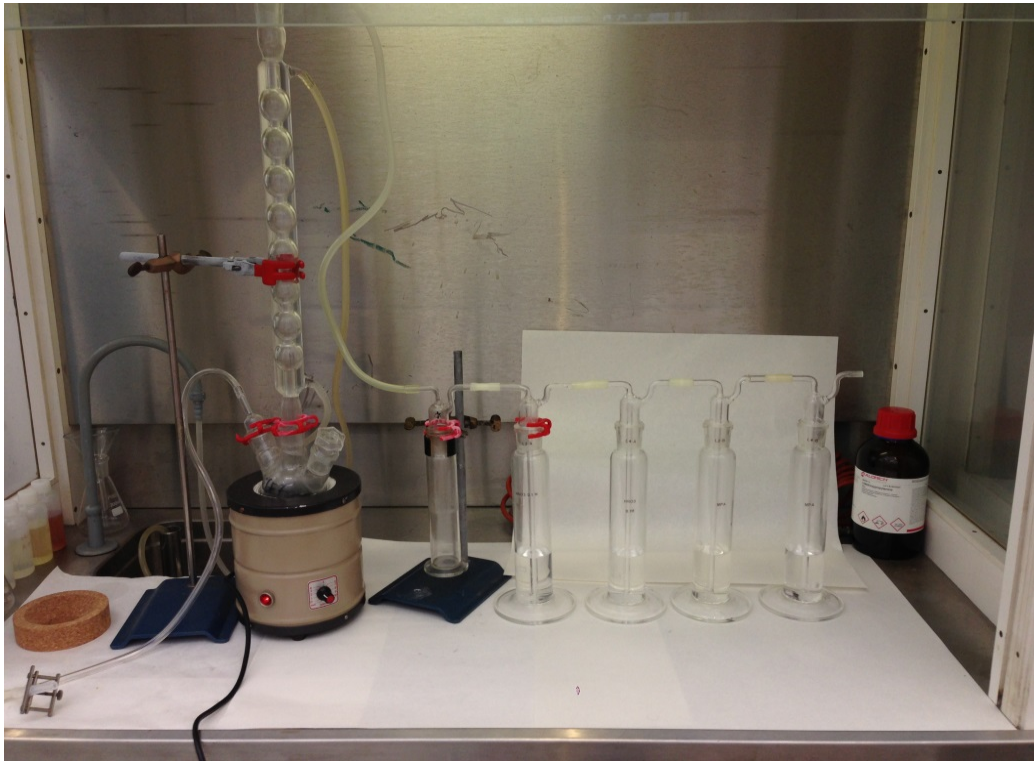
Figure 2.5.2 – Apparel for the wet oxidation acid digestion of the graphite sample for the ^{14}C determination.

The solutions of 3-MPA obtained from graphite samples dissolution are then measured by Liquid Scintillation Counting LSC with a LSC HIDEX 300SL TDCR. The concentrations of activity for each sample analysed are illustrated in Table 2.5.1.

	iGF1	iGF3	iGF4	iGF5	iGF6	iGF7	iGF8	iGF9	iGF10	iGF12	iGF13	iGF14	iGF15
kBq/g	8508	12886	8552	37769	4650	7315	4370	9520	49489	68583	6042	80704	76744

Table 2.5.1 – Concentration of activity of irradiated graphite samples before treatment

Solvent treatment Ultrasound assisted on i-graphite samples

The test for applying the organic solvent treatment by exfoliation has been performed on 3 of the 13 characterised samples.

For each different sample, 10 mg of i-GF powder, 5 mL of solvent was added (DMF, DMA and NMP).

The time of sonication is set on 3, 5 and 10 hours for each group of the same sample but different solvent, in a sonication bath at the power of 30W – 37 kHz.

The solutions obtained have then centrifuged at 500 rpm for 90 min followed by filtration on PVDF 0.1 μm filters. These filters were then dried in vacuum oven and weighed.

The filtrated solution then is supposed to contain the ^{14}C extracted by mean of this process. In order to confirm this, each organic solution coming from the process above described (3 for each of the 3 different organic solvents, corresponding to the 3 organic solvent used and 3 different time of sonication) has been analysed for the measure the ^{14}C content.

The results are shown in Table 2.5.2; values of the Removal Efficiency in percentage (RE%) for each test are also shown. The Removal Efficiency (in %) is defined as a percentage that represents the activity removed from the original matrix relative to the activity before the applied process.

Sample ID	weight (g)	solvent (5 mL)	time (h)	Initial Activity (Bq)	Removed Activity (Bq)	RE%
iGF1	0,0108	DMF	3	91.89	1.12	**1.22**
	0,0100		5	85.08	7.71	**9.06**
	0,0113		10	96.14	9.87	**10.26**
	0,0111	DMA	3	94.44	0.21	**0.23**
	0,0112		5	95.29	4.27	**4.48**
	0,0110		10	93.59	11.49	**12.28**
	0,0112	NMP	3	95.29	0.85	**0.89**
	0,0107		5	91.04	2.02	**2.22**
	0,0104		10	88.49	8.47	**9.57**
iGF3	0,0109	DMF	3	140.46	0.87	**0.62**
	0,0107		5	137.88	5.69	**4.13**
	0,0111		10	143.03	12.63	**8.83**
	0,0102	DMA	3	131.44	1.34	**1.02**
	0,0114		5	146.90	11.11	**7.56**
	0,0102		10	131.44	19.01	**14.46**
	0,0101	NMP	3	130.15	3.14	**2.41**
	0,0110		5	141.74	5.59	**3.95**
	0,0109		10	140.46	14.01	**9.98**
iGF4	0,0103	DMF	3	88.08	1.45	**1.65**
	0,0113		5	96.63	3.26	**3.37**
	0,0114		10	97.49	7.89	**8.10**
	0,0112	DMA	3	95.78	0.37	**0.39**
	0,0103		5	88.08	1.10	**1.25**
	0,0107		10	91.50	3.72	**4.07**
	0,0109	NMP	3	93.21	1.73	**1.85**
	0,0120		5	102.62	3.80	**3.70**
	0,0120		10	102.62	13.68	**13.33**

Table 2.5.2   Summary of the tests performed on i-GF samples and relative results

	CAST		
	Final report on results from Work Package 5:		
	Carbon-14 in irradiated graphite (D5.19)	EURATOM	

Results and Discussion

In order to have an idea on the efficiency of this exfoliation-like process for the treatment of the irradiated graphite and in particular with respect to the radiocarbon, these preliminary and first results, as shown in Table 2.5.2, can be represented plotting the values of removal efficiency RE% for each solvent used towards the sonication time, for each iGF sample.

This is illustrated in Figure 2.5.3.
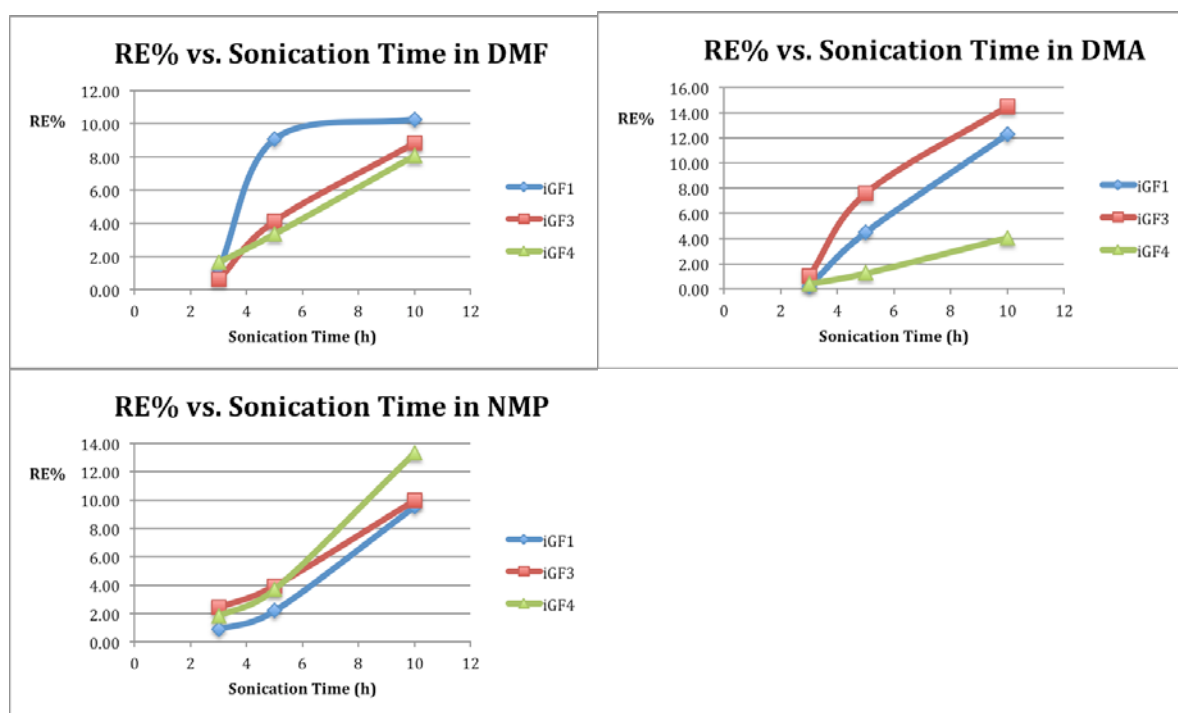
Figure 2.5.3 *(from top-left clockwise)* **Removal efficiency in % for each organic solvent (DMF, DMA and NMP) with respect to different sonication times for 3 different irradiated graphite samples.**

At first glance what comes out is that the efficiency of removal of the activity in terms of ^{14}C increases with the respect to the sonication time. This is well explained by the fact that, as already demonstrated in the previous report, the exfoliation of the graphite increases with respect to the sonication time. So, this allows to the solvent to easily reach the target radiocarbon in the closed porosity and extract it.

Moreover, no solvent seems to be better than one another as all of them play the same property in solvating the radiocarbon without particular capacity.

Anyway, the yields in extraction (RE%) obtained range from 0.2 to about 15 %. Although these values are relatively low, they can be considered the first ones obtained with this kind of treatment since no other values are produced in the literature by the same process to be compared. These results should be considered promising to keep on by this route.

The exfoliation method is a reliable method to remove some ^{14}C from nuclear graphite, paving the way for the production of graphite for recycling and/or safe disposal. To support this method, a lot of evidence has been collected. It is very clear that the sonication allows the solvent to easily reach the target radiocarbon in the closed porosity and extract it: successful exfoliation requires the overcoming of the Van der Walls attractions between adjacent layers. Solvents with surface tension (γ) ~ 40 mJm^{-2} are the best solvents for the dispersion of graphene and graphitic flakes, since they minimize the interfacial tension between solvent and graphite. Solvents used in this work show a surface tension between 36.7 mJm^{-2} (DMA) and 40.1 mJm^{-2} (NMP). Unfortunately, these solvents have some disadvantages: NMP is an eye irritant and may be toxic to the reproductive organs, while DMF may have toxic effect on multiple organs. Therefore, the search of alternative solvents (possibly "green" and with low toxicity) is highly recommended: the mixture water/acetone is a first step to achieve graphene dispersions in a low-boiling point solvent.

It has been demonstrated that the process is applicable to nuclear graphite: its linearity has been demonstrated through UV-Vis analyses. This is one of the most important parameters to validate an analytical procedure, and is defined as its ability, within a given range, to obtain test results that are directly proportional to the concentration of analyte in the sample. The absorption coefficient (α) at 660 nm of filtrate in NMP, DMA and DMF follows a Lambert and Beer behaviour with no substantial influence by the nature of the solvent: this confirms the robustness of the method. Furthermore, the reproducibility of the sonication process has also been taken into account. It is well known that the sonic energy input to a sample is sensitive to the water level, the exact position in the bath, the volume of dispersion, vessel shape and so on: for this reason, nominally identical baths tend to give

different results. In this work, the samples have been sonicated in a fixed position, in one sonic bath. Since the sonication temperature can reach more than 50°C, to avoid the collateral effects of the overheating the sonic bath was connected to a refrigerating system. It has been also demonstrated that the ratio powder/solvent has a crucial position in the optimization of the whole procedure. The recovery of exfoliated graphite increases when the ratio powder/solvent is low: to maximize the effect of the solvent it could be very useful to operate with a recovery and recycling system, also due to the fact that the solution produced from the exfoliation of nuclear graphite is highly radioactive.

The extracting abilities of each solvent are quite comparable. Since the partially removed activity is independent of the yield degree, these results can be interpreted on the basis that not all the ^{14}C species in the irradiated graphite are the same and only the ones not chemically bonded or in those forms that have some chemical or physical-chemical affinity with the extracting media are likely to be removed.

These first results are promising enough to promote further investigations in this direction. Furthermore, there is no doubt that the basic aqueous mixture is more efficient in the removal of ^{14}C respect to the organic solvents. NaOH increases the production of carbonate (highly soluble in water) confirming that the next experiments have to be designed following this evidence, focusing on efforts to develop a "total green" procedure.

REFERENCES

Bourlinos, A. B., Georgakilas, V., Zboril, R., Steriotis, T. A. and Stubos, A. K. (2009), Liquid-Phase Exfoliation of Graphite Towards Solubilized Graphenes. Small, 5: 1841–1845. doi:10.1002/smll.200900242.

Choi, E.-Y., Choi, W. S., Lee, Y.B. and Noh, Y-Y, Production of graphene by exfoliation of graphite in a volatile organic solvent, Nanotechnology, 22 (2011), 365601 (6pp).

Hernandez, Y., V. Nicolosi, M. Lotya, F. Blighe, Z. Sun, S. De, I. T. McGovern, B. Holland, M. Byrne, Y. Gunko, J. Boland, P. Niraj, G. Duesberg, S. Krishnamurti, R. Goodhue, J. Hutchison, V. Scardaci, A. C. Ferrari, J. N. Coleman, High-yield production of graphene by liquid-phase exfoliation of graphite, Nature Nanotechnology, Vol. 3, September 2008, 563-568.

Khan, U., O'Neill, A., Lotya, M., De, S. and Coleman, J.N., High-Concentration Solvent Exfoliation of Graphene, Small 2010, 6, No.7, 864-871.

2.6 Forshungzentrum Juelich GmbH (FZJ)

According to the current nuclear waste management strategy in Germany, discharged irradiated graphite (i-graphite) will be disposed of in the deep geological repository for low and intermediate level radioactive waste (i.e. waste with negligible heat generation) Schacht Konrad. This requires reliable information on the radionuclide inventory of i-graphite and information about i-graphite behaviour under the conditions relevant to the repository. The former is relatively easy to obtain from routine analyses of i-graphite. However, the latter is concerned with comprehensive investigations of the radionuclide behaviour in i-graphite, namely with the understanding of release mechanisms and the availability of reliable models capable of predicting the radionuclide release and transport in the short-and long-term.

[14]C is a radionuclide of major concern regarding the disposal of i-graphite and. has relatively long half-life (5,700 years). It is a weak β-emitter (156 keV) and if incorporated in the human body may cause internal radiation hazard. [14]C can be present in i-graphite in different chemical forms, like elemental C, CO_2 or organic C species, which have different retention behaviour in i-graphite. Besides that, a partitioning of ^{14}C between gaseous phase and aqueous solution ubiquitous for the underground repository may be affected by a number of factors, e.g. pH, temperature, salinity etc.

The main objective of the present work is to account for the sources of major graphitic wastes in Germany, their ^{14}C inventory and to understand the release behaviour of ^{14}C from i-graphite under conditions relevant to the repository Schacht Konrad. For that the kinetics of ^{14}C release from i-graphite and the corresponding speciation of volatile ^{14}C were investigated in order to answer the question, whether and to what extent German i-graphite can be disposed of in Schacht Konrad. As a sub-goal the effect of an upstream decontamination by thermal treatment on the behaviour of the labile ^{14}C fraction in i-graphite had to be evaluated in order to point on the benefits and disadvantages of i-graphite pre-treatment. The conditions of thermal treatment were selected based on the outcomes of EU project CARBOWASTE. Different destructive (total incineration, LCS) and non-destructive (autoradiography, SEM) techniques were used to characterize i-graphite.

	CAST	
	Final report on results from Work Package 5:	
	Carbon-14 in irradiated graphite (D5.19)	

MAIN RESULTS OF THE PROJECT CAST WP5

Contribution to the Task 5.1

Within this Task the main i-graphite streams in Germany were actualized. These are summarized in the Table 2.6.1.

Table 2.6.1: Total amount and main sources of i-graphite in Germany*

Reactor	Location	Operational period	Mass of Graphite [t]
High Temperature Reactors			
AVR	Jülich	1967-1988	238.1
THTR	Hamm-Uentrop	1983-1989	618.4
Material Research Reactors (MTR)			
Rossendorfer Ringzonenreaktor (RRR)	Rossendorf	1962	5.34
FRF-1 / FRF-2	Frankfurt	1958-1968	7.7
FRH	Hannover	1973-1997	1.0
TRIGA HD I/II	Heidelberg	1966-1999	1.6
FRMZ	Mainz	since 1965	4.4
FRN	Oberschleißheim	1972-1982	27.7
FMRB	Braunschweig	1967-1995	1.5
FRG-1 / FRG-2	Geesthacht	1958-2010 / 1963-1993	11.1
FRJ-1	Jülich	1962-1985	12.9
RFR	Rossendorf	1957-1991	3.9
FRJ-2	Jülich	1962-2006	30
		Total:	963.6**

*Only publically available information for i-graphite sources is shown.
**Some unaccounted amount of i-graphite may come from other MRT, like FRM-1/FRM-2 etc.

The major amount of i-graphite is stored in the interim storage and reactor facilities. Thirteen metric tons of i-graphite have been already disposed in the ASSE test repository. The 42 drums contain moderator and absorber pebbles. However, the waste containers were observed to extensively rust on the storage conditions. This requires consequent measures to

prevent radionuclides release. Within the project time in was not possible to get any samples or publically available information on the ^{14}C release from i-graphite disposed in ASSE.

The rest of i-graphite is planned to be disposed in the repository for the waste with negligible heat production – Schacht Konrad. The total ^{14}C activity being allowed for Konrad is $4 \cdot 10^{14}$ Bq. With an overall storage capacity of 303,000 m^3 this results in $1.32 \cdot 10^9$ Bq/m^3, as an average. For the disposal of ^{14}C-waste in Konrad, the release rate must be evaluated within the safety analyses. Most restrictive ^{14}C limits arise from safety issues for internal operation (T ~ 50 °C), classified by annual ^{14}C release from the waste container, which must not exceed 1% of the total ^{14}C inventory. This provides the limit of $1.8 \cdot 10^{10}$ Bq per container or about 22,000 waste-containers will be needed to accommodate the allowed total ^{14}C activity of $4 \cdot 10^{14}$ Bq.

Contribution to the Task 5.2

Within this task different i-graphite from German HTR and MTR were characterized. The results are demonstrated in the Table 2.6.2.

Table 2.6.2: Results of characterization of i-graphite from MTR and HTR in Germany [1, 6].

Nuclide	Specific Activity, Bq/g						
	THTR-300 reflector	AVR reflector	AVR carb. bricks	FRJ-1 TC**	FRJ-2 reflector	RFR TC (block 3)	RFR TC (block 4)
[3]H	n.d.*	$1.2 \cdot 10^6$	$3.8 \cdot 10^7$	$5.1 \cdot 10^2$	$2.7 \cdot 10^6$	$3.8 \cdot 10^1$	$9.4 \cdot 10^2$
[14]C	$1.36 \cdot 10^2$	$7.8 \cdot 10^3$	$1.8 \cdot 10^6$	$4.1 \cdot 10^2$	$9.8 \cdot 10^4$	$2.8 \cdot 10^3$	$1.2 \cdot 10^4$

*n.d. – no data; **TC – thermal column.

The experimental work within CAST project at FZJ was carried out on RFR i-graphite (block 4 of the head part of thermal column) [1, 2], as it was available in sufficient amount to perform characterization, thermal treatment and leaching tests. Sampled RFR i-graphite was characterized prior the leaching tests [3], in order to define inventories of ^{14}C and other radionuclides, as well as their spatial distribution in i-graphite. This information enabled a

CAST
Final report on results from Work Package 5:
Carbon-14 in irradiated graphite (D5.19)

quantification of the released fractions of ^{14}C and other radionuclides and will help to understand the mechanism of their release.

One of the important findings was made during i-graphite pre-leaching characterization using a combination of autoradiography and SEM/EDX techniques, when major fractions of APs were shown to be associated with the porosity (see Figure 2.6.1). The results of autoradiographic investigation demonstrate the presence of hot-spots (red spots if Figure 2.6.1A), whereas SEM/EDX confirmed the hot-spots to be pores with only measurable carbon signal in it (Figure 2.6.2B and C).
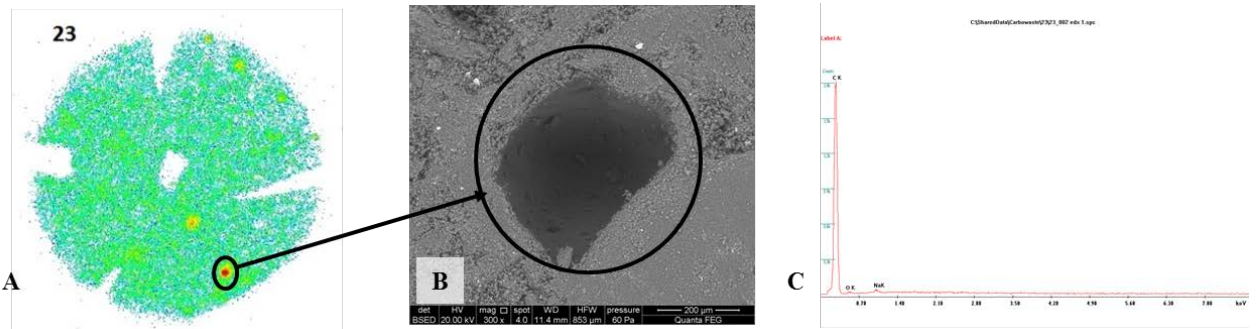
Figure 2.6.1: Graphite hot-spots characterization with autoradiography/SEM/EDX: (A) – autoradiography image, (B) - SEM image of the hot-spot area, (C) - EDX spectrum.

No significant amounts of impurities around hot-spots may indicate that the increased activity in these areas was due to radioactive ^{14}C. This result was consistently observed for all graphite samples analyzed and is in a good agreement with an assumption that the highest fraction of ^{14}C inventory has originated from activation of ^{14}N (via $^{14}N(n,p)^{14}C$ reaction) or ^{17}O (via $^{17}O(n,\alpha)^{14}C$ reaction), trapped in the pores or absorbed on the pore surface. The ^{14}C activated from ^{13}C (via $^{13}C(n,\gamma)^{14}C$ reaction) must be uniformly distributed in the graphite, and therefore cannot be the reason of hot-spots, but rather contributes to the background on the autoradiography images.

Along with the i-graphite characterization the improvement of gas-sampling equipment for leaching tests was performed. This equipment was originally developed within CarboDISP project [1, 6]. Application of the washing bottles with the smaller volume (4-5 mL) enables

low-level activity measurements for ^{14}C released into the gas phase and provides for the detection limit of $3.0 \cdot 10^{-2}$ Bq/g.

Contribution to the Task 5.3

In this Task the leaching behaviour of ^{14}C under conditions relevant to the final disposal was investigated. The release kinetics of ^{14}C described hereafter addresses the behaviour of ^{14}C when graphite is encapsulated in a cementitious matrix and exposed to conditions relevant to the Konrad repository (ambient atmosphere and pressure, T<50°C). This information provides for the ground for classification of RFR i-graphite as a special nuclear waste and defines the packaging type for final disposal in Schacht Konrad. The main parameters of leaching tests were discussed and summarized in D5.4 [4].

During storage of i-graphite in deionized water (DIW) and cementitious media (1M NaOH) ^{14}C was predominantly released into the gas phase as CO_2, whereas other volatile species of ^{14}C, like CO or C_{org}, were detected in the gas phase as well (Figure 2.6.2). As it was technically impossible to differentiate between CO and volatile organic species, a sum fraction of these species (CO+C_{org}) is shown on the graph.
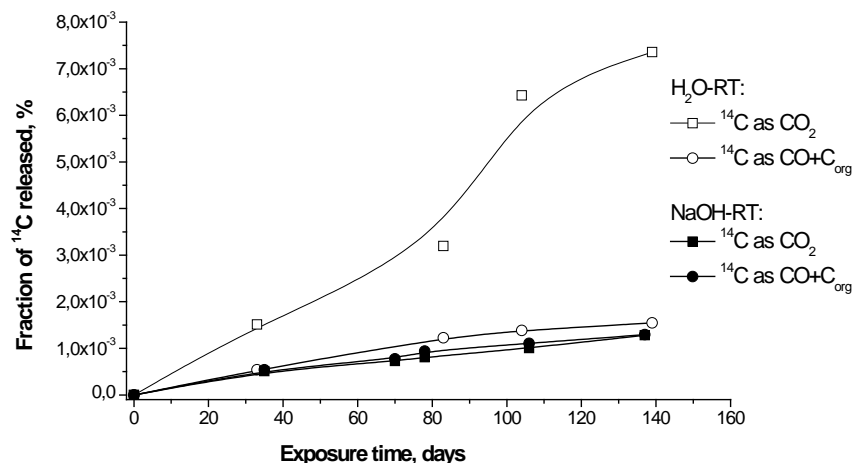
Figure 2.6.2: Kinetics of ^{14}C release from RFR-graphite at RT: in water (opened symbols) and in 1 M NaOH (filled symbols).

The results are summarized in the Table 2.6.3 show that over the given exposure time of ca. 140 days, the total release of volatile ^{14}C in DIW at room temperature (RT) is $8.9 \cdot 10^{-3}\%$, which is more than 3 times higher than from NaOH ($2.6\ 10^{-3}\%$) on the respective temperature conditions. In the volatile fraction released in an i-graphite/DIW system, the fraction of $^{14}CO_2$ prevails ($7.35 \cdot 10^{-3}\%$), whereas detected $CO+C_{org}$ fraction is much lower, $1.5 \cdot 10^{-3}\%$. In the system with NaOH, the release of $^{14}CO_2$ is much lower ($1.28 \cdot 10^{-3}\%$) and very similar to the $CO+C_{org}$ fraction ($1.28 \cdot 10^{-3}\%$). The fractions of volatile $CO+C_{org}$ released in water and NaOH systems are rather similar, i.e. around $1.5 \cdot 10^{-3}\%$.
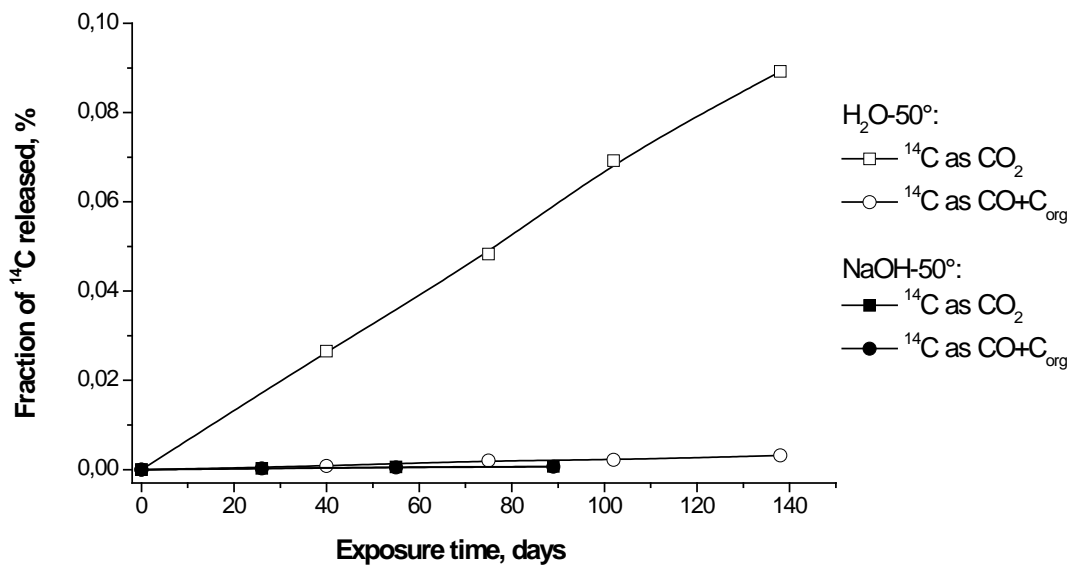
The fractions of non-volatile ^{14}C released in DIW and NaOH at RT (i.e. ^{14}C in the leachates) are significantly higher compared to the respective volatile ones. Thus, the dominant fraction of ^{14}C released remains in the solution. Here the higher amount of ^{14}C remains in the basic solution presumably in form of $Na^{14}CO_3^-$ and $^{14}CO_3^{2-}$ species in form of $H^{14}CO_3^-$ than in DIW at neutral pH. This consistently determines the lower volatile ^{14}C fraction from the i-graphite/NaOH system compared to the i-graphite/DIW system.

Table 2.6.3: Cumulative fractions of ^{14}C (in %) released into the leaching solution and the gas phase respectively (t=140 d).

Conditions	H$_2$O/RT	NaOH/RT	H$_2$O/50°C	NaOH/50°C
Gas phase	$8.9 \cdot 10^{-3}$	$2.6 \cdot 10^{-3}$	0.09	$8.9 \cdot 10^{-3}$
Solution	0.16	0.65	0.43	1.04

At 50°C the total volatile ^{14}C fraction reaches 0.089 %, which is more than an order of magnitude higher than the respective release on the RT conditions ($2.6 \cdot 10^{-3}\%$). Speciation of ^{14}C has shown (Figure 2.6.3) that this increase is mostly due to CO_2 release, whereas the fraction of $CO+C_{org}$ is close to the detection limit and is not significantly affected by the temperature increase. This behaviour is consistent with the decrease of CO_2 solubility in water with the temperature [7], however can be also explained by the higher release rates of volatile ^{14}C compared to the RT. In contrast to the system with DIW, the total release of volatile ^{14}C-spiecies in leaching experiments in NaOH is slightly lower ($1.3 \cdot 10^{-3}\%$) than the respective release at RT. The resulting speciation of ^{14}C in the gas phase indicated almost

equal fractions of CO_2 and $CO+C_{org}$, similar to the RT experiments. Examination of the leaching solution demonstrated a rather high concentration of dissolved ^{14}C (1.04%), presumably in form of carbonate. Thus, it can be concluded that the release of volatile ^{14}C is generally higher in DIW and increases with the temperature; application of NaOH as a leaching solution results in the higher fraction of ^{14}C being absorbed in the aqueous phase.

Figure 2.6.3: Kinetics of ^{14}C release from RFR-graphite at 50°C: in water (opened symbols) and in 1 M NaOH (filled symbols).

The obtained release fractions of volatile ^{14}C were subsequently used for the evaluation of the release rate R_n of ^{14}C (see Figure 2.6.4). The highest release rate was found for the i-graphite/DIW system at 50°C. Significantly lower is the R_n for i-graphite/DIW at RT. For both i-graphite/NaOH systems, the leaching rate was found to vary insignificantly. Hence, it can be concluded that the release of volatile ^{14}C from untreated i-graphite can be considerably retarded if i-graphite is encapsulated in some kind of cementitious environment.
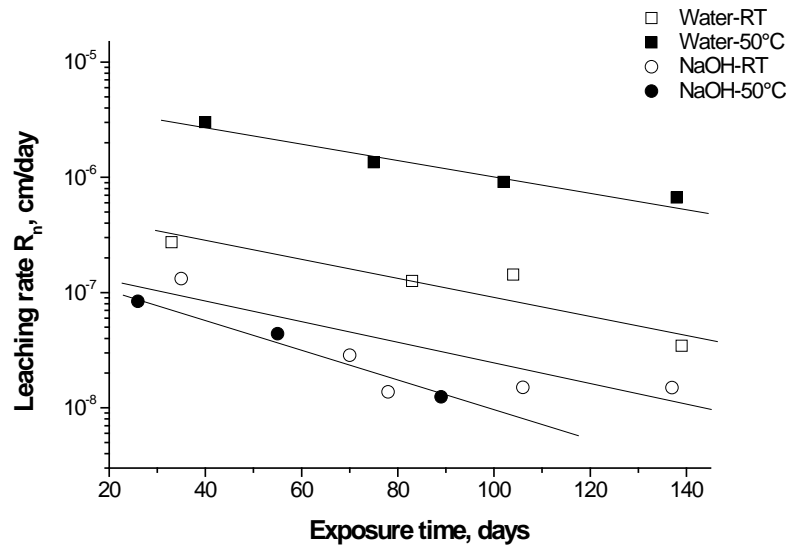
Figure 2.6.4: Leaching rate R_n of ^{14}C from RFR i-graphite in DIW and NaOH at RT and 50°C.

In order to assist conclusions about the disposability of i-graphite, to choose associated appropriate treatment steps (if required) and to select a suitable packaging approach, the annual release rates for ^{14}C are evaluated and compared to requirements from the Waste Acceptance Criteria (WAC) for the repository Schacht Konrad [1, 8]. The results (Table 2.6.4) show that in a case of i-graphite/1M NaOH, the annual release rates of ^{14}C does not exceed the required WAC of 1%, which enables the highest allowed ^{14}C loading of RFR i-graphite, i.e. $1.8 \cdot 10^{10}$ Bq per container or corresponds to the 22,000 containers with i-graphite to be disposed with the total allowed ^{14}C activity of $4 \cdot 10^{14}$ Bq.

Table 2.6.4: The annual release rates for ^{3}H and ^{14}C from RFR graphite, in %/year.

Radionuclide	i-graphite/DIW		i-graphite/1M NaOH	
	RT	**50°C**	**RT**	**50°C**
^{3}H	$2.53 \cdot 10^{-1}$	$8.48 \cdot 10^{-1}$	$8.81 \cdot 10^{-1}$	$5.69 \cdot 10^{-1}$
^{14}C	$2.56 \cdot 10^{-2}$	$2.56 \cdot 10^{-1}$	$7.3 \cdot 10^{-3}$	$6.9 \cdot 10^{-3}$

Various other APs were also detected in the leaching solution, whereas only ^{137}Cs was systematically found in every sample; ^{60}Co was detected only in NaOH solution at 50°C. No isotopes of Eu were detected in any leaching solution.

The results of thermal treatment (on Ar, at 1300°C, ca. 19 h) demonstrated a selective separation of ^{14}C fraction of 5.5 – 8 % with only little mass loss of 0.4%. As no oxidation of graphite is expected Ar stream, an easily-removable ^{14}C fraction is suggested to be separated by desoprtion, which is presumably bound to the outer surfaces via physisorption and is separated by desorption [9, 10]. Further leaching tests with treated i-graphite revealed only the background level of total released ^{14}C activity within ca. 140 days. These results indicate that thermal treatment at 1300°C enables the separation of a relatively easy removable fraction of [14]C (labile fraction) and improves the robustness of RFR i-graphite as a nuclear waste to be disposed of in Konrad. However, separation of an insignificant fraction of the ^{14}C inventory does not look like a beneficial treatment approach, especially taking into account a necessity of secondary waste management and additional costs outbalancing the advantage of the waste volume reduction. A proper encapsulation of RFR i-graphite in a cementitious material alone provides for the WAC to be met and does not require costly energy consumption compared to the thermal treatment, and, therefore, thermal treatment is unlikely to be considered as a part of i-graphite disposal plan in Germany [10].

REFERENCES

1   Toulhoat, N. et al. D5.2. WP5 Annual Progress Report of EU project CAST, p. 45, 2014.

2   Bach, F.-W. BMBF-Abschlussbericht: Trennen von graphitischen Reaktorbauteilen; Universität Dortmund; Förderkennzeichen 02S7849, 2004.

3   Shcherbina, N. et al. Final evaluation of leach rates of treated and untreated i-graphite from the Rossendorf Research Reactor. D5.12 of EU project CAST, 2017.

4   Petrova, e. at al. Definition of the scientific scope of leaching experiments. D5.4 of EU project CAST, 2015.

5   Vulpius, D. et al. Thermal treatment of neutron-irradiated nuclear graphite. // Nucl. Eng. Des. 265, 294–309, 2013.

6   Kuhne et al. Entsorgung von bestrahltem Graphit (CarboDisp). Abschlussbericht, 2015.

7   Carroll, J.J., Slupsky, J.D., Mather, A.E. The solubility of carbon dioxide in water at low temperature. // J. Phys. Chem. Ref. Data, 20, 1201, 1991.

8   Brenneke, P. Anforderungen an endzulagernde radioaktive Abfälle (Endlagerungsbedingungen, Stand Dezember 2014), Technical report SE-1B-29/08-REV-I, 2014.

9   Burchell, T.D. Graphite: properties and characteristics. Chapter 2.10 in: Konings, R.J.M. (ed.) Comprehensive nuclear materials, 2, 285-305, 2012.

10   Engle, G.B., Kelly, B.T. Radiation damage of graphite in fission and fusion reactor systems. // J. Nucl. Mater. 122(1-3), 122-129, 1984.

11   Shcherbina et al. Final evaluation of leach rates of treated and untreated i-graphite from the Rossendorf Research Reactor D5.12 of EU project CAST, 2017.

CAST
Final report on results from Work Package 5:
Carbon-14 in irradiated graphite (D5.19)

2.7 Centro de Investigationes Energéticas Médioambientales y Tecnològicas (CIEMAT)

Throughout WP5 within the CAST project, CIEMAT has been involved in four tasks. Tasks related to the data interpretation, compilation and/or analysis and those that imply experimental work. In the first aforementioned group are the Tasks 5.1 "Review of CARBOWASTE and other relevant R&D activities to establish the current understanding of inventory and release of ^{14}C from i-graphites" and 5.5 "Data interpretation and synthesis – final report", while in the second are the Tasks 5.3 "Measurement of release of ^{14}C inventory from i-graphites" and 5.4 "New waste forms and ^{14}C decontamination techniques for i-graphites".

CIEMAT participation in Tasks 5.1 and 5.5.

Regarding the Tasks 5.1 and 5.5, CIEMAT provided its contribution to the deliverables D5.4 "Definition of a recommended scientific scope of leaching experiments and harmonized leaching parameters", special contribution in the sections 2.1 Standardized leach test methods and 3. Discussion

D5.5 "WP5 Review of Current Understanding of Inventory and Release of ^{14}C from Irradiated Graphite", both generated as an output of the Task 5.1 and the current report D5.19 "Final report on results from WP5" corresponding to the Task 5.5.

CIEMAT participation in Task 5.3.

In order to achieve the objectives of the Task 5.3, CIEMAT developed both analytical methods and QA procedures to determine the release of ^{14}C from irradiated graphite samples and the speciation in the aqueous and gaseous phases. The descriptions and the conclusions of these works were depicted in the report D5.15 "WP5 CIEMAT Final Report on ^{14}C Leaching from Vandellós I Graphite". To achieve the objectives before mentioned, leaching experiments were planned considering two different scenarios: The first one, in which the leaching solution simulates the expected conditions in a cement based repository where a granitic - bentonite mixture has been used as backfill material (see Table 2.7.1 for

granitic - bentonite water (GBW) composition). The other one, Milli-Q® water type 1 as a high efficiency chemical removal agent was used for reference or comparison purposes.

Table 2.7.1. Granitic - bentonite water composition.

Al	< 0,03	mg/L
B	< 0,03	mg/L
Br⁻	15,7	mg/L
Ca	100	mg/L
Cl⁻	6,7	g/L
CO$_3$$^=$	< 12	mg/L
Electric	16,8	mS/cm
F⁻	< 0,5	mg/L
HCO$_3$⁻	32,4	mg/L
K	44	mg/L
Mg	580	mg/ml
Na	4,1	g/L
NO$_3$⁻	115	mg/L
pH	7,2	
Si	4,1	mg/ml
SiO$_2$	11.9	mg/L
SO$_4$$^=$	2.0	g/L

Test samples used in these works consisted on core-drilled samples of sleeve graphite from the Spanish NPP Vandellós I. During operation, the sleeves were placed inside the reactor pool while removing the fuel; it means that non-activation products like ^{137}Cs, transuranic, etc., have been incorporated from those present in the pool. The treatment applied to manage this waste, and the characterization processes carried out in the years of dismantling, have made it impossible to analyse volatile compounds other than ^{3}H and ^{14}C. Therefore, ^{99}Tc and ^{129}I were not measured, and ^{36}Cl were not detected above detection limit.

To perform the characterization of the initial sample, an aliquot (ca. 20 mg) of the powdered sample produced after each drilling was introduced in a combustion oven, where the sample is burned to 900 ºC in an oxygen stream. The gases formed are passed through a catalyst bed (CuO, Pt), where the carbon compounds are converted to CO_2, which is trapped in a specific cocktail, and finally the vial obtained was analysed by LSC. After the first results are

obtained, where no ^{14}C activity has been detected, the samples are measured again with ultra-low level LSC equipment (Quantulus).

Additionally, another aliquot of the powder sample (ca. 1 g) was placed into a glass vial (counting geometry) and measured by gamma spectrometry with a HPGe Detector, to determine the activity of the high energy beta-gamma emitters present in the initial sample. The results of ^{14}C and the most representative high energy beta-gamma emitters of the irradiated graphite samples are indicated in Table 2.7.2.

Table 2.7.2. Radiological characterization of graphite cylinders 1 to 6.

Sample	Mass (g)	H$_{avg}$ (mm)	Ø$_{avg}$ (mm)	^{14}C (Bq/g)	2u (%)*	^{60}Co (Bq/g)	2u (%)	^{137}Cs (Bq/g)	2u (%)
V-I-1	1,9688	12,68	11,28	1,22E+04	7,42	5,56E+01	3,57	2,03E+03	6,27
V-I-2	2,0222	12,51	11,09	1,35E+04	7,34	4,98E+01	3,71	3,98E+02	6,28
V-I-3	2,1861	14,07	11,11	1,08E+04	7,26	1,08E+01	5,00	2,88E+01	6,63
V-I-4	1,8077	12,15	11,08	1,13E+04	7,27	1,42E+02	3,61	2,17E+02	6,32
V-I-5	1,9102	11,70	11,07	1,12E+04	10,88	5,87E+01	3,78	4,20E+01	6,62
V-I-6	2,0964	12,51	11,05	1,10E+04	7,23	2,34E+01	4,08	1,40E+01	7,04

* The range "a ± 2u" represents a 95% level of confidence where the true value "a" would be found. The value of "U" or "2u" is the value which is normally used and reported by analysts and is hereafter referred to as "measurement uncertainty".

The leaching experiments started on June 2016 with the V-I-1 and V-I-2 core-drilled samples, whose main characteristics are depicted in Table 2.7.3. Once graphite cylindrical samples were obtained, the leaching process, based on the standard ISO 6961 "Long-Term Leach Testing of Solidified Radioactive Waste Forms" [1], were carried out using hermetic containers and on the basis detailed in the Table 2.7.4. The final setup of the experiment is depicted in the Figure 2.7.1.

Table 2.7.3. Specimens 1 to 6 - physical properties.

Sample Ref.	Mass (g)	H_{avg} (mm)	$Ø_{avg}$ (mm)	S (cm²)	V (cm³)	$Ø_{avg}$ / H_{avg}	ρ (g/cm³)
V-I-1	1,9688	12,68	11,28	6,49	1,27	0,89	1,55
V-I-2	2,0222	12,51	11,09	6,29	1,21	0,89	1,67
V-I-3	2,1861	14,07	11,11	6,85	1,36	0,79	1,60
V-I-4	1,8077	12,15	11,08	6,15	1,17	0,91	1,54
V-I-5	1,9102	11,70	11,07	5,99	1,13	0,95	1,70
V-I-6	2,0964	12,51	11,05	6,26	1,20	0,88	1,75

Table 2.7.4. General conditions of graphite leaching experiments.

Parameter	Leaching Conditions
Specimen geometry	Cylinder block 11 x 12 mm (Ø x H)
Leachant	Pure / GBW (synthetic)
Temperature (°C)	Room temperature
Vessel / Stirring	PTFE / No
$V_{leachate}$/$S_{specimen}$	0,18 - 0.20 m
Initial gas phase composition	Synthetic air (21 % oxygen, 79 % nitrogen)
Regime	Total renewal of the leachate (static).
Sampling	14, 28, 56, 90, 180 and 360 days from first immersion 14, 14, 28, 34, 90 and 180 leachate ages
Analyses	**Pre-leaching:** Solid phase: ^{14}C inventory & γ-spectrometry Leachant: Background ^{14}C inventory, pH & EC **Post-leaching:** Leachate: ^{14}C inventory, speciation (GC-MS, IC), γ-spectrometry, pH & EC Gas phase: Speciation (GC-MS)
Evaluation of results	Incremental leaching rate as a function of time of leaching (cm/day)

	CAST		
	Final report on results from Work Package 5:		
	Carbon-14 in irradiated graphite (D5.19)	EURATOM	

Figure 2.7.1. Leaching containers for deionized water and GBW.

After each interval, initially the gas sample (volatile species) is collected through the gas sample extraction valve, by means of a gas-tight syringe, and immediately injected into the GC-MS system. Once this previous step has been completed, the container is opened, the specimen is withdrawn from the leachant, the leachate is filtered, and finally transferred to a polyethylene bottle (the whole process is depicted in Figure 2.7.2).

	CAST	
	Final report on results from Work Package 5:	
	Carbon-14 in irradiated graphite (D5.19)	EURATOM

Gas sample is collected with a gas tight syringe and immediately injected into the GC-MS (speciation).

The container is opened and the leachate filtered and transferred to a PEHD bottle (filter paper and liquid are stored for ulterior analysis).

- pH & EC
- γ-spectrometry
- ^{14}C inventory
- GC-MS, IC (speciation)

The PFTE insert cleaned up with deionized water, refilled with fresh leachant and the reactor closed with its headspace purged with synthetic air.

Berghof ©

Figure 2.7.2. Leaching process sampling methodology.

The results of ^{14}C and the main high energy beta-gamma emitters (^{137}Cs and ^{60}Co) found in the leachates after each leaching step are indicated in Table 2.7.5 for deionized water and Table 2.7.6 for GBW.

Table 2.7.5. Results of ^{14}C, ^{137}Cs and ^{60}Co in deionized water as leachate (Vol. = 120 mL)

Leachant: Deionized Water.				Activity (Bq/g)	
Leaching Step (days)	^{14}C	^{60}Co	**2u (%)**	^{137}Cs	**2u (%)**
15	< 3,00E-03	1,73E-03	40,93	4,74E-01	4,39
28	0,267 ± 0,1	-	-	9,33E-02	5,62
56	< 2,40E-02	-	-	9,35E-02	6,16
90	< 2,40E-02	-	-	1,25E-01	5,12
182	< 2,40E-02	-	-	7,85E-02	6,96
359	< 2,40E-02	9,33E-03	13,18	1,07E-01	5,51

103

Table 2.7.6. Results of ^{14}C, ^{137}Cs and ^{60}Co in GBW as leachate (Vol. = 120 mL)

Leaching Step (days)	Leachant: Granite-bentonite water.			Activity (Bq/g)	
	^{14}C	^{60}Co	2u (%)	^{137}Cs	2u (%)
15	< 2,40E-02	2,15E-02	8,15	2,05E-01	4,75
28	< 2,40E-02	5,71E-03	18,14	1,22E-02	14,49
56	< 2,40E-02	6,61E-03	19,88	7,29E-03	29,36
90	< 2,40E-02	5,83E-03	16,26	7,23E-03	18,62
182	< 2,40E-02	5,41E-03	26,47	7,27E-03	35,49
359	< 2,40E-02	9,20E-03	13,04	9,30E-03	19,35

Throughout the CAST Project and regarding the analytical requirements for speciation, a methodology to determine permanent gases (CO, CO_2), C1 to C5 hydrocarbons, alcohols and aldehydes has been developed using a Gas Chromatograph coupled to a Mass Spectrometer (GC-MS). To analyse permanent gases, hydrocarbons C1 to C5 and CO_2, it was decided to use a column that is a combination of Molsieve 5A and PoraBondQ, named Select Permanent Gases/CO_2 HR (Agilent). A column to analyse different alcohol and aldehydes was set up. The column used was DB-624UI (L = 60 m; ID = 0,25 mm and F = 1,40 mm). In this case the following temperature-time profile, used in order to separate the different peaks, was applied: 40 ºC (2 min); 1 ºC / min to 45 ºC (5 min.); 1 ºC / min to 50 ºC (5 min) and 50 ºC (2 min) with a Split 100:1. The technique of head space sampling was used with 30 seconds of incubation time with a temperature of 40 ºC.

Also, the methodology to determine short chain carboxylic acids by an Ion Chromatography System using a conductivity detector has been implemented. In this case a Dionex ICS-900 Ion Chromatography System (ICS) with Ionic Reagent Free Controller (RFC) has been used. This equipment permits the analysis of short chain carboxylic acids with a AS11-HC column. As part of method used in the experiments, a set of standard mixed solutions of acetate, formate and oxalate ranging from 0.01 ppm to 1 ppm. The chromatograms of the calibration standards in deionized water medium are shown in Figure 2.7.3.

	CAST	
	Final report on results from Work Package 5:	
	Carbon-14 in irradiated graphite (D5.19)	
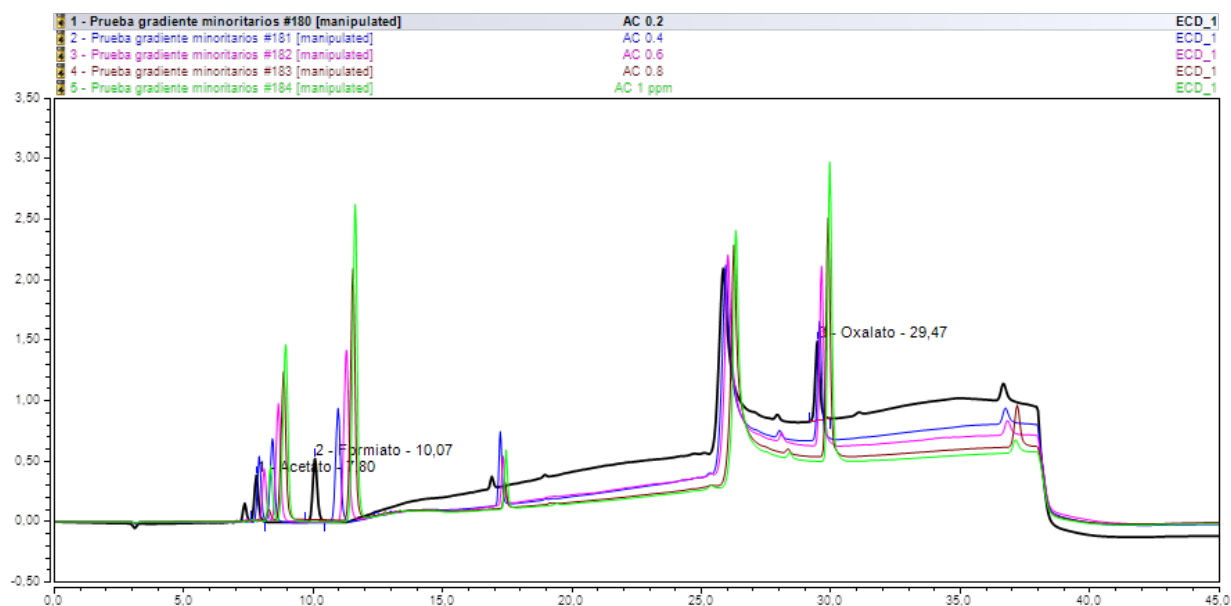
Figure 2.7.3. Chromatograms of the calibration standards in deionized water.

The results of the different leachates, obtained with the column AS-11 and with concentrations gradients of 1.5 mM KOH (0-8 min); 25 mM KOH (8-30 min) and 1.5 mM KOH (30 - 40 min) and a flow of 1 mL/min, are shown in Table 2.7.7.

Table 2.7.7. ICS results obtained from deionized water leachates.

Leachant: Deionized Water.	Concentration (mg/L±2U)					
Compound	Day 15	Day 28	Day 56	Day 90	Day 182	Day 359
Acetate	< 0.002	< 0.002	< 0.002	0.043±0.001	< 0.002	< 0.002
Formate	0.067±0.001	< 0.005	0.08±0.02	0.21±0.01	< 0.005	< 0.005
Oxalate	< 0.01	< 0.01	0.14±0.06	0.034±0.001	< 0.01	< 0.01

CIEMAT participation in Task 5.4.

Regarding the task 5.4, CIEMAT manufactured a new impermeable graphite matrix denominated (IGM), and investigated the behaviour of this material (corrosion progress and leaching rates of radionuclides) in contact with two types of aqueous media, deionized water and granitic - bentonite water. The first IGM [2] samples with irradiated graphite

manufactured in the worldwide have been made with this technology at CIEMAT facilities. An additional research line consisted on the validation of the ^{14}C decontamination procedure based on the thermal treatment of the Vandellós I NPP graphite. This thermal treatment will try to separate ^{14}C contents without a significate corrosion of the matrix, in order to maintain the structural properties and mass of the graphite. The outcome of these works was reported in the document D5.13 "Vandellós I graphite compilation report: thermal decontamination and IGM waste form results".

Impermeable Graphite Matrix (IGM)

The porous structure of Graphite enables the penetration of aqueous phases into the graphite and the radionuclides can be leached. Impermeable graphite matrix (IGM) would inhibit ingress of water and disable the release of radionuclides resulting in a safer final disposal. A ratio 80-20 graphite-glass is adopted to maximize the mass of graphite conditioned according to the pore volume determined in previous studies [4]. The method allows the production of encapsulated graphite without increasing the disposal volume.

The system used in the experiments, shown in Figure 2.7.4, is a specific hot vacuum press at lab scale to manufacturing the IGM specimens at control area.

Figure 2.7.4. Hot Press (ALD-France (FNAG) Tecnology) and IGM specimens

Graphite powder is mixing with the glass (80 % of graphite – 20 % of glass), in order to obtain a density $\approx$ 2,2 $\cdot$ g/cm^3 in the final form. The obtained specimens are shown in the picture. With this methodology two IGM samples have been manufactured for this project. The procedure for leaching experiment [1], [6] is the same already described in CIEMAT contribution to Task 5.3.

Characterization methods

The ^{14}C in the leachate was separated quantitatively by a catalytic furnace Harvey OX500 using specific trapped solutions. Activity of ^{14}C in the leachate was analyzed by LSC systems (Packard Tricarb 3110 TR/LL LSC and Quantulus LSC system.

Determination of organic dissolved species (carboxylic acids) with an Ionic Chromatograph Dionex ICS-900 Ion Chromatography System with Ionic Reagent Free Controller (RFC) with an AS11-HC column. The results of the deionized water leachates, obtained with the column AS-11, with a gradient of concentrations.

Gamma emitters were measured in the leachate with a Canberra HPGe Detector.

The gas and leachate volatile species were measured with an Agilent Gas Chromatograph-Mass Spectrometer 7890B system (Agilent DB624UI 60m column type for liquid samples and Molsieve 5A Porabond Q column for permanent gases and CO_2).

The methodology to analyze leaching gases in the optimal conditions with a Molsieve 5A column and alcohols and aldehydes with DB-624UI was developed throughout the project.

IGM Leaching. Results and Discussion

✓ **Macroscopic physical characteristics of specimens**

Physical characteristics (size and weight) of the specimens used in the experiments are shown in Table 2.7.8:

Table 2.7.8. Physical properties

Sample Ref.	IGM Mass (g)	i-graphite (%)	H_{avg} (mm)	$Ø_{avg}$ (mm)	ρ (g/cm^3)
IGM-4	7,6945	81,2	11,5	20,67	2,04
IGM-5	7,8097	78,8	11,01	20,7	2,01

✓ **pH and electrical conductivity (EC) of leachant**

The pH and electrical conductivity of leachant and leachate are determined before and after each leaching step. In the case of granitic - bentonite water the pH and EC variations are not possible to quantify with the techniques available due to the high concentration of ions in solution. pH and the EC increase due to the appearance of certain amounts of ions in solution when deionized water is used as leachant.

The concentrations of the ions found in the leachate in the crystal matrix studies (mentioned in the introduction) verify that the increase in conductivity coincides effectively with the presence of dissolved ions, this behavior is also expected in the case of granitic - bentonite water used as leachant. The additional increase of the ion concentration by dissolution may result in ion concentrations in the leachant leading to the precipitation of secondary phases.

✓ **Identification and concentration of carboxylic acid in the leachant**

The organic carbon present in the leachates are formate ($HCOO^-$) and rarely oxalate $(COO)_2$. The high concentrations of anions masked the detection of carboxylic anions. Additionally, the expected concentrations of carboxylic acids in the leachant are also low independently of the macro-components that interfere in the determination.

✓ **Activity of ^{14}C of the waste form and leachant**

The results obtained are lower than Minimum Detectable Activity (MDA). This leads to leaching rate (Rn) for ^{14}C of lower than 6,15 E-09 cm/day.

✓ **Leaching rate of ^{14}C and the correlation with other gamma emitters (^{60}Co and ^{137}Cs)**

The activity concentration is > MDA except for ^{137}Cs in the first leaching step likely due to surface contamination. With these data is not possible to establish a leaching trend for this radionuclide. In the case of deionized water only in the first steps it possible to find ^{137}Cs close to MDA. Assuming the detection limit as release the following maximum leach rate could be calculated: ^{137}Cs < 1E-03 cm/day

The principal beta-gamma emitters detected were ^{60}Co and ^{137}Cs in granitic - bentonite water. In all steps less than 0.1 % of ^{60}Co was leached except for last step where was higher. For ^{137}Cs less than 1% of ^{137}Cs was leached except in the first step.

Regarding the main beta-gamma emitters detected in the leaching test with granitic - bentonite water, in the Figure 2.7.5 are shown the leaching rates (R_n) of ^{137}Cs and ^{60}Co versus the time.
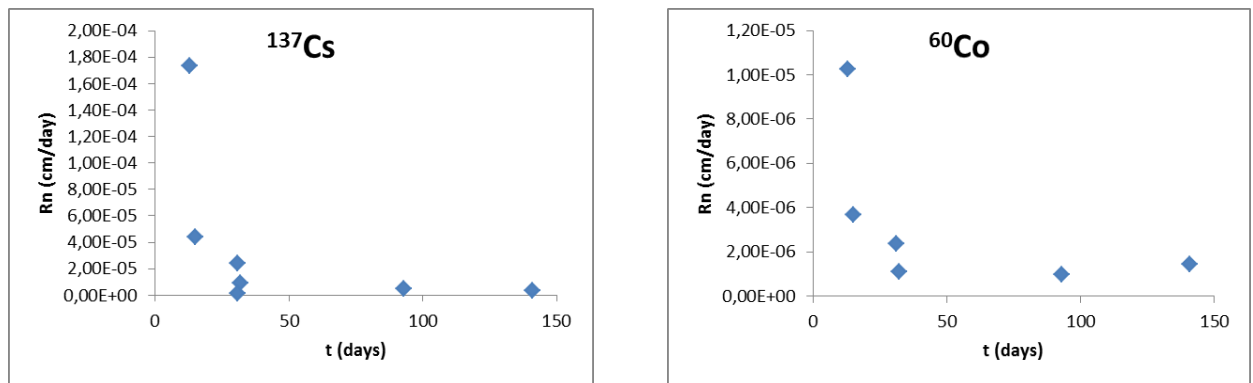
Figure 2.7.5. Leaching rates of ^{137}Cs and ^{60}Co in granitic - bentonite water

The obtained results reveal a difference in leaching behavior in deionized water and granitic - bentonite water. However, the low leaching rates (except the fast release fraction after 13 days which are related to surface effects) indicate the enclosing potential of IGM.

✓ **Identification of volatile carbon species in leachate gases by GC-Mass Spectrometry**

Alcohols and aldehydes have not been detected in any step of the leaching process, the absence of signal for these organics could be due to there not being enough time to form these molecules from the graphite or there are no thermodynamic and kinetic conditions for the formation from the materials of the waste form.

On the other hand, CO has been detected, but it is not possible to determine the presence of ^{14}C in CO due to the technique to trap this gas is not available.

THERMAL TREATMENT

It is demonstrated in other i-graphite [7] types that the thermal treatment is effective in the selective decontamination of radiocarbon. Chemical behavior of ^{14}C is not different of ^{12}C, only different bonds of activated forms or different positions in the structure of i-graphite can distinguish, for this reason the release of ^{14}C also implies the release of ^{12}C and consequently a corrosion of the treated matrix [8], [9].

Thermal treatment system consists of a rotating furnace from ALD France with, a single quadrupole mass spectrometer by AMG Coating (Figure 2.7.6)

CAST
Final report on results from Work Package 5:
Carbon-14 in irradiated graphite (D5.19)
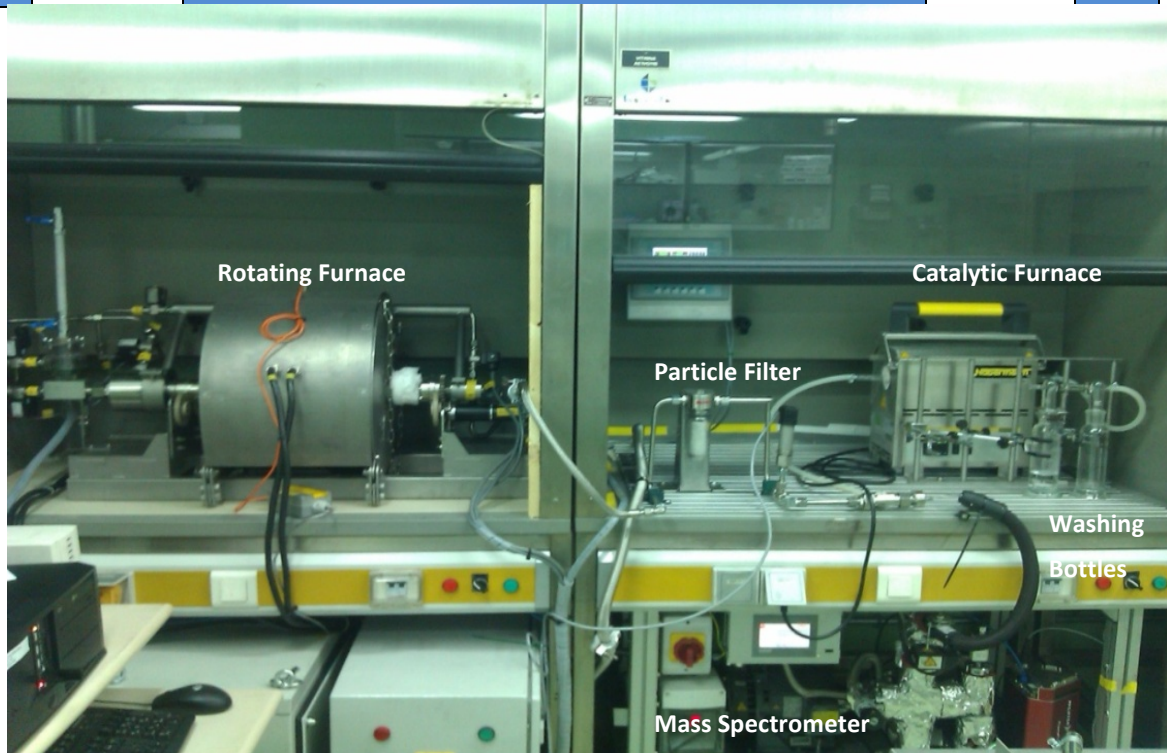
Figure 2.7.6. Thermal Treatment Facility

The release of ^{14}C throughout thermal treatment without significate mass loss is being investigated by a partial oxidation.($C+O_2 \rightarrow CO_2$; and $C + 1/2\ O_2 \rightarrow CO$)

The variables that have a relevant influence on the oxidation of graphite and consequently in the corrosion rate of carbon are: The influence of treatment temperature, the influence of oxidizing agent, the influence of active gas flow and the influence of grain size.

The studies are faced separately in order to parameterize the effect of the variables independently.

Carbon dioxide is the specie to be trapped and measured at the end of the experiment due to the ^{14}C treated in an oxidant atmosphere will be released as $^{14}CO_2$ or ^{14}CO. $^{14}CO_2$ is trapped in NaOH and the corrosion rate of carbon is calculated by precipitation with barium nitrate as $BaCO_3$.

Corrosion rates are summarized in Table 2.7.9 as well as the main data of these experiments for different temperatures and flow rates of oxygen.

Table 2.7.9. Experiments with virgin graphite at 700ºC, 900ºC and 1100ºC

Experiment	Mass (g)	T(ºC)	O_2 (litres/hour)	Corrosion Rate (% C)
TR-7-10-1	2,0058	700	10	39,93
TR-7-10-2	2,0029	700	10	89,57
TR-9-5-1	2,0129	900	5	71,55
TR-9-5-2	2,0021	900	5	97,76
TR-9-10-3	1,9907	900	10	6,03
TR-9-10-4	2,0163	900	10	45,83
TR-11-10-1	2,0043	1100	10	87,71
TR-11-10-2	2,0161	1100	10	67,93

The mass balance of some experiments are much lower than others due to problems of determination of treated mass because of mass losses from static charge problem in the injector.

The irradiated graphite used came from sample GC-2 (coarse grain size) from the sleeves of fuel elements. The activity was determined as: $3.50 \cdot 10^4$ Bq/g of tritium and $1.42 \cdot 10^4$ Bq/g for radiocarbon.

An increase of CO and CO_2 release, in inert atmosphere, is observed when temperature is reaching 400 ºC. This behavior is observed when the slope of temperature is performed with the i-graphite is into the tube.

The first step was to study the release of ^{14}C in inert atmosphere (Ar) and the second one the release with a low amount of oxidizing agent (O_2). The irradiated graphite was introduced directly in the glass tube in order to minimize cross contamination and mass losses in the experiments.

CAST
Final report on results from Work Package 5:
Carbon-14 in irradiated graphite (D5.19)

Experiment # 1

The graphite was firstly treated in inert atmosphere (Ar) and oxidize at 700ºC in a 3 litres/hour O_2 flux for 4 hours in this Experiment.

The qualitative releases of CO/CO_2 were measure by the MS. The total amounts of ^{12}C for each treatment period and the final amount was obtained by gravimetric method, getting 94.20% of the initial mass of graphite (1.0060 g).

Tritium recovery from the first HCl washing bottle was 13 % (relative to initial inventory). This low recovery rate leads to increasing the volume of HCl (from 100 mL to 200 mL) and adding a second HCl washing bottle.

There were no releases of ^{14}C with inert atmosphere treatment, nevertheless when oxygen is injected at this temperature the ratio ^{14}C / ^{12}C is around 1.5, and after one hour treatment 51 % of ^{14}C was release with a corrosion rate of 36%.

Experiment #2

The thermal pre-treatment in inert atmosphere was performed at 1100 ºC for 1 hour; Holding the gas flux the temperature was reduced to 300 ºC at this temperature a oxidation treatment with 5 litres/hour of oxygen for half an hour. After that an inert treatment at 1100ºC with Ar for 0.5 hours. Finally, the consumption of matrix at 1100ºC with 5 litres/hour O_2 was done.

The temperature and gas fluxes in Experiment#1 and #2 tried to saturate the graphite surface with oxygen at low temperature (≈400 ºC) chemisorbed on it and when the temperature increases the superficial and more labile ^{14}C reacts with the chemisorbed oxygen and produces these amounts of CO and CO_2 registered.

The mass of carbon obtained in this experiment was 91.1 % regarding initial graphite mass (m_0 =1.0139 g). Additionally, a 32 % of ^3H was recovery in this process.

It is observed that, once oxygen is chemisorbed, in treatment process at 1100 ºC in inert atmosphere a depletion of ^{14}C has a ratio of 2.6 regarding ^{12}C depletion in 30 minutes.

CAST
Final report on results from Work Package 5:
Carbon-14 in irradiated graphite (D5.19)
EURATOM

That indicates chemisorption is higher at low temperature and reaction (and consequently corrosion) is produced at higher temperature. Data obtained are plotted in Figure 2.7.7:
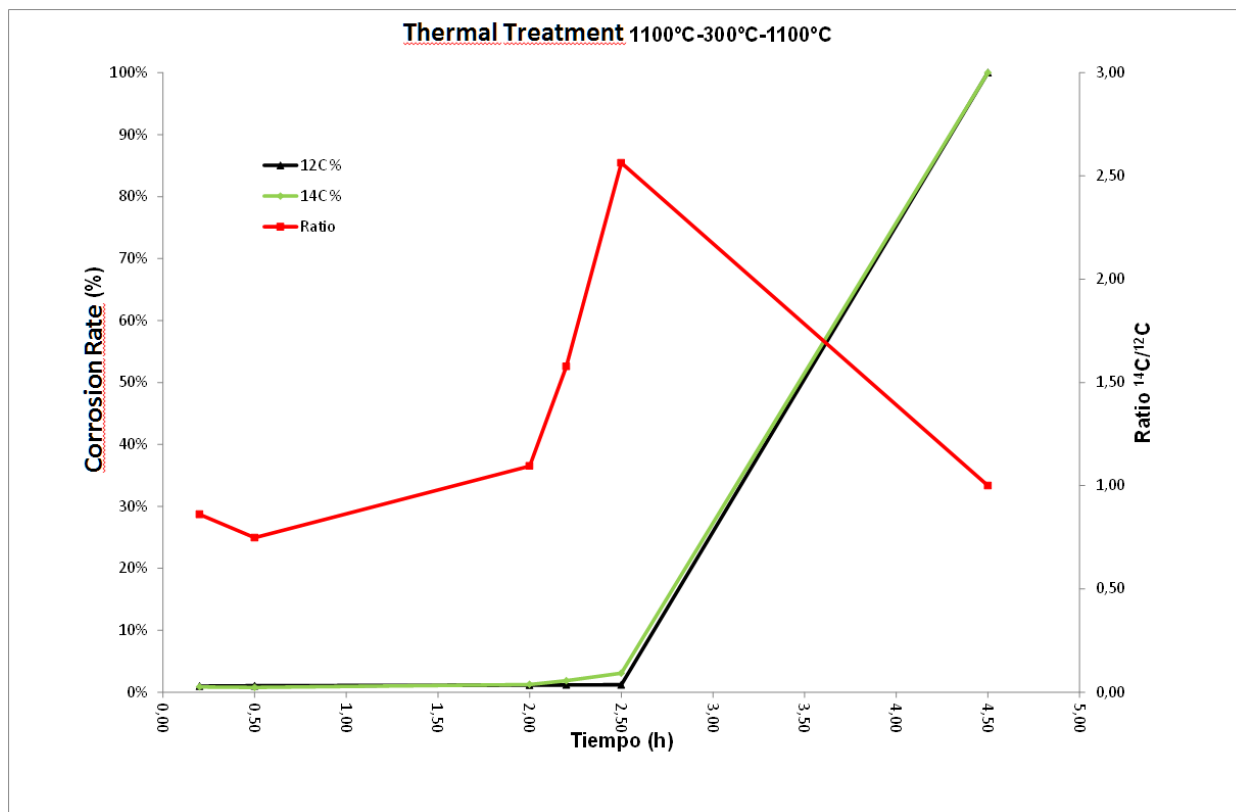
Figure 2.7.7. ^{14}C and ^{12}C release rate by thermal treatment at 1100ºC-300ºC-1100ºC

Experiment #3

This experiment differs from Experiment #1 in the flux of O_2 used – 3 litres/hour in this case.

The amounts of ^{12}C and ^{14}C were determined as in Experiment#1 and #2. The obtained mass of carbon, in this case, by precipitation as carbonate was 97 % (relative to the initial mass m_0= 0.9801 g). Release of ^{3}H was 24%.

There is not a selective release of ^{14}C regarding ^{12}C (or total carbon) when 1100 ºC is applied for thermal treatment. ^{14}C released came from graphite corrosion instead of decontamination after 2 hours of treatment.

Experiment #4

Conditions of Experiment #4 are the same than Experiment#1, already discussed. The graphite was treated with Ar for 4 hours at 700º C, after that oxygen treatment with a flux of 3 litres/hour of O_2 for 4 hours)

In this case the release of ^{14}C in inert atmosphere is very low at this temperature, similar to the results obtained in Experiment#1, on the other hand in oxidizer atmosphere ratios of $^{14}C/^{12}C$ closed to 2 were observed, getting a ^{14}C release of 11% versus a release of 5% for ^{12}C 10 minutes after oxygen flux started. This percentage became 58% for ^{14}C and 31% for ^{12}C in 1 hour. Data of this experiment are plotted in the Figure 2.7.8.

Determinations of ^{14}C and ^{12}C were performed in the same way that is described for the other experiments. In Experiment-4 the mass of graphite obtained by precipitation was an 86.5 % of an original mass of $m_0 = 1.0169$ g. The recovery of ^3H was 32 %.
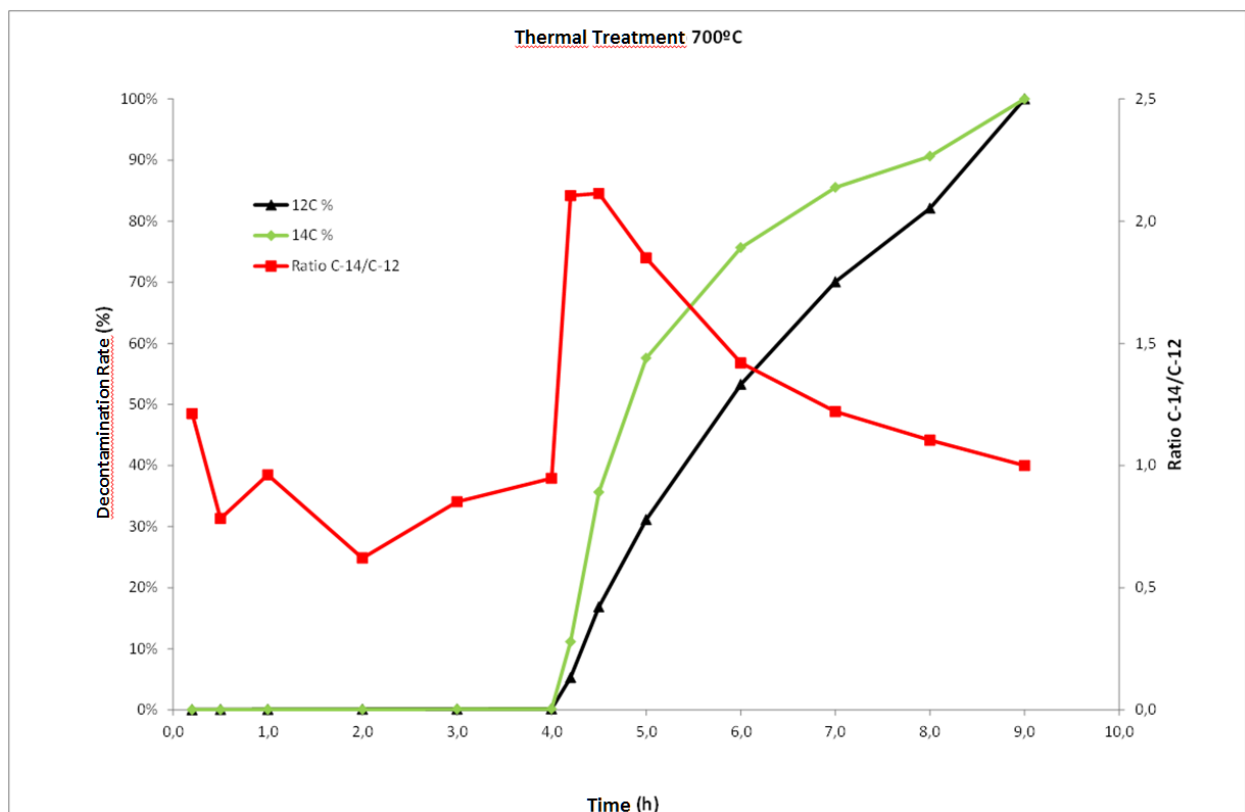
Figure 2.7.8. ^{14}C and ^{12}C release rate by thermal treatment at 700ºC

For studying the influence of the total flow and the flow of the oxidant agent in the corrosion rate some experiments were performed. The temperature was established in 700 ºC, 600 ºC, 500 ºC and 400 ºC. The flows selected were 20, 50 and 100 litres/hour. The results are in the following tables:

Figure 2.7.9 plots the corrosion rates vs treatment temperatures for three oxygen flows tested and shows the behavior/evolution of oxidation in such a way that is easier to select the treatment conditions (temperature and oxygen flux) to get the minimum of corrosion and maximum of ^{14}C decontamination.
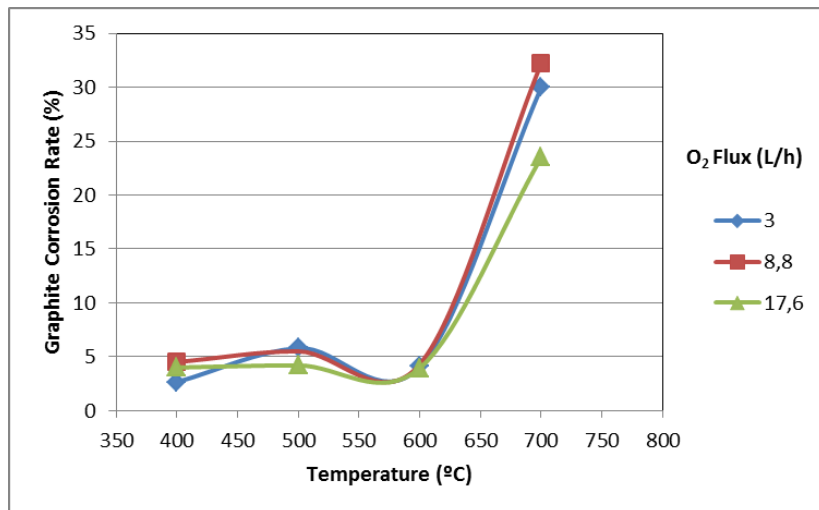
Figure 2.7.9. Corrosion rate for different fluxes vs treatment temperature

The slope of corrosion rate vs temperature is practically null for temperatures < 600 ºC and the corrosion values in this range is ≈5%. However the slopes for temperatures > 600 ºC is in the range 0.20 - 0.28 being lower for high flux (17.6 litres/hour).

In order to achieve the lowest corrosion rate of graphite and the highest decontamination factors of ^{14}C the work temperature will be in the range of 400 ºC – 600 ºC and the O_2 flow rate lower than 9 litres/hour.

The corrosion of the total mass of graphite can be higher than 100 % due to the increasing of C coming from the absorption of atmospheric CO_2 depending on the delayed time for

sampling and analysis (sometimes higher than 24 hours) the increment in some cases is lower than 10 %.

It was observed in all experiments that CO_2 and CO concentrations increased during some minutes in inert atmosphere starting from 400 ºC, (temperature of reaction for O_2). The explanation that sounds most plausible is that both O_2, chemisorbed in the surface and pore system, and the labile C which is also in the graphite surface (may be as CN groups) react at elevated temperatures without addition of an additional oxidant.

Summary

Regarding the Task 5.3 it is worth pointing out the following:

- Although significant heterogeneity has been observed both in the detection and in the activity of the high energy beta-gamma emitters, the ^{14}C content of the core samples tested shows a good correspondence, with an average specific activity of 1,17E+04 Bq/g and a standard deviation of the 8,74 %.

- Among all the analyses of leachate samples carried out, including pure water and GBW, only one value, corresponding to the 28 days leaching step in pure water, presented a value of ^{14}C higher than the detection limit. It is more likely that this could be because of bad filtering of the sample or cross contamination in the equipment than because of the leaching process itself.

- Using pure water as leachant, in the ICS analyses, acetate was detected, although close to the MDA, after 90 days of leaching time; formate after 15, 56 and 90 days and oxalate in the 56 and 90 periods. However, this technique cannot be used to analyze GBW solutions because of the high concentration of anions and cations present in this media.

- Both alcohols and aldehydes in leachates have not been detected in any step of the leaching process, and regarding gas samples, nor was CO (whose values were again below MDC (< 3.5 ppm)).

- After all the leaching steps were completed, the graphite core samples were dried, weighed and measured, without presenting any significant dimensional change (< 1 %), cracks or crumbles.

Regarding the Task 5.4 it is worth pointing out the following:

IGM samples

- In deionized water the pH and the conductivity increase, which means a certain amount of ions is dissolved from the IGM into the leachant.

- The organic carbon has been found in deionized water as formate ($HCOO^-$) in leachants from day 28, 91, 184 and 215. An oxalate $(COO^{2-})_2$ could be detected only in one leachate sample after 28 days.

- Both alcohols and aldehydes in leachates have not been detected at any time of the leaching process.

- In the case of granitic - bentonite water the pH and conductivity are practically the same before and after each step due to the higher ion concentration in the leachant which masked the presence of ions dissolved from the waste form.

- CO was not found in the gas phase of the leaching process with a MDC (< 3.5 ppm), except for the first and second leaching period with granitic - bentonite water where the concentration is: 30.9 mg/l and 10.4 mg/l. This is may be also related to the carbonate content in the leachate.

- After 356 days of leaching in granitic - bentonite water the following leaching rates has been observed: 1,44E-06 cm/day for ^{60}Co and 3,52E-06 cm/day for ^{137}Cs.

- The values obtained for ^{14}C are lower than Minimum Detectable Activity. This leads to leaching rate (Rn) for ^{14}C of lower than 6,15 E-09 cm/day.

- The Leaching rate (R_n) for ^{60}Co and ^{137}Cs in granitic - bentonite water, decreases with the time and after 356 days it will be constant.

- The durability of the IGM glass matrix has been validated by leaching experiments.

- The methodology has been established to manufacture the IGM samples in lab scale.

- It is possible to close the pore system in the irradiated graphite without to increase the volume of the waste.

Thermal Treatment

- The data obtained with virgin graphite experiments have allowed adjustment of the elements of the experimental system: Devices and methods which will be the base of the system at pilot plant scale.

- Ratio ^{14}C/Total C results are not definitive neither conclusive and they have to be improved because the corrosion rate of the graphite is higher than the one desired. Reasons for this behavior are guessing to base on the use of powder graphite that increases the surface and the corrosion kinetic due to the higher availability of ^{12}C. Further experiments can demonstrate the influence of the grain size in the corrosion kinetic.

- A decontamination ratio around 58% of ^{14}C versus 31% of ^{12}C in a 1-hour treatment at 700ºC in a 3 litres/hour of oxygen flux was obtained.

- The smallest amount of ^{14}C in inert atmosphere obtained in the Experiment 1 is in contrast with the experiment performed with other graphite type reactors as Merlin and AVR. The different behavior can be explained by the loss of ^{14}C of the graphite surface during reactor operation. UNGG reactors use graphite as moderator and CO_2 as coolant and average operation temperature is 400º C. In these conditions CO_2 reacts with graphite producing ^{14}CO. The radiocarbon comes from the graphite surface more probably from the activation of ^{14}N impurities of coolant and/or nitro-derivates in the graphite. Due to the release of majority of ^{14}C in the surface the one in the graphite comes from the activation of the ^{13}C and forms part of the structure.

- Experiment 2 demonstrates that oxygen saturation of the surface at 300º C, allows to obtain ^{14}C without high corrosion rate ($^{14}C/^{12}C = 2,6$) with a thermal treatment in inert atmosphere. This indicates that surface bound ^{14}C is not completely released during operation which can be release by chemisorbed oxygen in the surface to be decontaminated.

- The set of experimental data indicates that a lower treatment temperature and lower reactivity of the oxidant agent increase the $^{14}C/^{12}C$ ratio.

REFERENCES

[1]   ISO (International Organization for Standarization), "Long-Term Leach Testing of Solidified Radioactive Waste Forms", ISO 6961-1982(E).

[2]   Reference ALD-F patent EP2347422

[3]   J. Cobos, L. Gutiérrez, N. Rodríguez, E. Iglesias, G. Piña, E. Magro (CIEMAT). Irradiated Graphite Samples Bulk Analyses at CIEMAT. CARBOWASTE report (T.3.2.4).

[4]   Proceedings of ICAPP 2011, Nice, France, May 2-5, 2011; Paper 11267: Impermeable graphite: A new development for embedding radioactive waste; J. Fachinger1, K.H. Grosse1, R. Seemann2, M. Hrovat2 1FNAG, 2ALD Vacuum technologies, Wilhelm Rohn Str. 35;63450 Hanau; Germany

[5]   E. Magro, M. Rodríguez Alcalá, J. L. Gascón, G. Piña, E. Lara, L. Sevilla. WP5 CIEMAT Final Report on ^{14}C leaching from Vandellós I Graphite (D5.15)

[6]   "Leaching methods for conditioned radioactive waste". R.Carpentiero, P.Bienvenu, A.G.de la Huebra, C.Dale, D.Grec, C.Gallego, M.Rodriguez, F.Vanderlinden, ºP.I.Voors, J.Welbergen, R.Maz, J.Fazs. Report WG-B-02, Abril 2004.

[7]   J. Fachinger, W. von Lesa, T. Podruhzina. Decontamination of nuclear graphite. Nuclear Engineering and Design 238 (2008),3086-3091.

[8]   R. Holmes, B. Marsden, A. Jones. Mechanisms Involved in the Removal of Radioisotopes from Nuclear Graphite. First year report of PhD study, University of Manchester.

[9]   J. Cleaver. Thermal Treatment of irradiated Graphite for the Removal of ^{14}C.

CAST
Final report on results from Work Package 5:
Carbon-14 in irradiated graphite (D5.19)

2.8 Institutul National de Cercetare-Dezvoltare pentru Fizica si Inginerie Nucleara "Horia Hulubel" (IFIN-HH)

IFIN-HH's research activities were mainly performed in connection with Tasks 5.1, 5.2 and 5.3 within Work Package 5 (WP5) of the CAST Project.

During the first four years of the CAST Project, with respect to the RTD program, IFIN-HH participated in the Task 5.1 – "Review of CARBOWASTE and other relevant R&D activities to establish the current understanding of inventory and release of C-14 from i-graphites", Task 5.2 – "Characterisation of the C-14 inventory in i-graphites" and Task 5.3 "Measurement of release of C-14 inventory from i-graphites" is a fourth, i.e. this year activity. In the Task 5.1, IFIN-HH reviewed relevant existing information on the C-14 inventory in irradiated graphite and release of C-14 from irradiated graphites". For the Task 5.2, IFIN-HH explored the use of accelerator mass spectrometry to measure C-14 distributions in i-graphite and beta imaging to determine the distribution of C-14 and H-3 on graphite surfaces and prepared deliverable D5.7 "Report on C-14 distribution in irradiated graphite from research reactor VVR-S using accelerator mass spectrometry and beta imaging". In the Task 5.3 "Measurement of release of C-14 inventory from i-graphites" IFIN-HH developed a separation technique, based on silica gel columns and oxidation at high temperature over a CuO catalyst be decoupled with LCS device (TRICARB 2800 TR PerkinElmer) in order to measure the release rate of C-14 into gas and solution phase from irradiated graphite (intact and crushed samples from VVR-S reactor and prepared and prepared deliverable D5.14 "Release of C-14 from irradiated VVR-S graphite to solution and gas phase (Task 5.3). In conjunction with FZJ". In the last Task of WP5 (Task 5.5) that summarises and synthesises in a final report the work undertaken in the previous Tasks by all participants. The outcome of this Task is this deliverable D5.19 "Final report on results from WP5").

For the Task 5.1, IFIN-HH activities are completed. The main objective of the IFIN-HH in the first year of its input to Work Package 5 was to update the inventory of C-14 in the irradiated graphite arising from thermal column of VVR-S Reactor and radioactive wastes containing organic and inorganic C-14 compounds. Based on that, the draft input for

deliverable D5.5 "Review of current understanding of inventory and release of C-14 from irradiated graphites" was produced and sent to the RWM for the incorporation into the draft deliverable in the end of the first Project year. Some comments regarding IFIN-HH input were received. The IFIN-HH input then was updated based on the comments, and revised input for deliverable D5.5 was produced and sent to the RWM for the incorporation into the final deliverable. The final version of deliverable D5.5 is available on CAST Project public website.

For the Task 5.2, IFIN-HH activities are completed today. It should be noted, that samples extracted from discs 4, 5 and 6 of the thermal column (samples with high C-14 concentration were measured at 9 MV Tandem Accelerators, for a more accurate determination of C-14 concentration, at the beginning of this year when beam time at 9 MV Tandem accelerators was assigned. The results were included in this year report. The draft input draft for the deliverable D5.7 was produced and sent to Radioactive Waste Management (WP5 leader) for review and comments. Some comments regarding this report were received and were taken into account preparing the final version of the report.

For the Task 5.3 "Measurement of release of C-14 inventory from i-graphites" IFIN-HH activities are completed prepared the input for the deliverable D5.14 "Release of C-14 from irradiated VVR-S graphite to solution and gas phase", was produced and sent to RWM for the review and comments. Some comments regarding this report were received and were taken into account preparing the final version of the report.

MAIN RESULTS OF PROJECT CAST WP5

The aim of the research activities performed by IFIN-HH in the WP5 of the CAST project was to characterize the activity distribution of C-14 in the i-graphite of the thermal column of VVR-S research reactor and the release of C-14 from irradiated graphite to solution and gas phase. In connection with the first goal IFIN-HH developed a technique to characterize the C-14 concentration on the surface of the irradiated graphite form reactor VVR-S using accelerators mass spectrometry (AMS) 1 MeV and 9 MeV facilities. The method is suitable for a continuous measurement of the C-14 concentration in the depth of the material, providing a depth profile throughout the thickness of the graphite samples.

The total C-14 and H-3 activities in the i-graphite samples collected from the thermal column were measured based a separation technique, based on silica gel columns and oxidation at high temperature over a CuO catalyst that selectively oxidize components in the gas to H_2O and CO_2.

The text below presents only the summary of the work performed, whereas the full details are available in the CAST project deliverable.

Research reactor VVR-S

The VVR-S nuclear reactor from IFIN-HH is a research reactor with a maximum thermal power of 2 MW moderately cooled and reflected with distilled water, fuelled with enriched uranium 10% in the beginning and 36% subsequently.

Commissioned in 1957 and dedicated to nuclear physics research and radioisotopes production. Until 1984 the reactor was operated by nuclear fuel type EK-10 (10% enrichment) and from 1984, this fuel was replaced by S-36 (36% enrichment). The reactor was operational until 1997 when the reactor was definitively shut-down. On average, the reactor was operated 5 days per week at full or variable power levels. During 40 years of operation, the VVR-S reactor produced 9.59 Gadd. The maximum flow of the thermal neutrons was $2 \times 10^{13} \, \text{n/cm}^2\text{s}$.

A horizontal cross section of the reactor core is presented in the Figure 2.8.1.

Currently, the VVR-S Reactor is undergoing the decommissioning. The i-graphite grades, which are investigated in IFIN-HH, have been taken from thermal column of the VVR-S Research Reactors. The mobile thermal column (Figure 2.8.2) is made of 6 graphite discs placed on a mobile truck. Graphite bar-made discs are installed into a 20 mm wall thickness aluminium cylinder. Initially, the thermal column is provided with a cooling system that axially penetrated the graphite plate connected to the water-cooling system. As from the exploitation experience, it was concluded that this system is not necessary; it was given up. The horizontal tubes of the cooling system were filled with nuclear grade graphite rods of the same type as the discs of the thermal column (Figure 2.8.3).
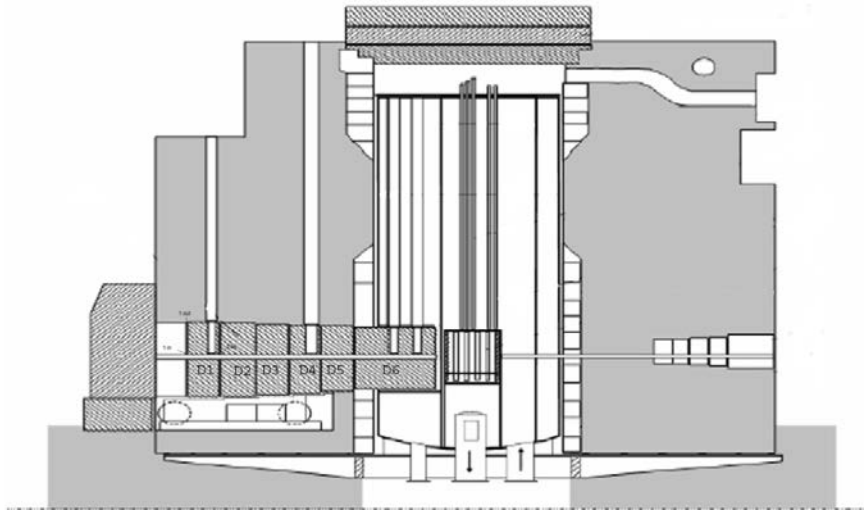
Figure 2.8.1: Vertical cut-view through the VVR-S reactor and the movable thermal column

Figure 2.8.2 Thermal column   **Figure 2.8.3** Thermal column disc no 6

The thermal column may be retreated by means of a rolling mechanism that drives the truck on which the graphite plates are mounted.

Irradiated graphite samples

Samples were collected after the final shut down and fuel removal of the reactor core. The irradiated graphite investigated at IFIN-HH has been taken from nuclear grade graphite rods which were used to fill the horizontal tubes of the cooling system of the thermal column of the VVR-S Research Reactor.

Two pieces of i-graphite have been cut from each graphite rod. One piece was cut from the rod's edge near to the reactor vessel (Samples 6-1, 5-1, 4-1, 3-1, 2-1, 1-1) and the other piece from the opposite part of the rod (Sample no 6-2, 5-2, 4-2, 3-2, 2-2, 1-2). An additional piece has been cut from the middle of the graphite rod located in the disc no 6. (Figure 2.8.4)
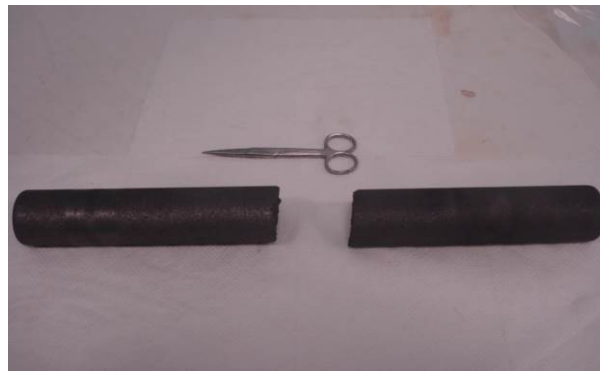
Figure 2.8.4 Irradiated graphite samples

Accelerators Mass Spectrometry (AMS) facility based on the 9 MV and 1 MV accelerators of IFIN-HH for measurements of C-14 concentration in i-graphite

Accelerators Mass Spectrometry (AMS) is a very unique and special method of selecting and counting atoms of a certain kind individually. It has the highest analysis sensitivity known today: 10^{-16} (ratio: isotope/element). By use of reference samples, it provides quantitative results expressed in suitable units (Bq/g, atoms/cm^3, atoms/l, etc.) which is a certain advantage compared to other employed methods.

AMS is measuring the rare isotopes concentration in a sample material if this is in solid state. The sample material has to be transformed into a confined ion beam, with good emittance, so that it can be transported on a long path through a particle accelerator and through many analyzers.

A typical AMS facility consists of four major parts: the ion injector (containing the ion source), the tandem accelerator; the high energy analyzing systems and the particle discrimination and detection system.

In this project depending on the concentrations of carbon two different AMS facilities were used, as follows:

1)   The AMS facility of the 9 MV Tandem accelerators:

- for C-14 exceeding the natural level of 10^{-12} for the ratio $^{14}C/^{12}C$ and for performing the depth profiling of the concentration in materials.

2)   The AMS facility at 1 MV Tandetron :

- for C-14 concentrations below the natural level of 10^{-12} for the ratio $^{14}C/^{12}C$.

The AMS facility at 9 MV Tandem Accelerators is shown schematically in Figure 2.8.6 and photos of the injector and the accelerator are presented in Figure 2.8.5 and 2.8.6, below.
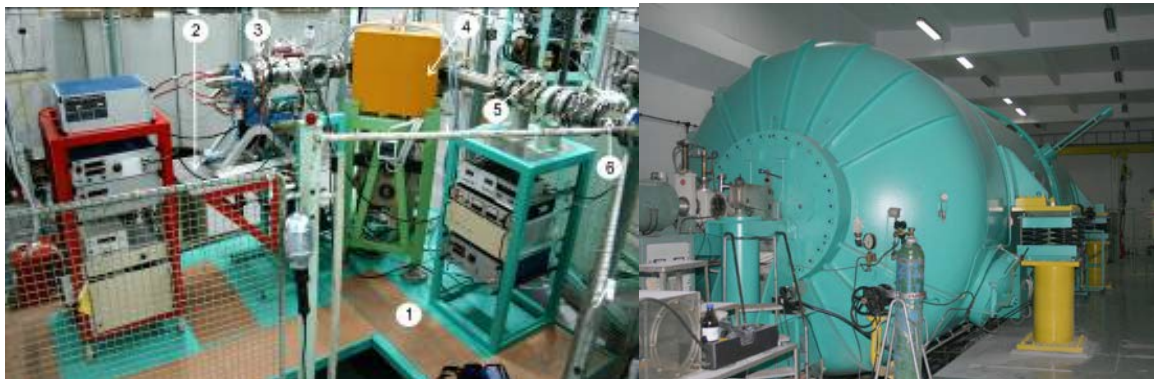
Figure 2.8.5 and Figure 2.8.6.
Left: Injector deck of the 9 MV Tandem AMS facility in Bucharest: 1) Injector platform polarized at -100 kV; 2) second platform polarized at -30kV in respect to the first platform; 3) the ion source (40 NC-SNICS); 4) 900 analyzing magnet; 5) slits and retractable Faraday cup; 6) pre-acceleration NEC tubes.
Right: the tandem 9 MV FN accelerator.

The second AMS facility, devoted to hyper-sensitive analyses is presented in Figure 2.8.7.

	CAST		
	Final report on results from Work Package 5:		
	Carbon-14 in irradiated graphite (D5.19)		
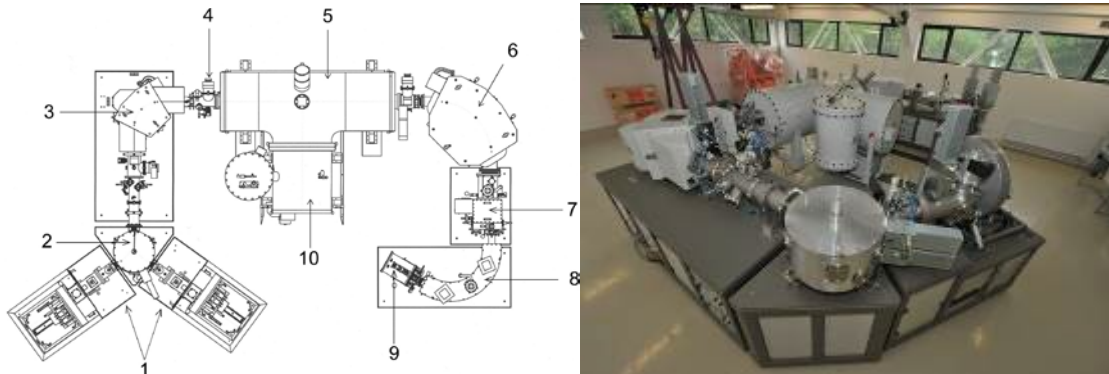
Figure.2.8.7. Left: the general layout of 1 MV HVEE AMS facility.
(1) Two ion beam injectors equipped with SNICS ion sources of type SO110 – 50 sample carousel HVEE and focusing ion lenses; (2) electrostatic switching system; (3) injection Magnet with multi beam switcher (bouncer); (4) faraday cup and Q-Snout device; (5) 1 MV tandetron accelerator, with gas stripper channel; (6) analyzing Magnet; (7) three offset Faraday cups; (8) electrostatic analyzer; (9) particle detector; (10) Cockcroft–Walton type HV power supply. Right: photograph of the facility.

Determination of C-14 in graphite samples collected from graphite column of the VVR-S reactor using AMS 1 MV facility

The sampling for the AMS analysis was performed from several positions inside and outside the graphite coating of the rod. About 20 mg of material of the samples (from both face of the samples) were transformed to powder and loaded and pressed into 8 sample holders of the ion source, together with reference and blank carbon samples (reference sample HOxII: 18.40 dpm/g/ 0.31 Bq/g).

The numerical results of the AMS measurements are listed in Table 2.8.1. All results were corrected for the background value and calibrated according to the reference samples.

Table 2.8.1 C-14 concentration in graphite samples

Sample	Outer side		Inner side		Average	
	Average (Bq/g)	Standard deviation	Average (Bq/g)	Standard deviation	Average (Bq/g)	Standard deviation
D1-2	0.64	0.04	6.85	0.45	0.69	0.04
D2-2	2.39	0.24	2.71	0.08	2.68	0.08
D2-1	3.73	0.3	8.48	0.43	5.29	0.25
D3-2	16.04	0.27	28.74	0.72	17.56	0.25
D3-1	20.28	0.95	29.13	1.61	22.55	0.82
D4-2	29.92	0.37	29.33	6.42	29.92	0.37
D4-1	14.88	0.22	27.95	0.13	24.67	0.11

C-14 concentration for disc 6 and 5 could not be measured, due to limitation of the 1MV AMS machine to concentrations exceeding the natural level of radiocarbon. These samples were re-measured at the AMS facility from the 9 MV accelerators that possess calibrated beam attenuators and are able to measure higher concentrations (by about a factor of 10^3).

AMS determination of C-14 in graphite samples of high radiocarbon concentrations collected from graphite column of the VVR-S

For measurement of high concentrations of radiocarbon samples and to provide the depth profile of the evolution of these concentrations towards the bulk, we used the AMS Depth profiling facility at the 9 MV tandem accelerators.

Since depth profiling is requiring a specialized ion source and special prepared acquisition we took advantage of the upgraded work performed at this machinery. Regarding the AMS measurement, since C-14 measurement implies the elimination of molecular interferences on the high energy side of the accelerator a velocity filter (Wien Filter) is a good the solution. Many interferences occur during C-14 measurements like $^{12}CH_2$, ^{13}CH, $^7Li_2$, ^{14}N etc. The elimination or reduction of these interferences was the major task of these measurements at this stage of the project, since the AMS facility at the 9 MV accelerators is not designed for such special analyses as are the dedicated C-14 machines today.

	CAST	
	Final report on results from Work Package 5:	
	Carbon-14 in irradiated graphite (D5.19)	

In our test experiments, we used the C-13 ion beam for tuning that is about 100 times less intense than the C-12 ion beam and therefore more suitable for the adjustment of the beam. Figure 2.8.8 shows the results of measurements performed in this AMS experiment. Four sectors from the disc 6, one from disc 5 and two rom disc 4 were measured. Disc 6 is located close to the active region, as mentioned before. C-14 concentrations are ranging from a maximum value of 74 kBq/g close to the reactor fission vessel down to about 2.6 kBq/g at the end of disc 6. In the next disc, first sector is even lower in the C-14 concentration. Exact values are given in Table 2.8.2.
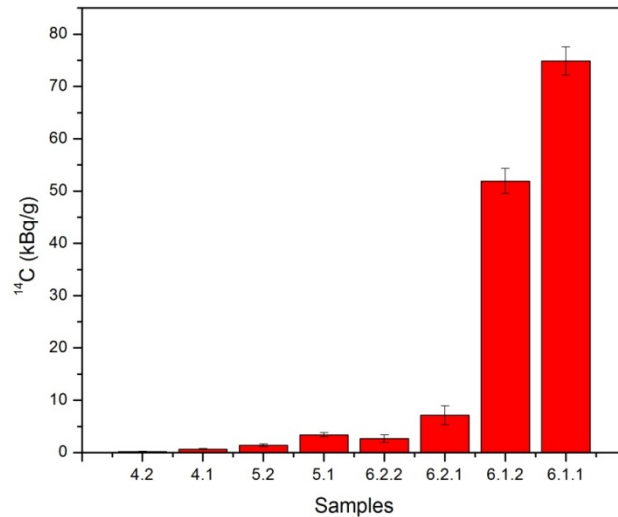
Figure 2.8.8: AMS measurement of C-14 concentrations in disc 6, disc 5 and disc 4 of the thermal column of the decommissioned VVR-S reactor

Table 2.8.2: C-14 measured values by AMS in the thermal column

Sample	4.2	4.1	5.2	5.1	6.2.2	6.2.1	6.1.2	6.1.2
C-14 (Bq/g)	212.7	653.3	1381.5	3402.1	2649.8	7121.2	51919.8	74850.7
Standard deviation	48.43	99.53	241.84	431.02	721.84	1830.65	2405.52	2673.14

Measurement of the total C-14 and H-3 concentration in the irradiated graphite

IFIN-HH developed gas sampling apparatus based on silica gel columns and oxidation at high temperature over a CuO catalyst be decoupled with LCS device (TRICARB 2800 TR PerkinElmer) in order to measure the total content of C-14 and H-3 of the i-graphite collected from the thermal column of the VVR-S reactor.

A layout of the apparatus designed at IFIN-HH is presented in Figure 2.8.9.
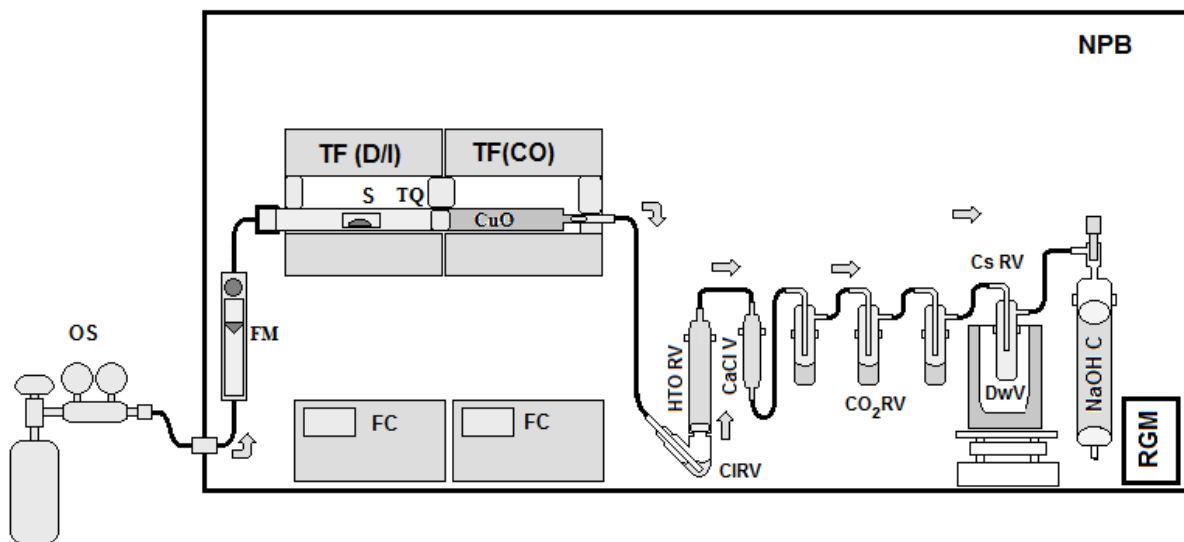
Figure 2.8.9: Schematic view of the oxidizer with separate retention of radionuclides of interest.
(QS- Oxygen supply; FM-Flow-meter; TF (D/I)- Tube furnace (Degassing/incineration); TF (CO)-Tube Furnace (catalytic oxidation); TQ- Quartz tube; S- Sample; CuO - CuO wire oxidation bed; ClRV – ^{36}Cl retention vials and saturator; HTORV- HTO retention cartridge; CO_2RV-ansembly with 3 CO_2 retention vials; CSRV- CARBOSORB retention vials ; DwV- Dewar vessel; NaOH C- retention cartridge with NaOH, RGM- Radioactive gas monitor).

Samples were taken from several positions along the thermal column of the rector. The weight of the samples was: 100.3-104.1 mg.

Based on activity value, sample weight and yield the specific activity of C-14 in each i-graphite sample was calculated.

C-14 and H-3 inventory in the thermal column of the VVR-S reactor

The result regarding the distribution of C-14 and H-3 specific activity along the axial direction in the graphite columns of the VVR-S reactor is presented in the next Figures 2.8.10 and 2.8.11 respectively.

Figure 2.8.10. C-14 specific activity distribution (kBq/g), along the thermal column of VVR-S reactor

Figure 2.8.11. H-3 specific activity distribution (kBq/g), along the thermal column of VVR-S reactor

CAST
Final report on results from Work Package 5:
Carbon-14 in irradiated graphite (D5.19)
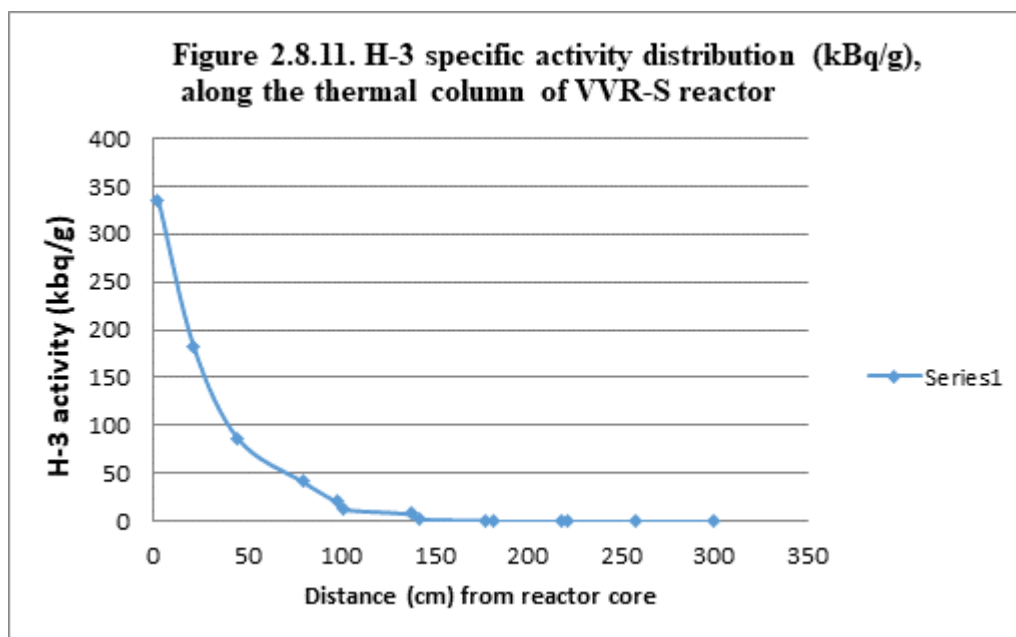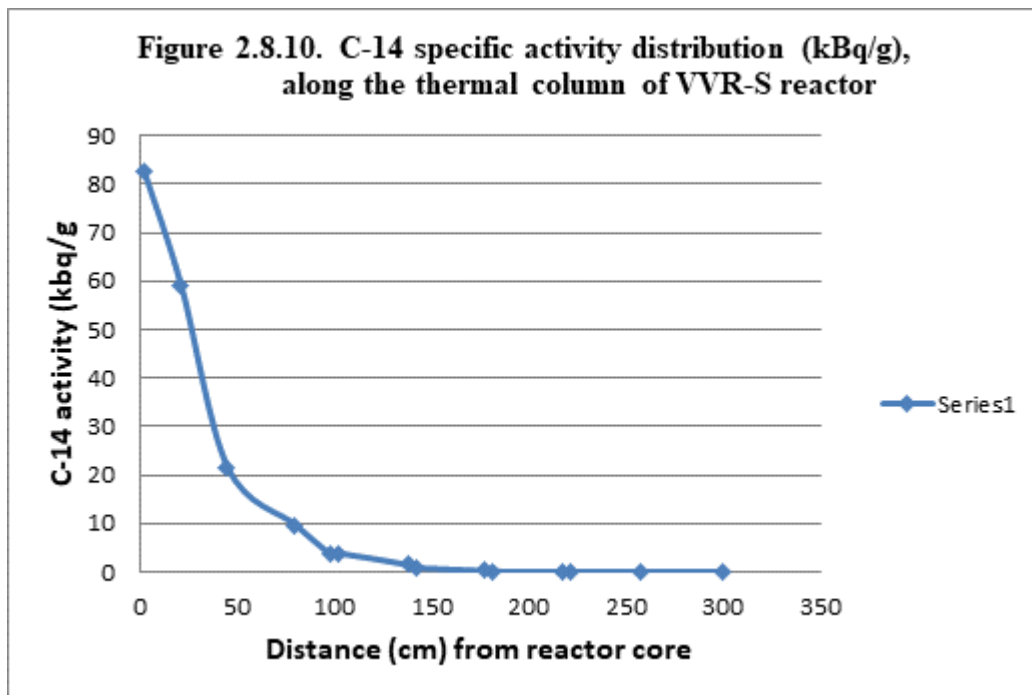
Estimation of C-14 inventory in the thermal column of VVR-S reactor

Based on the results of the specific C-14 activity and knowing the correspondence of the measured specific C-14 activity to the exact location in the graphite column and by applying quantities and masses of the graphite columns in the respective group, the integral C-14 activity in the graphite column was calculated, see Table 2.8.3.

Table 2.8.3 Estimation of C-14 inventory in the thermal column of VVR-S reactor

Graphite disc	1	2	3	4	5	6
Diameter (cm)	115	110	110	105	105	100
Length (cm)	40	40	40	40	40	40
Weight (kg)	715	660	670	595	610	1360
Average C-14 specific activity (Bq/g)	4.4	9.5	80.6	549.3	2665,6	35288.7
Average H-3 specific activity (Bq/g)	19.2	60.1	149.9	1918.1	10277.8	133414.2
Total C-14 activity in the graphite disc (Bq)	3.1×10^6	6.2×10^6	0.54×10^8	0.32×10^9	1.6×10^9	4.79×10^{10}
Total H-3 activity in the graphite disc (Bq)	28×10^6	39×10^6	1.0×10^8	1.1×10^9	6.3×10^9	18.1×10^{10}

Release of C-14 and H-3 from i-graphite to liquid phase.

Experimental methodology and results.

For the leaching test the graphite sampling was performed from the small graphite rod located around the central graphite rod of the disc no 6, which is near the reactor core. One piece was cut from rod's edge near the reactor vessel (**Sample 6.1**) and the other piece from the opposite part of the rod (**Sample 6.2**). From each piece collected from the graphite rod, two separate samples have been taken (e.g. Sample 6.1-1, Sample 6.2-1) (See Figure 2.8.12).
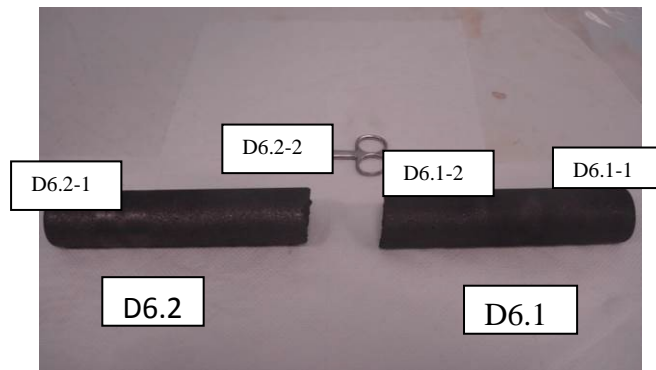
Figure 2.8.12: Irradiated graphite samples collected from the small rod of disc no 6

The graphite samples were placed in two 1-liter flasks with thread screw caps with 4 outlets/ inlets and were submerged in solution of 0.1 M of sodium hydroxide. The 700 ml of solution added to each flask ensured that the graphite samples were completely submerged.

To evaluate C-14 and H-3 long-term release in solution, under conditions relevant to a cement-based geological disposal facility, the leaching test was performed under nitrogen atmosphere in closed vessels and the sampling was performed at different time periods: the 1st, 7th 14th, 21st, 28th, 42nd days, 3rd, 6th, 9th and 12th months.

The starting inventory of C-14 in graphite samples was 6191.5 kBq for sample 6.1.1 and 338.4 kBq for sample 6.1.2 respectively; the inventory of H-3 was 21802.2 kBq for sample 6.1.1 and 2024.3 kBq for sample 6.1.2

The amount of C-14 and H-3 released in the liquid phase was measured by liquid scintillation counting using a TRICARB 3110 TR counter.

The C-14 average leaching rate (Bq/day and per g) and H-3 average leaching rate (Bq/day per g) were calculated by dividing the respective activities measured by the sampling period and the sample weight, (Table 2.8.4).

Table 2.8.4 Carbon-14 and Tritium average release rate into liquid phase

Sampling period	Graphite	sample 6.1.1	Graphite	sample 6.1.2
Day	C-14 average release rate (Bq/day per g)	H-3 average release rate (Bq/day per g)	C-14 average release rate (Bq/day per g)	H-3 average release rate (Bq/day per g)
1	259.6	30.66	9.39	0.744
7	92.55	6.43	1.77	0.032
14	43.02	3.26	0.92	0.112
21	27.66	2.73	1.30	0.013
28	30.58	3.05	0.66	0.039
42	3.69	1.01	0.08	0.009
56	1.88	1.24	0.04	0.009
77	1.03	0.43	0.03	0.007
180	0.32	0.10	0.02	0.006
270	0.24	0.04	0.02	0.005
365	0.13	0.01	0.01	0.001

Release of C-14 and H-3 from i-graphite to gas phase. Experimental methodology and results

Intact samples from VVR-S irradiated graphite have been cut from graphite disc no 6 and sealed in a glass vessel provided with 4 outlets and inlets. The first two trapping vessels contain 5 ml of sulfuric acid 0.1 N (for tritium trapping) each and the following three vessels contain 5 ml of Carbo-Sorb E (for C-14 trapping).

The sulfuric acid solutions in the first two vessels were mixed together. An aliquot (2 ml of retention solution) was transferred to a 20 ml LSC vial, and 16 ml of ULTIMA GOLD cocktail was added. The same procedure was followed for the vessels containing Carbo-Sorb, but this time Permafluor scintillator was used. C-14 and H-3 activity was measured by a TRICARB TR 2800 liquid scintillation counter.

Fourteen days after the samples were sealed, the vessel was connected to a catalytic oxidizer furnace that contains a CuO catalyzer inside. The C-14 and H-3 compounds released in the gas phase were oxidized in a low oxygen flow rate atmosphere and trapped separately in 5 vials (Figures 2.8.13 and 2.8.14). The measurement continued for one hour after the connection with the furnace was opened. At the end of the measurement the vessel containing the graphite samples was resealed and the experiment was repeated after 2 months.

Figure 2.8.13: Apparatus for C-14 and H-3 retention
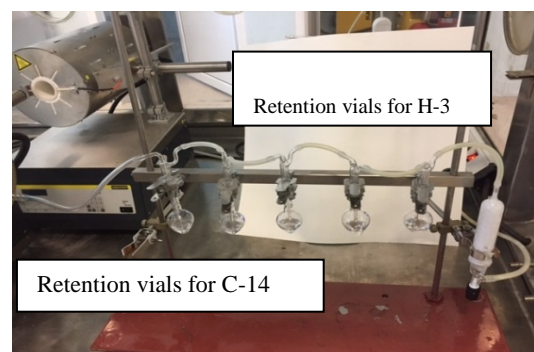
Figure 2.8.14: Vials for C-14 and H-3

The results are presented in Table 2.8.5.

Table 2.8.5 Carbon-14 activity and tritium activities in the gas phase

Sampling period (days)	C-14 total activity (Bq)	Background (Bq)	H-3 total activity (Bq)	Background (Bq)
14	0.9±12.5%*	0.5±0.3**	0.8±12.5%*	0.3±0.2**
60	12.15±12.5%*	0.5±0.3**	10.95±11.3%*	0.3±0.2**

* - overall uncertainties-estimated

**-2σ counting uncertainties

Conclusions

- Although the leaching experiment was primarily designed to measure C-14 release from irradiated VVR-S graphite to liquid and gas phase, the apparatus also allowed the measurement of H-3; these experimental results have been reported.

- The experiments to measure the release of C-14 and H-3 into liquid and gas phase were performed over a 12 months period. The irradiated graphite was collected from the thermal column of the VVR-S Reactor (at IFIN-HH). Two intact graphite samples were taken from the graphite rod located near the reactor core (graphite disc no 6) for use in the liquid leaching test. The mass of the samples were: 83.37 g and 79.88 g respectively. The graphite samples involved in the gas phase release experiment were taken from the same graphite rod. T

- The experiments were primarily designed to measure the total release of C-14 and H-3 into liquid and gas phase. The liquid leaching test was performed under condition similar to those relevant to geological disposal (NaOH solution 0.1 M, pH=10, anoxic conditions). Over the 365 days that the leaching experiment was running for, 2.27% of the initial C-14 inventory of graphite in sample 6.1.1 was released to the immersion solution, and 1.13% of the initial C-14 inventory of graphite in sample 6.1.2 was released to the immersion solution. In the case of H-3,

the percentages of the initial H-3 inventory released into the liquid phase were 0.073% and 0.016% respectively for these samples.

- The leaching rates for C-14 and H-3 were calculated by dividing the activity measured by the sampling period. As it can be seen, these leaching rates were high in the first period of the leaching test (30 days) with a maximum in the first week and then decreasing for both radioisotopes. Generally, the leaching rate for H-3 decreased with time to a lower value compared with C-14 leaching rate.

- The rate of release of C-14 into liquid phase decreased to 130 Bq /day per kg after 365 days for graphite sample 6.1.1 and to 10 Bq/day per kg for graphite sample 6.1.2.

- The rate of release of H-3 into liquid phase decreased to 10 Bq /day per kg after 365 days for graphite sample 6.1.1 and to 1 Bq/day per kg for graphite sample 6.1.2.

- The total C-14 released from graphite samples 6.1.1 and 6.1.2 and retained in solution represented approximately 2.271% of the initial estimated inventory and respectively 1.130%.

- The total H-3 released from graphite samples 6.1.1 and 6.1.2 and retained in solution represented approximately 0.073% of the initial estimated inventory and respectively 0.016%.

- The experimental results regarding the release of C-14 and H-3 from VVR-S irradiated graphite to liquid show that a major fraction of the total release occurs in the first months and a slower release on long time scale. However, these results should be applied cautiously for a long-time prediction.

- The total C-14 and H-3 released to gas phase represent approximately 0.00676% and respectively 0.00184% of the estimated inventory in the graphite samples.

- The extension of these results over a long period of time should be applied with caution due to the fact that small cracks could appear in graphite block in geological repository conditions and as a result, the release rate could increase.

However, on the basis of results presented herein, it is clear that the majority of C-14 and H-3 present in the samples of irradiated graphite tested is not released in leachate or as a gas over the timescale of the experiment; this is consistent with international work on other irradiated graphite.

CAST
Final report on results from Work Package 5:
Carbon-14 in irradiated graphite (D5.19)

2.9   Radioactive Waste Management (RWM)

Over the course of the EC CAST project, Radioactive Waste Management Limited (RWM, UK) undertook its role as Work Package 5 leader.

RWM contributed a summary of the results and understanding from their existing studies on carbon-14 release from irradiated graphite to WP5 of CAST under Task 5.1.

The release and migration of gaseous carbon-14-containing species has been identified as a key issue for geological disposal of intermediate-level radioactive wastes in the UK. A significant component of the carbon-14 in the UK radioactive waste inventory is present in irradiated graphite [see e.g. 2010 UK RWI, 2011] and this graphite has the potential to be a source of gases containing carbon-14 if it undergoes degradation or reaction in a repository environment. Earlier scoping calculations, undertaken prior to the EC CAST project, have shown that, if it is assumed that the carbon-14 in graphite reacts to form carbon-14-bearing methane ($^{14}CH_4$) and that this migrates as a free gas to the biosphere, there could be an impact on the calculated risk from the gas pathway [NDA, 2012]. An understanding of the release of carbon-14 from irradiated graphite under disposal conditions is therefore of importance to the post-closure safety case for a geological disposal facility (GDF) in the UK.

The current UK baseline for the disposal of irradiated graphite wastes envisages packaging in waste containers that will be emplaced in disposal vaults, which will be backfilled with a cement-based material designed to maintain a high pH environment in the vaults following their resaturation with groundwater. Conditions in a GDF are expected to become anoxic in the post-closure period as a result of the consumption of available oxygen by metal corrosion processes.

In initial experimental studies in the UK, small releases of gaseous carbon-14 were measured from samples of irradiated graphites (from the Windscale Advanced Gas-cooled Reactor (WAGR) [BASTON et al. 2004, HANDY, 2006] and the British Experimental Pile 0 reactor (BEP0) [MARSHALL et al, 2011, BASTON et al 2012]) on immersion in

alkaline solutions. The majority of the carbon-14 remained in the graphite although there was also some release of carbon-14 in a form that was retained in the liquid phase (possibly as the aqueous species $^{14}CO_3^{2-}$ resulting from the release of $^{14}CO_2$). In the measurements on BEP0 graphite, gaseous ^{14}CO and $^{14}CO_2$ were not distinguished, but the fraction of CO_2 in the gas phases was assumed to be negligible, due to its high solubility in alkaline solution. All of these studies were performed under oxic conditions and the impact of anoxic conditions on the speciation of released carbon-14 was not known.

Subsequent work has examined the release of gaseous carbon-14 from irradiated graphite from Oldbury Magnox power station [BASTON et al 2012, BASTON et al 2014]. The main objectives were to:

- determine the speciation and rate of gaseous release of carbon-14 from irradiated Oldbury graphite when in contact with alkaline solution under anoxic conditions and compare this to the release under oxic conditions;

- scope the effects of changes in pH, particle size and temperature on carbon-14 speciation and rate of release under anoxic conditions; and

- provide data and understanding for a possible update to the treatment of the releases of carbon-14 from irradiated graphite in assessment models.

Oldbury Graphite Studies

Experimental Summary

Eight segments (each about 30g in weight) of irradiated Magnox graphite were obtained. The segments had been cut from a cylindrical spacer piece obtained from an installed set that was removed from Oldbury Reactor 2 in 2005, some 38 years after installation.
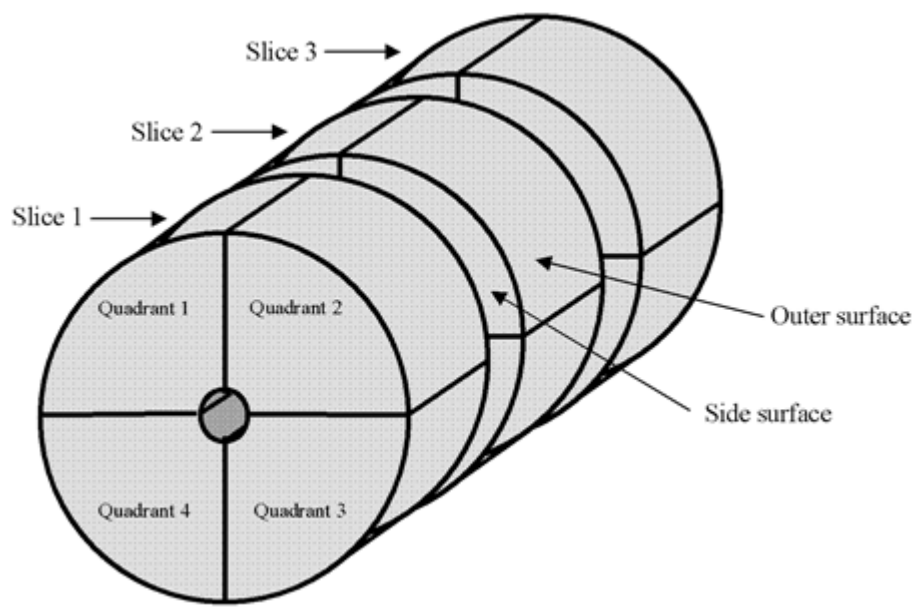
Figure 2.9.1: Schematic diagram of graphite sample locations [BASTON et al 2014].
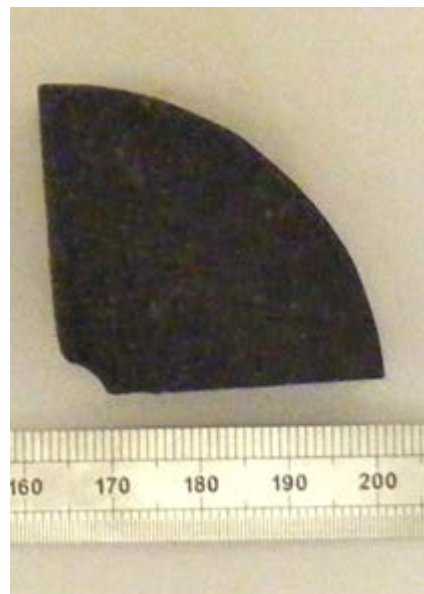
Figure 2.9.2: Graphite quadrant 635-BLOCK-1-2-2 [BASTON et al 2014].

Powdered sub-samples of the outer and inner (i.e. cut) surfaces of two of the segments were analysed for their radionuclide content to provide an estimate of the radionuclide inventory in each experiment.

Table 2.9.1. Specific activities of Carbon-14 measured in four samples taken from irradiated graphite block [BASTON et al 2014].

C-14 Specific activity (Bq g^{-1})			
1-2-3 Side	**1-2-3 Outer**	**1-3-1 Side**	**1-3-1 Outer**
$7.3 \times 10^4 \pm 0.9 \times 10^4$	$9.4 \times 10^4 \pm 1.0 \times 10^4$	$7.6 \times 10^4 \pm 0.5 \times 10^4$	$9.4 \times 10^4 \pm 0.7 \times 10^4$

The mean specific activity is $8.4 \times 10^4 \pm 1.1 \times 10^4$ Bq g^{-1}.

Seven leaching experiments were performed, each using a single segment of the irradiated graphite. Six experiments were designed to measure gaseous releases (with solution analysis on termination in some cases) and one to measure solution phase releases (only) with time for up to about one year after immersing the graphite in solution. The solution release experiment was performed independently from the gas release experiments, to avoid the possibility of disturbing the conditions in the reaction vessels in the gas-sampling experiments. Duplicate gas-release experiments and the solution release experiment were performed under anoxic, pH 13 conditions (in 0.1 mol dm^{-3} NaOH solution) at ambient temperature ('baseline' conditions) to simulate the post-closure conditions for disposal of graphite wastes in a cement-based GDF. The effects of oxic conditions, near-neutral pH, higher temperature (50°C) and reduced particle size (powdered sample) on the rates and speciation of gas-phase releases were investigated in variant experiments. Details of the seven experiments are summarised in Table 2.9.2.

Table 2.9.2: Summary of experimental conditions for leaching of irradiated Oldbury graphite [BASTON et al 2014].

Code.	Name	Solution pH	Atmosphere	Temperature	Graphite form	Duration
Run 1	Oxic	13	Air	Ambient	Intact	3 months
Run 2	Baseline 1	13	Nitrogen	Ambient	Intact	12 months
Run 3	Baseline 2	13	Nitrogen	Ambient	Intact	12 months
Run 3b	Solution sampling	13	Nitrogen	Ambient	Intact	12 months
Run 4	Neutral pH	7	Nitrogen	Ambient	Intact	3 months
Run 5	Powdered graphite	13	Nitrogen	Ambient	Powder	3 months
Run 6	Higher temperature	13	Nitrogen	50°C	Intact	3 months

The speciation of gaseous carbon-releases was investigated using a sampling apparatus capable of separating carbon dioxide, carbon monoxide and volatile hydrocarbons / organic compounds. A schematic diagram of the experimental set-up is shown in Figure 2.9.3.
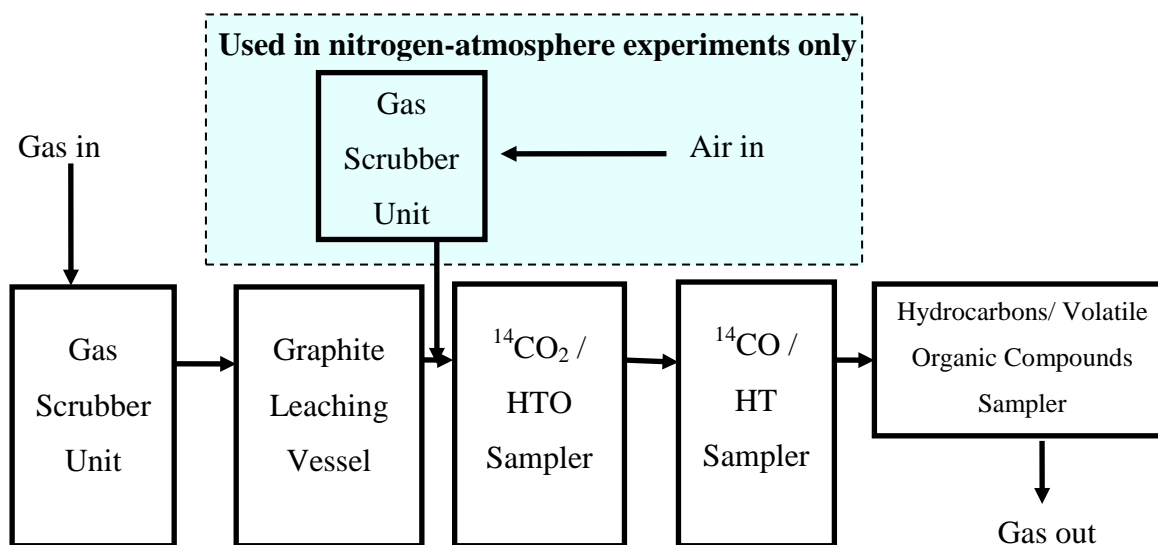
Figure 2.9.3: Schematic diagram of experimental apparatus [BASTON et al 2014]

Summary of Results

The cumulative activities of $^{14}CO_2$, ^{14}CO and $^{14}CH_4$ released to the gas phase on leaching are presented in Table 2.9.3. Figure 2.9.4 shows the total cumulative fractional release of carbon-14 to the gas phase from each experiment and compares this to the more limited data obtained for irradiated WAGR and BEP0 graphites.

Figure 2.9.5 shows the cumulative fractional release of carbon-14 to solution in the solution monitoring experiment (Run 3b). The solution concentrations in the gas monitoring experiments were measured only at the end, to avoid breaking the integrity of the system during the experiments. Figure 2.9.5 shows the uncertainty on the solution measurements as error bars, with the errors introduced by the uncertainty on the graphite inventory shown as the pink and blue lines (these are the upper and lower bound on fractional release based uncertainty in the graphite inventory and do not include uncertainties in solution concentration. In the solution monitoring experiment (Run 3b), 0.06% of the carbon-14 (1.6 kBq) was leached into solution in one year and appeared to still be rising. Solution phase measurements at the end of the baseline gas monitoring experiments showed similar fractional releases of carbon 14 in the range 0.06 to 0.08% at 12 months. Powdered graphite released 0.04% of the carbon-14 into solution in 3 months.

Table 2.9.3: Cumulative gaseous release of carbon-14 from irradiated Oldbury graphite [BASTON et al 2014].

Run	Conditions	Time (days)	Cumulative Gaseous C-14 Release			
			CO_2 (Bq)	CO (Bq)	Organic (Bq)	Total
1	Oxic, single piece of graphite pH 13, 20°C	7.0	0.04 ± 0.001	1.73 ± 0.02	1.67 ± 0.01	3.44 ± 0.02
		28.8	0.05 ± 0.001	2.13 ± 0.02	1.99 ± 0.01	4.17 ± 0.03
		70.9	0.07 ± 0.002	2.51 ± 0.03	2.38 ± 0.02	4.96 ± 0.04
2	Anoxic, single piece of graphite pH 13, 20°C	2.9	0.01 ± 0.001	0.44 ± 0.02	1.42 ± 0.07	1.87 ± 0.07
		7.0	0.03 ± 0.001	1.00 ± 0.04	2.45 ± 0.09	3.48 ± 0.09
		31.0	0.04 ± 0.002	1.47 ± 0.04	3.11 ± 0.09	4.62 ± 0.1
		94.0	0.05 ± 0.002	1.89 ± 0.05	3.88 ± 0.10	5.82 ± 0.11
		365.0	0.12 ± 0.004	2.42 ± 0.05	5.08 ± 0.12	7.62 ± 0.13
3	Anoxic, single piece of graphite, pH 13, 20°C	2.3	< 0.01	0.54 ± 0.03	0.94 ± 0.05	1.48 ± 0.06
		7.3	< 0.02	0.86 ± 0.04	1.96 ± 0.07	2.82 ± 0.08
		31.2	< 0.03	1.07 ± 0.04	2.34 ± 0.07	3.41 ± 0.08
		99.2	0.08 ± 0.04	1.37 ± 0.04	3.02 ± 0.09	4.47 ± 0.11
		366.0	0.29 ± 0.04	2.03 ± 0.05	4.46 ± 0.12	6.78 ± 0.13
4	Anoxic, single piece of graphite, pH 7, 20°C	7.1	30.7 ± 1.6	1.43 ± 0.07	3.45 ± 0.18	35.6 ± 1.6
		30.1	49.8 ± 1.7	1.7 ± 0.1	4.46 ± 0.19	55.9 ± 1.7
		93.1	121.9 ± 4.0	2.41 ± 0.11	5.44 ± 0.19	129.7 ± 4.0
5	Anoxic, graphite powder, pH 13, 20°C	7.0	0.09 ± 0.01	0.39 ± 0.02	0.91 ± 0.05	1.39 ± 0.05
		28.0	0.10 ± 0.01	0.68 ± 0.03	1.31 ± 0.05	2.09 ± 0.06
		91.0	0.52 ± 0.02	0.88 ± 0.03	1.52 ± 0.05	2.92 ± 0.07
6	Anoxic, single piece of graphite, pH 13, 50°C	6.9	0.10 ± 0.01	2.05 ± 0.11	5.26 ± 0.23	7.41 ± 0.26
		28.0	0.31 ± 0.02	2.72 ± 0.12	6.18 ± 0.23	9.21 ± 0.26
		94.2	0.39 ± 0.02	2.92 ± 0.12	6.59 ± 0.24	9.9 ± 0.27
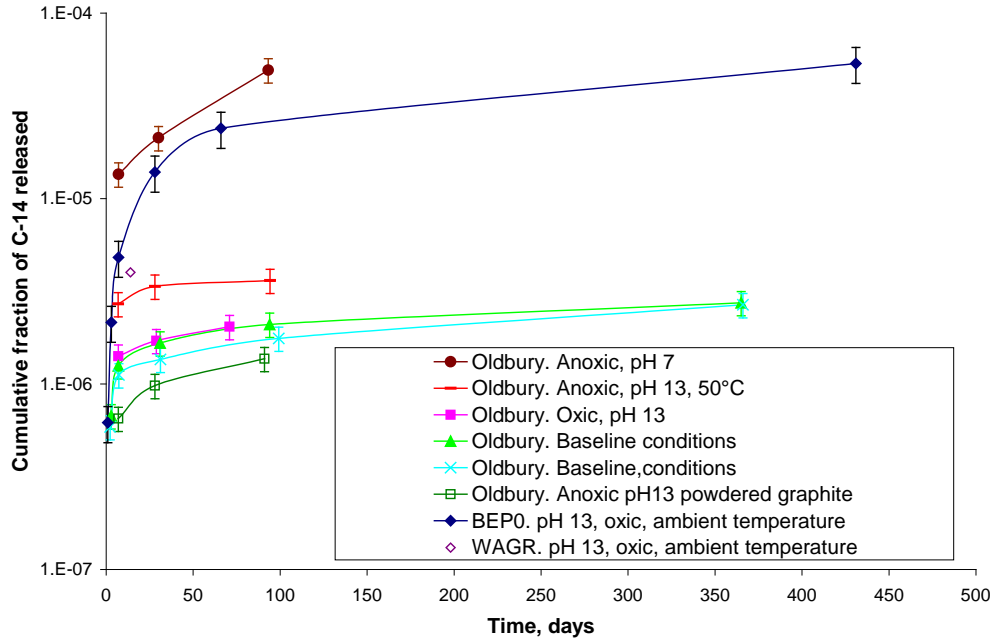
Figure 2.9.4: Total cumulative releases of carbon-14 from Oldbury graphite to the gas phase compared with data for BEP0 and WAGR graphites; error bars show combined uncertainty of carbon-14 content of the graphite and the measurement in the gas phase [BASTON et al 2014].
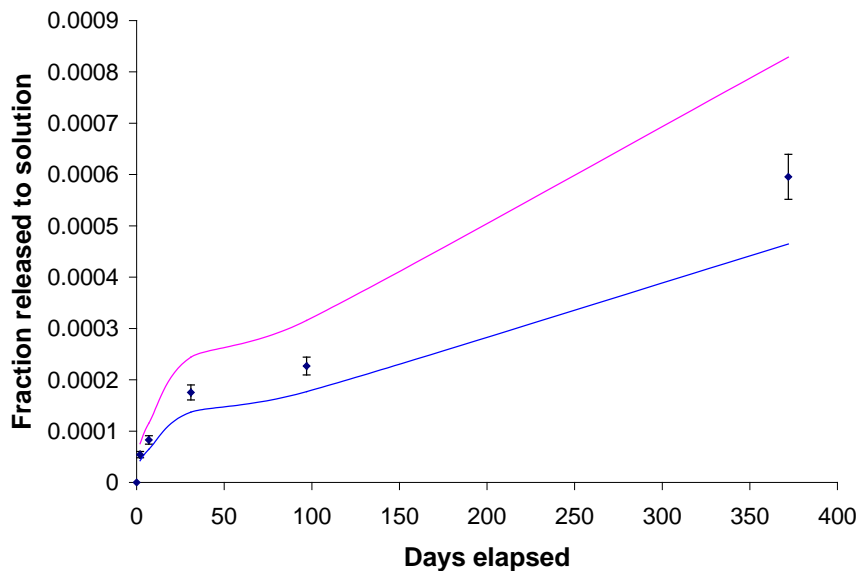
Figure 2.9.5: Fractional carbon-14 releases to solution in Oldbury graphite leaching experiment under anoxic conditions at pH 13 and ambient temperature. Error bars show the uncertainties on solution concentration measurements; pink and blue lines

show systematic errors based on the uncertainty in the graphite inventory [BASTON et al 2014]

Conclusions from the Study

The main conclusions from the study are given below.

- Under baseline conditions (anoxic, under pH 13 solution, ambient temperature), the predominant carbon-14 release was to the solution phase, with about 0.07% of the carbon-14 inventory being released into solution in one year. About 1% of the released carbon-14 was released to the gas phase.

- In all five of the gas-phase release experiments under high-pH conditions, broadly similar levels of total carbon-14 release were observed to the gas phase from each of the five graphite segments on comparable timescales.

- In all seven experiments, for both gaseous and solution-phase release, an initial phase of rapid carbon-14 release was observed, which was followed (beyond about 28 days) by a longer-term phase of slower release.

- Under baseline conditions (anoxic, under pH 13 solution, ambient temperature, single piece graphite sample):

  o an initial rapid release of ~3 Bq of carbon-14 to the gas phase was observed in the first week, which represents ~ 10^{-6} of the carbon-14 in the graphite;

  o the rates of release decreased with time but detectable quantities of carbon-14 were found in all gas samples. For the final cumulative sampling period, which ran from three to twelve months, a release of ~2 Bq was measured;

  o the gaseous carbon-14 was predominantly in the form of hydrocarbons and other volatile organic compounds and CO. The ratio of carbon-14 in hydrocarbons / organic compounds to CO was approximately 2:1. Less than 2% of the gas-phase release was in the form of $^{14}CO_2$.

- When the graphite was powdered, the rapidly releasable fraction of carbon-14 to the gas phase was found to be lower (by a factor of ~2) than from leaching intact segments, whereas the total solution phase release after 91 days was higher (by about 65%). This contrasting behaviour is most likely due to a loss of loosely-bound volatile carbon-14 species during the powdering process and an overall increase in release rate, primarily to solution, due to the increased surface area of the sample.

- At pH 7, levels of ^{14}CO and carbon-14 bearing volatile organic compounds were similar to the baseline values. However, the overall gaseous carbon-14 release was at least an order of magnitude higher than the baseline, due to significantly more $^{14}CO_2$ being released as gas from solution rather than being retained as dissolved carbonate.

- There is some evidence that increased temperature increases the release rate of carbon-14, but this observation is from a limited set of data.

- Under oxic conditions the total carbon-14 gaseous release rate was similar to the baseline condition values but the ratio of organic compounds to CO was closer to 1:1. The rates of carbon-14 release from Oldbury graphite were significantly lower than those measured previously from irradiated BEP0 graphite under oxic conditions, but the ratio of hydrocarbon / organic species to CO was higher.

- The differences between the fractional releases of carbon-14 from Oldbury and BEP0 graphites are likely to be due to differences between the original graphites, their irradiation histories, operating temperatures and coolant gases. The results of this study do not allow us to determine whether any one of these differences is a dominant effect although a wider comparison of irradiated graphites might.

Application in modelling gas generation

A tool commonly used in RWM work in relation to gas generation calculations for UK waste is SMOGG ("Simplified Model Of Gas Generation") [e.g. Swift & Rodwell, 2006; note this software is regularly updated, please check the RWM bibliography (https://rwm.nda.gov.uk/publications) for more recent versions]. SMOGG models the

generation of bulk and radioactive gases from waste packages or groups of waste packages. SMOGG includes a model for the generation of carbon-14 from irradiated graphite, which was developed on the basis of only limited data on gaseous carbon-14 releases from the sources available at the time. As a result of this study and other recent work [McDermott, 2011], an updated conceptual model for carbon-14 releases from irradiated graphite has been proposed, a revised mathematical model has been formulated and the data obtained for Oldbury Magnox graphite have been fitted to illustrate how the proposed model may be parameterised [BASTON et al, 2014]. This is implemented in SMOGG version 7.0 [Amec Foster Wheeler, 2016a and 2016b].

RWM irradiated graphite studies undertaken in parallel to the EC CAST project

Additional work RWM has been involved with over the duration of CAST has further considered carbon-14 / irradiated graphite (RWM, 2016; AMEC, 2016). A main purpose of reviewing the experimental evidence on carbon-14 release from graphite in these parallel studies was to provide information to revise the model used to calculate this release from graphite wastes and to parameterise the revised model for deployment in an update to SMOGG. The main requirements for the model are information on the rate and extent of release of the carbon-14 and on the speciation of the released carbon-14.

The key findings relating to the **rate and extent of carbon-14 release** are:

- In general, only a small fraction of the total carbon-14 inventory (up to ~1% for conditions expected in packages and in a GDF, and under 30% even for harsh acidic conditions) is released on leaching in solution over timescales of up to 4 years;

- A significant fraction of carbon-14 in irradiated graphite appears to be bound up as part of the graphite matrix and is inaccessible to leaching;

- There is an initial fast release followed by an approach to a steady state with a very low incremental release rate (continuing for at least 4 years in some cases);

- Total fractional releases and rates of release may depend on the type of graphite, its irradiation history and the reactor operational conditions.

The key findings relating to the **speciation of the released carbon-14** are:

The ratio of the solution to gas phase releases is typically of the order of 100, and ranges from about 10 to a few hundred;

- Carbon-14 is released to the solution phase in organic as well as inorganic ($^{14}CO_2$/carbonate) forms under alkaline conditions and the organic fraction may be a substantial component of the overall amount released;

- Gas phase releases include both volatile ^{14}C-organics (probably $^{14}CH_4$) and ^{14}CO ($^{14}CO_2$ is also purged from solution at near-neutral pH);

- The form of gaseous carbon-14 release is affected by the redox conditions; lower redox seems to favour ^{14}C-organics, but the total carbon-14 release to the gas phase may be similar;

- The proportion of each gas phase species differs between graphite samples from different sources.

The above findings provide empirical data on which to base a revised model for carbon-14 release from graphite. Some information is also available on the mechanisms of release, as well as on the location and form of carbon-14 in graphite.

The key findings on the **location and form of carbon-14** in graphite and on the **mechanisms of its release** are:

- The chemical form of carbon-14 is primarily elemental and is bound covalently in the graphite structure;

- There is evidence that the major fraction of the carbon-14 is distributed homogeneously throughout the graphite matrix (arising primarily from the activation of carbon-13) and that a minor fraction is distributed heterogeneously,

enriched in hotspots and on surfaces; the latter fraction of carbon-14 is potentially more accessible for leaching;

- The release of carbon from the surface of unirradiated graphite is dependent in part on the presence of oxygen; water is required to catalyse the reaction in some way at low temperatures;

- Oxygen-containing surface species have been observed on irradiated graphites that are chemically similar to the intermediates formed on carbon surfaces during oxidation at elevated temperatures; the release of $^{14}CO_2$ as a major product is consistent with the principal mechanism of carbon-14 release being an oxidation process;

- The association of hydrogen with active carbon sites could provide a mechanism for the formation of hydrocarbons and/or other volatile organic species;

- The graphite matrix is extremely resistant to oxidation at GDF temperatures and is unlikely to undergo further chemical oxidation once GDF conditions have become anaerobic and all surface oxygen species have been consumed.

The information on the location and form of carbon-14 in graphite and on the mechanisms of its release is provided by fundamental studies, rather than experiments specifically designed to provide data on the leaching behaviour of carbon-14 from graphite. It therefore complements the leaching data and provides additional justification for the key features that should be included in the revised model. Nonetheless, it does not provide sufficient information on the mechanisms of release to justify the use of a mechanistic model.

Based on the findings of the review of experimental evidence, it is considered that:

- A substantial fraction of the carbon-14 in graphite is not releasable;

- Some carbon-14 will initially be released rapidly, and some will be released more slowly at a rate reducing over time (i.e. the release cannot be defined by a single rate constant);

- Carbon-14 can be released to both the gas and aqueous phases. Carbon-14 released to the aqueous phase may exist as CO_2/carbonate and as organic species. Carbon-14 released to the gas phase may exist as a number of different species with potentially different consequences, including organic species (e.g. CH_4), CO_2 and CO;

- Release rates and speciation of the released carbon-14 may change depending on the conditions (e.g. pH, presence of oxygen).

The SMOGG model used by RWM to calculate gaseous carbon-14 release from graphite has subsequently been updated (SMOGG version 7.0 [Amec Foster Wheeler, 2016a and 2016b]). The main change to the model has been to include the release fractions. This results in much less carbon-14 being released in total. In addition, potential release of carbon-14 as three separate species ($^{14}CH_4$, ^{14}CO and $^{14}CO_2$) is explicitly accounted for.

An exercise has been undertaken to parameterise the updated model. Values for the fractions of carbon-14 released, carbon-14 release rates and speciation fractions for the released carbon-14 for several sets of conditions have been defined. For each parameter a best estimate, and upper and lower bounds have been specified to allow uncertainty in the parameters to be considered. Table 2.9.4 shows these release model parameters, and Table 2.9.5 presents speciation parameters (the fraction released as CO_2 is assumed to be the sum of the $^{14}CO_2$ measured in the gas phase (this is only significant for neutral pH conditions) and the total carbon-14 in solution, some of which could be organic. For high pH conditions, the proportion released as gaseous carbon dioxide is small in comparison to the fractions released as carbon monoxide and methane).

Table 2.9.4 Parameter values for carbon-14 release

Parameter	Lower bound	Best estimate	Upper bound
Rate constant for the rapid release of carbon-14 from graphite (k_{ca})	10 yr^{-1}	30 yr^{-1}	100 yr^{-1}
Rate constant for the slower release of carbon-14 from graphite (k_{cc})	1 10^{-3} yr^{-1}	1 10^{-2} yr^{-1}	1 10^{-1} yr^{-1}
Fraction of the carbon-14 activity in the graphite that is available for rapid release	0	2 10^{-4}	2 10^{-3}
Fraction of the carbon-14 activity in the graphite that is available for slower release	1 10^{-2}	5 10^{-2}	3 10^{-1}

Table 2.9.5 Parameter values for speciation of released carbon-14

Conditions	Fraction released as CO_2	Fraction released as CO	Fraction released as CH_4
Aerobic, neutral pH	0.99	0.0050	0.0050
Aerobic, high pH	0.99	0.0050	0.0050
Anaerobic, high pH	0.99	0.0033	0.0066

Tables 2.9.4 and 2.9.5 are offered as examples of possible parameterisation to be considered in modelling carbon-14 release from irradiated graphite in the context of deep geological disposal in a cementitious repository.

Figure 2.9.6 illustrates the revised conceptual model of carbon-14 release from irradiated graphite for use in the UK programme, including release rates and percentages of affected carbon-14; note that the majority of carbon-14 in irradiated graphite is not considered releasable under conditions appropriate to a deep geological disposal facility.
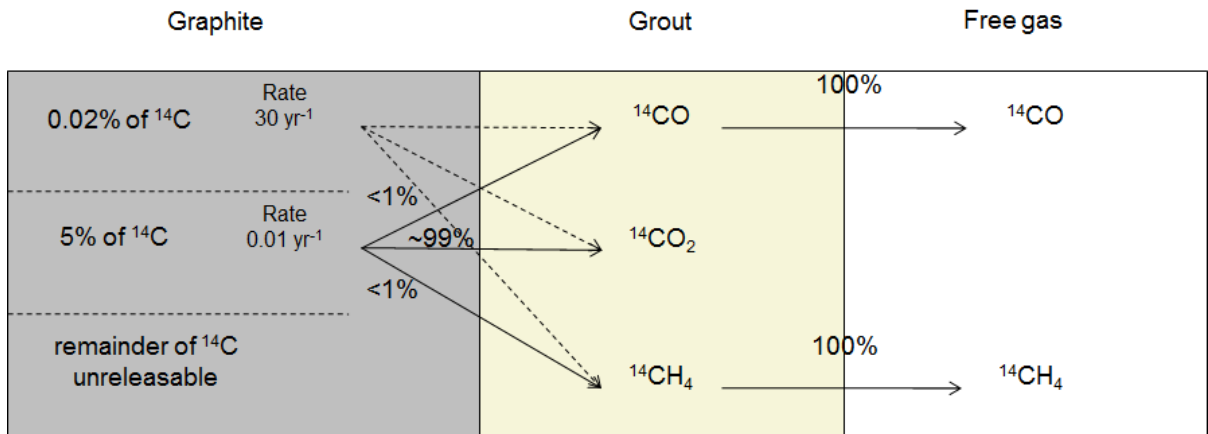
Figure 2.9.6 Improved conceptual model for carbon-14 release from graphite

	CAST	
	Final report on results from Work Package 5:	
	Carbon-14 in irradiated graphite (D5.19)	

References

AMEC report to RWM, Carbon-14 Project Phase 2: Irradiated Graphite Wastes, AMEC/200047/004 Issue 2, 2016, https://rwm.nda.gov.uk/publication/carbon-14-project-phase-2-irradiated-graphite-wastes/

Amec Foster Wheeler report to RWM, Specification for SMOGG Version 7.0: A Simplified Model of Gas Generation from Radioactive Wastes, AMEC/204651/001, Issue 2, https://rwm.nda.gov.uk/publication/specification-for-smogg-version-7-0-a-simplified-model-of-gas-generation-from-radioactive-wastes/, 2016a.

Amec Foster Wheeler report to RWM, User Guide for SMOGG Version 7.0: A Simplified Model of Gas Generation from Radioactive Wastes, AMEC/204651/002, Issue 2, https://rwm.nda.gov.uk/publication/user-guide-for-smogg-version-7-0-a-simplified-model-of-gas-generation-from-radioactive-waste/, 2016b.

BASTON, G.M.N., CHAMBERS, A.V., COWPER, M.M., FAIRBROTHER, H.J., MATHER, I.D., MYATT, B.J., OTLET, R.L., WALKER, A.J. and WILLIAMS, S.J. 2004. The Release of Volatile Carbon-14 from Irradiated Graphite in Contact with Alkaline Water, Serco Assurance Report SA/ENV-0654.

BASTON, G.M.N., MARSHALL, T.A., OTLET, R.L., WALKER, A.J., MATHER, I.D. and WILLIAMS, S.J. 2012. Rate and Speciation of Volatile Carbon-14 and Tritium Releases from Irradiated Graphite, Mineralogical Magazine 76(8), 3293-3302, 2012.

BASTON, G., PRESTON, S., OTLET, R., WALKER, J., CLACHER, A., KIRKHAM, M. and SWIFT, B. 2014. Carbon-14 release from Oldbury Graphite, Amec report AMEC/5352/002 Issue 3.

HANDY, B.J. 2006. Experimental Study of C-14 and H-3 Release from Irradiated Graphite Spigot Samples in Alkaline Solution, NNC Report 11996/TR/001.

MARSHALL, T.A., BASTON, G.M.N., OTLET, R.L., WALKER, A.J. and MATHER I.D. 2011. Longer-term Release of Carbon 14 from Irradiated Graphite, Serco Report SERCO/TAS/001190/001 Issue 2.

McDERMOTT, L. 2011. Characterisation and Chemical Treatment of Irradiated UK Graphite Waste, PhD thesis, University of Manchester.

NUCLEAR DECOMMISSIONING AUTHORITY, 2012. Geological Disposal, Carbon-14 Project, Phase 1 Report, NDA Report NDA/RWMD/092.

RADIOACTIVE WASTE MANAGEMENT, Geological Disposal: Carbon-14 Project Phase 2: Overview report, NDA Report no. NDA/RWM/137, 2016, https://rwm.nda.gov.uk/publication/geological-disposal-carbon-14-project-phase-2-overview-report/.

	CAST	
	Final report on results from Work Package 5:	
	Carbon-14 in irradiated graphite (D5.19)	

SWIFT, B.T. and RODWELL, W.R. 2006. Specification for SMOGG Version 5.0: a Simplified Model of Gas Generation from Radioactive Wastes, Serco Report SERCO/ERRA-0452 Version 6.

The 2010 UK RADIOACTIVE WASTE INVENTORY: Main Report, URN 10D/985, NDA/ST/STY(11)0004, 2011.

2.10 State Institution "Institute of Environmental Geochemistry National Academy of Science of Ukraine" (IEG NASU) summary

IEG NASU is involved in the review of the outcome of the IAEA project investigating conversion of i-graphite from decommissioning of Chernobyl NPP into a stable waste form. IGNS will also provide input on the use of graphite in the RBMK reactor, particularly the decommissioning of each category, classification, volume, weight and activity.

It is intended to draw together relevant existing information on the ^{14}C inventory in irradiated graphite, its form and leaching behaviour and treatment and packaging for geological disposal.

IEG NASU will review characterisation data on the speciation of ^{14}C in RBMK reactor, i-graphites and relevant information from decommissioning projects in Ukraine.

Progress in Task 5.1

The inventory of i-graphite in Ukraine is not made completely. In compliance with the requirements of the regulatory documents, the composition and activities of radionuclides accumulated in structural materials and structures during the operation of the NPP power unit must be evaluated before its removal from service.

At present the reactors of Chornobyl NPP, power units 1, 2, and 3 are shut down (1996, 1991, 2000) and are at the stage of final shutdown or preservation stage.

The waste inventory of irradiated graphite of Chornobyl NPP (Units 1-3) is 5687 tonnes (3732m^3) and of emergency graphite is 700 tonnes in the shelter.

After the shutdown of the RBMK reactor the graphite stack and graphite elements of channels may account for as much as 80% of the total amount of radioactive waste. However, the estimates are to a large extent dependent on the impurity content of the graphite.

Table 2.10.1. The waste inventory of irradiated graphite waste of Chernobyl NPP

Group	Volume, m^3	Weight, t	A$_{Specific.}$ Bq/g	Brand
Graphite stack	3732	5280	~ E+4 – E+5	GR-280
Graphite rings and bushings	328	372	~ E+4 – E+5	GRP-2-125
Graphite displacer control rods	22	35		GR-93

The mass of i-graphite of those reactors still needs to be quantified in more detail.

The duration of the reactor operation the graphite was in the nitrogen–helium medium, incidents due to leakage of water coolant into the stack occurred.

Three major contamination sources for the graphite are:

- Neutron activation of impurities;

- Delivery of radionuclides as a result of technological incidents during the reactor operation;

- External contamination of the graphite by radionuclides of corrosive origin those are present in the CP water.

Nuclear graphites have been manufactured from a range of raw materials using different manufacturing processes, this includes differing impurity levels. Original impurities in the reactor graphite include a large number (up to 30) of naturally occurring elements with the concentration 10^{-4}–10^{-6}% by mass, many of which form long-lived radionuclides through the neutron reactions.

Graphite waste management

At the Chernobyl NPP a considerable amount of equipment and special items used during the Power Units operation. Currently, they are stored in cooling pools, technological shafts, and in a reactors core of Units 1-3. A total amount of these special items (long-length waste)

is about 26.000 units. According to the design dimensions of these special items are from 6 to 22 meters in length and up to 145 mm in diameter.

Technological channels include 19 pcs. of the graphite sleeves and 163 graphite rings. Graphite removed using techniques and equipment removal graphite.

Removal device graphite rings and bushings

The primary packaging will be the 165 or 200 liters barrels placed in a concrete container GTZ-2.6. The limiting values of total activity in these primary packages should be:

- the 165-liter barrel of long-length special items (cuttings and milling) - 4,32 10^{12}Bq/barrel;

- the 200-liter barrel of graphite of low-and intermediate level (grinding matter) - 4,11 10^{10}Bq/barrel.

- Packages with graphite will be placed in temporary storage (up to 30 years) in an existing store of solid waste;

- Graphite waste emplaced in the storage/disposal container without grouting.

Progress in Task 5.3

IGNS will examine the effect of etching and removing the surface layer of graphite and study the long–term behaviour of 14C in concrete waste packages.

As graphite is bombarded with neutrons, C-14 is produced through neutron capture by carbon-13 (C-13), nitrogen (N-14), and oxygen-17 (O-17) as seen in Equations 1, 2, and 3 [1].

$$\text{N-14} + n \rightarrow \text{C-14} + p \text{ (Eqn. 1)}$$

$$\text{C-13} + n \rightarrow \text{C-14} + \gamma \text{ (Eqn. 2)}$$

$$\text{O-17} + n \rightarrow \text{C-14} + \alpha \text{ (Eqn. 3)}$$
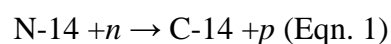
There is far less information of ^{14}C different forms penetration into graphite materials. At the same time the preliminary observation shows that study of radiocarbon penetration process into graphite materials is connected with many difficulties of methodological nature from complex micro relief of surface to wide range in physico-mechanical characteristics.

Removing a graphite material layer by layer can be executed by several ways, e.g. cutting. In the given work the external layers were consecutively deleted by polishing-out and measuring of activity of polished-out material layer after each treatment.

For measuring of activity used technology "vacuum pyrolysis" [2]:

1.   Material sample is mixed with manganese dioxide. Addition of manganese dioxide plays an important role. When the temperature is above 550 ^{o}C the manganese dioxide disintegrates with active oxygen liberation all over the volume of mixture. Oxygen liberation runs quietly, under the broad range of temperatures (550-940 ^{o}C).

2.   Carbon materials therewith are oxidized to carbon oxide and dioxide, and in such a form are absorbed by melted lithium.

3.   Resulted lithium carbide is subjected to hydrolysis.

4.   Gassing acetylene is converted into benzene on vanadium catalyst.

It allows fractional separation of analysed carbon material during one sample preparation procedure**.** Vacuum pyrolysis is considerable simplification and accelerates LS radiocarbon analyses.

REFERENECS

[1]   T. Podruhzina "Graphite as radioactive waste: corrosion behavior under final repository conditions and thermal treatment." Doctoral Dissertation. 2004.

[2]   V.V. Skripkin, N.N. Kovalyukh, Recent Developments in the Procedures Used at the SSCER Laboratory for the Routine Preparation of Lithium Carbide. Radiocarbon 1998, V.40, pp.211-214.

3   Summary (by organisation)

Centre National de la Recherche Scientifique (CNRS/IN2P3) laboratory: Institute of Nuclear Physics of Lyon (IPNL, France)

Ion irradiation of Highly Oriented Pyrolitic Graphite (HOPG) samples was carried out on ^{13}C pre-implanted samples. ^{13}C implantation was used to simulate ^{14}C displaced from its original structural site through recoil. In order to simulate neutron irradiation, the irradiations were carried out under temperature. Moreover, in order to monitor the ballistic and electronic effects independently, ion irradiation was carried out by varying the ion nature and energy.

We can now try to extrapolate these results to the structural modifications induced in graphite by irradiation in a reactor and also the behaviour of the ^{14}C in the irradiated graphite. The main structural modifications that the graphite undergoes in the reactor are linked to the ballistic damage; the low values of the electronic stopping power probably lead to little damage.

For a very damaged graphite structure (for example, coke grains which have remained in a reactor for several years in a high neutron flux zone), the irradiation will have little impact on the evolution of its structure. This is because the temperatures at which the UNGG reactors function, i.e. between 200 and 500 °C at the most, are insufficient in annealing the defects. However, the evolution of an initially slightly disordered graphite structure (in the case of coke grains irradiated with a low neutron flux), will be greatly affected by the irradiation flux and temperature. The result could therefore lead to very different structural states as a function of the position of the graphite in the reactor. Consequently, graphite irradiated with a low neutron flux and situated in a hot zone (500 °C) would probably be characterised by a structure similar to that of well-ordered graphite. However, graphite irradiated with a high neutron flux situated in a cold zone (200°C) would keep its damaged/disordered structure. Thus, both the nature and initial structural state of the graphite as well as the irradiation conditions in the reactor are likely to generate significant structural heterogeneity in the graphite moderator in the UNGG reactors.

CAST
Final report on results from Work Package 5:
Carbon-14 in irradiated graphite (D5.19)

Concerning ^{14}C, apart from the ^{14}C formed by activation of ^{14}N located close to free surfaces for which a great part has probably been removed through radiolytic corrosion, both temperature and irradiation would tend to be stabilise it in the irradiated graphite structure: in planar sp^2 structures (in both aromatic cycles and chains) or three dimensional sp^3 structures (allowing interstitials carbon atoms to bond between the basal layers). The proportion of these structures would be variable and linked with the irradiation history. Thus, in case of disposal, the ^{14}C stabilisation, especially into sp^2 aromatic structures, should lead to reduced leaching rates in comparison to ^{14}C present in degraded and porous graphite. Furthermore, in case of prior purification, ^{14}C stabilised into the "hot" parts of the irradiated graphite should be more difficult to extract in comparison to ^{14}C present in "cold" and disordered zones. Moreover, as the majority of the ^{14}C would have been produced in zones submitted to high neutron flux and greatly disordered, these ^{14}C enriched zones would then be easier to decontaminate using CO_2 gasification based or steam reforming processes due to the selective gasification of the most degraded areas. Thus, keeping a reduced mass loss of around 5%, it has been shown that around 20% of the total ^{14}C could be gasified in SLA2 or G2 graphites.

Lithuanian Energy Institute (LEI) summary

The aim of LEI work was to perform the neutron activation modelling of Ignalina Nuclear Power Plant (Ignalina NPP) Unit 1 reactor RBMK-1500 graphite stack and determine C-14 inventory. In order to achieve this aim, new numerical models for neutron activation were developed and activity distribution of C-14 within whole reactor graphite stack was obtained. Then, combining this data with the available C-14 activity measurement results, estimation of C-14 inventory in the graphite stack was made.

Modelling of neutron flux was performed using MCNP 5 ver. 1.6 code. The newly developed model envelopes the whole reactor core with the graphite stack consisting of 2488 graphite columns and surrounding structures. The modelled neutron flux was grouped into 238 energy groups (the most detailed discrete neutron energy group structure used in SCALE 6.1 codes system) and was used by COUPLE code from SCALE 6.1 codes system, for automated preparation of problem-specific cross-section data for ORIGEN-S code (also

CAST
Final report on results from Work Package 5:
Carbon-14 in irradiated graphite (D5.19)

from SCALE 6.1). Having problem-specific cross-section data and using total neutron flux, the neutron activation modelling of the whole reactor RBMK-1500 graphite stack was performed. The modelling results revealed the theoretically possible 3D distribution of the C-14 inventory in the reactor graphite stack, i.e. possible C-14 inventory heterogeneity.

Results of a preliminary study (performed by Ignalina NPP and Nature Research Centre staff, Lithuania) to estimate experimental C-14 activity in the GR-280 grade graphite of Ignalina NPP Unit 1 reactor were also taken into account. By having the modelled distributions of specific C-14 activity in each group of the graphite columns (in normalised units), by knowing the correspondence of measured (from the mentioned study) specific activity of C-14 to the exact point (location) of the modelled specific activity distribution, and by applying quantities and masses of the graphite columns in the respective group, the integral C-14 activity in the graphite stack was evaluated.

Regia Autonoma pentru Activitati Nucleare – Institute for Nuclear Research (RATEN ICN)

The thermal column of TRIGA Reactor is a graphite block (1716 x 1144 x 710 mm) made up of 98 rectangular graphite cells (12 rows x 8 bricks) in Aluminium cladding and it is placed into the reactor pool on the North side of the steady-state core. It was built up in 1985, using sintered graphite blocks with a density of 1.72 g/cm^3 and various geometries. The graphite was imported in the '50s from a UK producer but documents of its origin were lost. No information on its characteristics and on the impurity content could be found.

In CAST WP5, RATEN ICN proposed to update the ^{14}C inventory in the irradiated graphite from thermal column of the TRIGA 14MW reactor and to evaluate the ^{14}C release in alkaline conditions (relevant to disposal in cementitious environment), both in terms of total ^{14}C as well as inorganic and organic fractions.

The results of the leaching tests confirm the very low release rate of the ^{14}C. At the end of the leaching tests (376 days), around 1.33E3 Bq of ^{14}C in aerobic conditions and 450 Bq in anaerobic condition was released as dissolved species, representing 1.75%, respectively 1.85% from the initial ^{14}C activity of the i-graphite subject to the leaching test.

CAST
Final report on results from Work Package 5:
Carbon-14 in irradiated graphite (D5.19)
EURATOM

Both for anaerobic and aerobic conditions, the leaching rates are high in the first days of immersing and it decrease after that, indicating a two-stage process: an initial quick release (less than 9E-02 % of inventory/day for the first 48 days) followed by a slower release rate (around 4E-3 % of inventory/day).

The ratio between inorganic and organic ^{14}C release during the leaching test is almost constant, with more organic than inorganic ^{14}C released under anaerobic conditions (with an average fraction of organic ^{14}C of around 65% from the total ^{14}C released) and more inorganic than organic ^{14}C in aerobic conditions (with an average fraction of inorganic ^{14}C of around 68% from the total ^{14}C released).

No ^{14}C was measured in gas phase, but it is expected for this high-pH conditions that any $^{14}CO_2$ released from the irradiated graphite to remain in solution as carbonate.

Agence nationale pour la gestion des déchets radioactifs / EDF (Andra / EDF, France)
Studies on French i-graphites have shown that, during leaching experimentations, carbon 14 release rate is very slow for the graphite stack. French studies also highlighted that tests have to be specifically design for carbon 14 studies. The influence of some parameters, such as the chemical composition of the leaching liquor, has been observed.

Because of the low release rate of carbon 14 in graphite leaching tests, an experimental methodology was specifically designed to increase carbon 14 release so as to identify the organic and inorganic released species in the gas and liquid phases: powdered graphite sample, specific sampling procedure, and agitation of the leaching reactor.

These tests have shown that most of the release carbon 14 was in the liquid phase (up to 95% of the released carbon 14), mostly in the form of inorganic species (carbonates). But, it has also been observed that 30% of the release carbon 14 was in an organic form in the liquid phase. Due to the low leaching rate, it has not been possible to identify the organic species.

CAST
Final report on results from Work Package 5:
Carbon-14 in irradiated graphite (D5.19)

Agenzia Nazionale per le Nuove Technologie, L'Energia e lo Sviluppo Economico Sostenibile (ENEA, Italy)

ENEA participated in Tasks 5.4 "Exfoliation of irradiated nuclear graphite by treatment with organic solvent assisted by ultrasound", within Work Package 5 (WP5) of the CAST Project. ENEA efforts in CAST have been focused on the possibility to remove efficiently ^{14}C, from nuclear graphite, to produce graphite for recycling and/or safety disposed as LL&ILW.

In the draft delivered at the end of the first Project year WP5 (D 5.2), after the analyses of literature data, it was identified the suitable sample set and a preliminary plane of the exfoliation process ultrasound assisted. In to the second project year draft WP5 (D 5.6) it was reported the optimization of the experimental parameters which has been accomplished through a comparison of HOPG and nuclear graphite behaviour when testing the liquid exfoliation method (LEM) with N-Methyl-2-pyrrolidone (NMP); N,N-Dimethylacetamide (DMA); N,N-Dimethylformamide (DMF).

Some preliminary data of ^{14}C removed activity from nuclear graphite are showed in the draft version of the WP5 - year3 (D.5.9). Since any literature data have been published on this approach, any further comparison was possible.

Taking into account these outcomes, additional experiments have been performed. The final version of Deliverable D5.11 described the obtained results in terms of percentage rates of removal efficiency with respect to the initial amount of ^{14}C in pristine nuclear graphite and to the exfoliated nuclear graphite.

The exfoliation method is a reliable method to remove some ^{14}C from nuclear graphite, paving the way for the production of graphite for recycling and/or safe disposal. To support this method, a lot of evidence has been collected.

It has been demonstrated that the ratio powder/solvent has a crucial position in the optimization of the whole procedure. The recovery of exfoliated graphite increases when the ratio powder/solvent is low: to maximize the effect of the solvent it could be very useful to

operate with a recovery and recycling system, also due to the fact that the solution produced from the exfoliation of nuclear graphite is highly radioactive.

The extracting abilities of each solvent are quite comparable. Since the partially removed activity is independent of the yield degree, these results can be interpreted on the basis that not all the ^{14}C species in the irradiated graphite are the same and only the ones not chemically bonded or in those forms that have some chemical or physical-chemical affinity with the extracting media are likely to be removed.

These first results are promising enough to promote further investigations in this direction. Furthermore, there is no doubt that the basic aqueous mixture is more efficient in the removal of ^{14}C respect to the organic solvents. NaOH increases the production of carbonate (highly soluble in water) confirming that the next experiments have to be designed following this evidence, focusing on efforts to develop a "total green" procedure.

Forshungzentrum Juelich GmbH (FZJ, Germany)

The main objective of the work performed at FZJ was to account for the sources of major graphitic wastes in Germany, their ^{14}C inventory and to understand the release behaviour of ^{14}C from i-graphite on conditions relevant to the repository Schacht Konrad. For that the release kinetics of volatile and soluble ^{14}C were investigated in order to answer the question, whether and to what extent German i-graphite can be disposed of in Schacht Konrad. As a sub-goal the effect of an upstream decontamination by thermal treatment on the behaviour of the labile ^{14}C fraction in i-graphite had to be evaluated in order to point on the benefits and disadvantages of i-graphite pre-treatment.

Different types of i-graphite were characterized in order to account for the total inventory of ^{14}C in i-graphite accumulated in Germany. A number of leaching tests under different conditions were performed with i-graphite from Rossendorf Research Reactor (RFR), in order to evaluate the leaching rates and leaching kinetics of ^{14}C from i-graphite. The release of radiocarbon was found to occur into the aqueous and gas phase, and in both cases the inorganic $^{14}CO_2$ species represents a dominant fraction. The volatile fraction was also shown to contain some relatively small amount of organic ^{14}C-species or ^{14}CO. At higher

temperature and in water solution the release of volatile $^{14}CO_2$ is significantly enhanced. Simulation of i-graphite behaviour in cementitious media by using 1M NaOH as a leaching solution demonstrated the major part of leached ^{14}C remains in the aqueous phase. At a respective annual release rate of ^{14}C of less than $7.3 \cdot 10^{-3}$ %/year (if encapsulated in the cementitious material), the highest allowed storage capacity of i-graphite in the Schacht Konrad can be achieved even without prior treatment (e.g. thermal decontamination). An application of thermal treatment of i-graphite allows a selective separation of only a minor ^{14}C fraction, i.e. 8%, but results in unmeasurable release rates of volatile ^{14}C from treated i-graphite in neutral and basic solution. This finding indicates that thermal treatment on the given conditions does not provide for separation of a significant part of ^{14}C from RFR i-graphite to achieve the clearance level, requires costly energy consumption and may result in unwanted secondary waste generation. Given that a proper encapsulation of RFR i-graphite in a cementitious material alone may provide for WAC to be met, a thermal treatment of RFR i-graphite is now considered to be redundant.

Centro de Investigationes Energéticas Médioambientales y Tecnològicas (CIEMAT, Spain)

Regarding the Task 5.3 it is worth pointing out the following:

- Although significant heterogeneity has been observed both in the detection and in the activity of the high energy beta-gamma emitters, the ^{14}C content of the core samples tested shows a good correspondence, with an average specific activity of 1,17E+04 Bq/g and a standard deviation of the 8,74 %.

- Among all the analyses of leachate samples carried out, including pure water and granitic – bentonite (GBW), only one value, corresponding to the 28 days leaching step in pure water, presented a value of ^{14}C higher than the detection limit. It is more likely that this could be because of bad filtering of the sample or cross contamination in the equipment than because of the leaching process itself.

- Using pure water as leachant, in the ICS analyses, acetate was detected, although close to the MDA, after 90 days of leaching time; formate after 15, 56 and 90 days and oxalate in the 56 and 90 periods. However, this technique cannot be used to

analyze GBW solutions because of the high concentration of anions and cations present in this media.

- Both alcohols and aldehydes in leachates have not been detected in any step of the leaching process, and regarding gas samples, nor was CO (whose values were again below MDC (< 3.5 ppm)).

- After all the leaching steps were completed, the graphite core samples were dried, weighed and measured, without presenting any significant dimensional change (< 1 %), cracks or crumbles.

Regarding the Task 5.4 it is worth pointing out the following:

IGM samples

- In deionized water the pH and the conductivity increase, which means a certain amount of ions is dissolved from the IGM into the leachant.

- The organic carbon has been found in deionized water as formate ($HCOO^-$) in leachants from day 28, 91, 184 and 215. An oxalate ($COO^{2-})_2$ could be detected only in one leachate sample after 28 days.

- Both alcohols and aldehydes in leachates have not been detected at any time of the leaching process.

- In the case of granitic - bentonite water the pH and conductivity are practically the same before and after each step due to the higher ion concentration in the leachant which masked the presence of ions dissolved from the waste form.

- CO was not found in the gas phase of the leaching process with a MDC (< 3.5 ppm), except for the first and second leaching period with granitic - bentonite water where the concentration is: 30.9 mg/l and 10.4 mg/l. This is may be also related to the carbonate content in the leachate.

- After 356 days of leaching in granitic - bentonite water the following leaching rates has been observed: 1,44E-06 cm/day for ^{60}Co and 3,52E-06 cm/day for ^{137}Cs.

- The values obtained for ^{14}C are lower than Minimum Detectable Activity. This leads to leaching rate (Rn) for ^{14}C of lower than 6,15 E-09 cm/day.

- The Leaching rate (R_n) for ^{60}Co and ^{137}Cs in granitic - bentonite water, decreases with the time and after 356 days it will be constant.

- The durability of the IGM glass matrix has been validated by leaching experiments.

- The methodology has been established to manufacture the IGM samples in lab scale.

- It is possible to close the pore system in the irradiated graphite without to increase the volume of the waste.

Thermal Treatment

- The data obtained with virgin graphite experiments have allowed adjustment of the elements of the experimental system: Devices and methods which will be the base of the system at pilot plant scale.

- Ratio ^{14}C/Total C results are not definitive neither conclusive and they have to be improved because the corrosion rate of the graphite is higher than the one desired. Reasons for this behavior are guessing to base on the use of powder graphite that increases the surface and the corrosion kinetic due to the higher availability of ^{12}C. Further experiments can demonstrate the influence of the grain size in the corrosion kinetic.

- A decontamination ratio around 58% of ^{14}C versus 31% of ^{12}C in a 1-hour treatment at 700ºC in a 3 litres/hour of oxygen flux was obtained.

- The smallest amount of ^{14}C in inert atmosphere obtained in the Experiment 1 is in contrast with the experiment performed with other graphite type reactors as Merlin and AVR. The different behavior can be explained by the loss of ^{14}C of the graphite surface during reactor operation. UNGG reactors use graphite as moderator and CO_2 as coolant and average operation temperature is 400º C. In these conditions CO_2 reacts with graphite producing ^{14}CO. The radiocarbon comes from the graphite surface more probably from the activation of ^{14}N impurities of coolant and/or nitro-derivates in the graphite. Due to the release of majority of ^{14}C in the surface the one in the graphite comes from the activation of the ^{13}C and forms part of the structure.

- Experiment 2 demonstrates that oxygen saturation of the surface at 300º C, allows to obtain ^{14}C without high corrosion rate ($^{14}C/^{12}C = 2,6$) with a thermal treatment in inert

atmosphere. This indicates that surface bound ^{14}C is not completely released during operation which can be release by chemisorbed oxygen in the surface to be decontaminated.

- The set of experimental data indicates that a lower treatment temperature and lower reactivity of the oxidant agent increase the $^{14}C/^{12}C$ ratio.

Institutul National de Cercetare-Dezvoltare pentru Fizica si Inginerie Nucleara "Horia Hulubel" (IFIN-HH, Romania)

The main objective of the IFIN-HH in Task 5.3 of the Work Package 5 was to measure the release rate of C-14 (and tritium) into gas and solution phase from irradiated graphite (intact and crushed samples from VVR-S reactor will be used) in order to improve the understanding of the mechanism of release of C-14 from irradiated graphite in contact with aqueous solutions. An experimental apparatus has been designed and manufactured to measure the total release of C-14 (and H-3) to gas phase from irradiated graphite from the thermal column of the VVR-S Reactor.

Irradiated graphite, dismantled from the thermal column of VVR-S Reactor, contains different radioisotopes as activation products (APs), including carbon-14 (C-14) and tritium (H-3). In repository-relevant conditions, this graphite could be a source of gases containing C-14 and H-3.

In the experiments performed by IFIN-HH we have investigated the release of C-14 and H-3 from two intact samples of irradiated graphite which have been cut from the thermal column disc located near the reactor core. The samples were collected after the reactor was shut down and the spent fuels assemblies were transferred to the final repository. The graphite samples were submerged in a pH 10 solution of sodium hydroxide (NaOH) during the experiment to replicate the alkaline conditions that are likely to appear in an underground repository once grouted wastes became saturated with water. The C-14 and H-3 contents in submerged solution were measured at different times over a long period of time (12 month). The study also investigated the long-term release of C-14 and H-3 to the gas phase.

172

Radioactive Waste Management (RWM, UK)

Work reported by RWM considers the release of gaseous carbon-14 from irradiated graphite samples from Oldbury Magnox power station. Key conclusions from the study are that under baseline conditions, the predominant carbon-14 release was to the solution phase, with about 0.07% of the carbon-14 inventory being released into solution in one year and with about 1% of the released carbon-14 being released to the gas phase. An initial rapid release of ~3 Bq of carbon-14 to the gas phase was observed in the first week, and subsequently the rates of release decreased with time but detectable quantities of carbon-14 were found in all gas samples. For the final cumulative sampling period, a release of ~2 Bq was measured. Gaseous carbon-14 was predominantly in the form of hydrocarbons and other volatile organic compounds and CO, and less than 2% of the gas-phase release was in the form of $^{14}CO_2$. The differences between the fractional releases of carbon-14 from Oldbury graphite and that released from BEP0 graphite – a subject of previous study - are likely to be due to differences between the original graphites, their irradiation histories, operating temperatures and coolant gases; the results of this study do not allow determination of whether any one of these differences is a dominant effect although a wider comparison of irradiated graphites might.

The information on the location and form of carbon-14 in graphite and on the mechanisms of its release is provided by fundamental studies, rather than experiments specifically designed to provide data on the leaching behaviour of carbon-14 from graphite. It therefore complements the leaching data and provides additional justification for the key features that should be included in the revised model. Nonetheless, it does not provide sufficient information on the mechanisms of release to justify the use of a mechanistic model.

Based on the findings of the review of experimental evidence, it is considered that:

- A substantial fraction of the carbon-14 in graphite is not releasable;

- Some carbon-14 will initially be released rapidly, and some will be released more slowly at a rate reducing over time (i.e. the release cannot be defined by a single rate constant);

173

- Carbon-14 can be released to both the gas and aqueous phases. Carbon-14 released to the aqueous phase may exist as CO_2/carbonate and as organic species. Carbon-14 released to the gas phase may exist as a number of different species with potentially different consequences, including organic species (e.g. CH_4), CO_2 and CO;

- Release rates and speciation of the released carbon-14 may change depending on the conditions (e.g. pH, presence of oxygen).

The SMOGG model used by RWM to calculate gaseous carbon-14 release from graphite has subsequently been updated. The main change to the model has been to include the release fractions. This results in much less carbon-14 being released in total. In addition, potential release of carbon-14 as three separate species ($^{14}CH_4$, ^{14}CO and $^{14}CO_2$) is explicitly accounted for.

An exercise has been undertaken to parameterise the updated model. Values for the fractions of carbon-14 released, carbon-14 release rates and speciation fractions for the released carbon-14 for several sets of conditions have been defined. For each parameter a best estimate, and upper and lower bounds have been specified to allow uncertainty in the parameters to be considered.

State Institution "Institute of Environmental Geochemistry National Academy of Science of Ukraine" (IEG NASU, Ukraine)

In compliance with the requirements of the regulatory documents, the composition and activities of radionuclides accumulated in structural materials and structures during the operation of the NPP power unit must be evaluated before their removal. The first to be examined will be the main sources of radionuclides, which are the structures of the reactor, especially the graphite stack and other graphite elements.

No specific waste-acceptance criteria have been defined. However, work is in progress on this issue by SNRCU in compliance with international standards as expressed in ICRP 60 which defines acceptable public and operator doses. Irradiated reactor graphite management

determined by the Law of Ukraine "On Radioactive Waste Management» N 255/95-VR 30 June 1995 on the HLW and LLW

Issues to be addressed include:

- Uncertainty with terms of establishing a national geological repository, which may necessitate e.g. the construction of an interim storage facility;

- A lack of acceptance criteria for the disposal of graphite waste and appropriate container fleet, which in the future may result in a requirement to repackage i-graphite waste in storage;

- Verification techniques and equipment for the characterization of graphite waste are needed;

- There is a need for additional surveys of displacer graphite control rods to be undertaken and for the development of technology to deal with them;

- Handling graphite waste of the "Shelter".

CAST
Final report on results from Work Package 5:
Carbon-14 in irradiated graphite (D5.19)

4   Provision of Work Package 5 Key Findings to Work Package 6

This section presents a suggested output from CAST Work Package 5 to Work Package 6 Safety Case. It relates to and outlines the behaviour of irradiated graphite **in the context of deep geological disposal in a cementitious repository**.

It must be remembered that some national programmes participating in CAST Work Package 5 do not envisage this approach for the long-term management of irradiated graphite; for example, some consider long term storage in a surface facility or disposal to a near surface / shallow geological facility disposal.

A regulatory 'cap' on the total amount of carbon-14 permitted in a storage / disposal facility may also be in place. Treatment of irradiated graphite, e.g. to reduce the associated carbon-14 inventory, could be being considered as part of the overall management strategy for this waste, also encompassing management of any resulting secondary waste (see work reported in Section 2.5 (authored by ENEA), Section 2.6 (authored by FZJ) and Section 2.7 (authored by CIEMAT) for examples of research into possible approaches (ongoing / historical) to the treatment of irradiated graphite in national programmes.

As national programme requirements drive research activities related to irradiated graphite (and other inventory components), these activities themselves may involve considerations of varying end points to the management of irradiated graphite. Furthermore, the relative importance in the safety case of irradiated graphite-derived carbon-14 (in the aqueous phase) versus carbon-14 (in the gaseous phase) also can vary by waste management concept; this can affect the prioritisation of research activities.

It is suggested that the following is considered as an output of CAST Work Package 5 learning, for utilisation in CAST Work Package 6 Safety Case **in the context of deep geological disposal in a cementitious repository**:

- A substantial fraction of the carbon-14 in irradiated graphite is not releasable;

- Some carbon-14 would initially be released rapidly, and some would be released more slowly at a rate reducing over time (i.e. the release cannot be defined by a single rate constant);

- Carbon-14 can be released to both the gas and aqueous phases. Carbon-14 released to the gas phase may exist as a number of different species with potentially different consequences, including organic species (e.g. CH_4), CO_2 and CO;

- Release rates and speciation of the released carbon-14 may change depending on the conditions (e.g. pH, presence of oxygen).

Work reported in Section 2.3 (authored by RATEN ICN), Section 2.4 (authored by Andra / EDF), Section 2.6 (authored by FZJ), Section 2.7 (authored by CIEMAT), Section 2.8 (authored by IFNN-HH) and Section 2.9 (authored by RWM) of leaching experiments on a range of irradiated graphites from respective national programmes has presented information on the release of carbon-14 from this material that is broadly in agreement with the above suggested output from CAST Work Package 5 to CAST Work Package 6.

Furthermore, in relation to the first above bullet point ("*A substantial fraction of the carbon-14 in irradiated graphite is not releasable*"), work reported in Section 2.1 (authored by IPNL) concludes that both reactor temperature and irradiation would tend to be stabilise carbon-14 in the irradiated graphite structure: in planar sp^2 structures (in both aromatic cycles and chains) or three dimensional sp^3 structures (allowing interstitials carbon atoms to bond between the basal layers), affecting releasability. The IPNL work also notes that the proportion of these structures would be variable and linked with the relevant reactor irradiation history (i.e. irradiated graphite in a reactor should not necessarily be considered as a homogeneous medium in relation to the presence of carbon-14 and, by extrapolation, its possible behaviour as part of a waste management strategy).

It is also helpful to consider work reported in Section 2.5 (authored by ENEA), wherein it is suggested – in relation to work targeted at treating Latina NPP irradiated graphite - that ENEA results gained can be interpreted on the basis of not all the carbon-14 species in the irradiated graphite being the same, and that only the ones not chemically bonded or in those forms that have some chemical or physical-chemical affinity with the extracting media are

CAST
Final report on results from Work Package 5:
Carbon-14 in irradiated graphite (D5.19)

likely to be removed in experiments such as those undertaken by ENEA – this again implies a proportion of carbon-14 present in irradiated graphite is <u>not</u> releasable.

4.1 Modelling the behaviour of irradiated graphite

In order to parameterise any model for the behaviour of irradiated graphite in the context of deep geological disposal in a cementitious repository, the following information needs would be relevant:

- The initial total activity of carbon-14 in the graphite;

- The fractions of the carbon-14 activity in the graphite that are available for rapid and slower releases (any remaining fraction will not be releasable);

- Rate constants for the rapid release of carbon-14 under each set of conditions;

- Rate constants for the slower release of carbon-14 under each set of conditions;

- The fractions of carbon-14 released as CH_4 and CO under each set of conditions (the fraction not released as CH_4 or CO is assumed to be released as CO_2).

Various sets of conditions could be considered for which input values can be specified. Examples of these are:

- Aerobic, neutral pH: expected to be applicable to waste packaged without grouting;

- Aerobic, high pH: expected to be applicable to grouted waste during GDF operations and early post-closure;

- Anaerobic, high pH: expected to be applicable in the post-closure period, usually after resaturation.

There is a certain degree of empiricism to the above. Although some information regarding the potential mechanisms of release of carbon-14 from graphite has been obtained in CAST Work Package 5, the mechanisms are not currently fully understood. Therefore, it could be appropriate for any model to represent the important features of the release behaviour observed across various types of experiments. The limitation of this approach is that there would be uncertainty in the release calculated by the model on timescales that are substantially longer than those for which experimental data are available.

Parameterisation of any model ought to be cautious, taking into account the long timescales over which leaching of disposed irradiated graphite may occur. Furthermore, given the variability of the graphite used in different reactors, model parameterisation may need to be bespoke in the context of any one facility that has derived irradiated graphite. Additionally, work reported herein in Section 2.1 (authored by IPNL) and Section 2.2 (authored by LEI) indicates variation in the carbon-14 inventory in irradiated graphite in any one reactor; this variation could also affect carbon-14 release rates. If longer-term measurements were available, it could be possible to enhance understanding of carbon-14 release from irradiated graphite, leading possibly to the amendment of release rates and release fractions.

Work undertaken as part of RWM's programme on irradiated graphite has led to parameters being derived based on UK irradiated graphite, see Section 2.9 and Tables 2.9.4 & 2.9.5. It must be recalled that such example parameters are not necessarily transferable for consideration in relation to other waste management organisations' irradiated graphite and its potential behaviour **in the context of deep geological disposal in a cementitious repository**.

	CAST	
	Final report on results from Work Package 5:	
	Carbon-14 in irradiated graphite (D5.19)	

5   Collation of References

Centre National de la Recherche Scientifique (CNRS/IN2P3) laboratory: Institute of Nuclear Physics of Lyon (IPNL)

[Ammar 2015] M. R. Ammar, N. Galy, J.-N. Rouzaud, N. Toulhoat, C.-E. Vaudey, P. Simon, N. Moncoffre, Characterizing various types of defects in nuclear graphite using Raman scattering: Heat treatment, ion irradiation and polishing, Carbon 95 (2015) 364-373

[Bonal 2006] BONAL, J.-P. et ROBIN, J.-C. (2006). *Les réacteurs nucléaires à caloporteur gaz*, pages 27–32. CEA/DEN.

[Calizo 2007] I. Calizo, A.A. Balandin, W. Bao, F. Miao, C.N. Lau, Temperature dependence of the Raman spectra of graphene and graphene multilayers, Nano Letters, 2007, Vol. 7, No.9, 2645-2649

[Couzi 2016] M. Couzi, J.-L. Bruneel, D. Talaga, L. Bokobza, A multi wavelength Raman scattering study of defective graphitic carbon materials: The first order Raman spectra revisited, Carbon 107 (2016) 388-394

[Eapen 2014] J. Eapen, R. Krishna, T.D. Burchell, K.L. Murty (2014), Early damage mechanisms in nuclear grade graphite under irradiation, Materials Research Letters 2:1, 43-50

[Ewels 2003] C.P. Ewels, R.H Telling, A.A. El-Barbary, M.I. Heggie, Metastable Frenkel Pair Defect in Graphite: Source for Wigner Energy?, Physical Review Letter, Vol 91, 2 (2003)

[Ferrari 2007] A.C. Ferrari, Raman spectroscopy of graphene and graphite: Disorder, electron-phonon coupling, doping and nonadiabatic effects, Solid State Communications 143 (2007) 47-57

[Galy 2016] N. Galy, (2016) *Comportement du ^{14}C dans le graphite nucléaire: Effets de l'irradiation et décontamination par vaporéformage*, Thèse de Doctorat, Université Claude Bernard Lyon 1, LYCEN – T 2016-12

[Gauthron 1986] GAUTHRON, M. (1986). *Introduction au génie nucléaire Tome 1 : Neutronique et matériaux*. INSTN/CEA.

[Lehtinen 2011] O. Lehtinen and T. Nikitin (2011). "Characterization of ion-irradiation-induced defects in multi-walled carbon nanotubes." New Journal of Physics 13.

[Liu 2006] J. Liu, H.-J. Yao, et al. (2006). "Temperature annealing of tracks induced by ion irradiation of graphite." Nuclear Instruments and Methods in Physics Research Section B: Beam Interactions with Materials and Atoms 245(1): 126-129.

[Moncoffre 2016] N. Moncoffre et al., Impact of radiolysis and radiolytic corrosion on the release of ^{13}C and ^{37}Cl implanted into nuclear graphite: Consequences for the behaviour of ^{14}C and ^{36}Cl in gas cooled graphite moderated reactors, Journal of Nuclear Materials 472 (2016) 252-258

[Pageot 2014] J. Pageot, Etude d'un procédé de décontamination du ^{14}C par carboxy-gazéification des déchets de graphite nucléaire, thèse de doctorat de l'Université Paris-Sud, Andra, 2014.

[Pageot 2015] J. Pageot, J.-N. Rouzaud, M. Ali Ahmad, D. Deldicque, R. Gadiou, J. Dentzer, L. Gosmain, Milled graphite as a pertinent analogue of French UNGG

reactor graphite waste for a CO$_2$ gasification-based treatment, Carbon 86 (2015) 174-187

[Poncet 2013] B. Poncet, L. Petit, Method to assess the radionuclide inventory of irradiated graphite waste from gas-cooled reactors, J. Radioanal. Nucl. Chem. 298, 941-953, 2013

[Reich 2004] S. Reich, C. Thomsen, Raman spectroscopy of graphite, The Royal Society, Phil. Trans. R. Soc. Lond. A (2004) 362, 2271-2288

[Rouzaud 1983] Rouzaud, J.-N., Oberlin, A. & Beny-Bassez, C., 1983. Carbon films: Structure and microtexture (optical and electron microscopy, Raman spectroscopy). Thin Solid Films, 105(1), pp.75–96.

[Seitz 1956] F. Seitz, J.S. Koehler, Solide state physics 2, 305, 1956

[Silbermann 2013] SILBERMANN, G. (2013). *Effets de la température et de l'irradiation sur le comportement du* [14]*C et de son précurseur* [14]*N dans le graphite nucléaire. Etude de la décontamination thermique du graphite en présence de vapeur d'eau.* Thèse de doctorat, Université Claude Bernard Lyon 1, IPNL & EDF/CIDEN, LYCEN T 2013-12

[Silbermann 2014] G. Silbermann, N. Moncoffre, N. Toulhoat, N. Bérerd, A. Perrat-Mabilon, G. Laurent, L. Raimbault, P. Sainsot, J.-N. Rouzaud, D. Deldicque, Temperature effects on the behavior of carbon 14 in nuclear graphite, Nuclear Instruments and Methods in Physics Research B 332, 106–110, 2014.

[Telling 2003] R.H Telling, C.P. Ewels, A.A. El-Barbary, M.I. Heggie, Wigner defects bridge the graphite gap, Nature Materials, Vol 2 May 2003 doi:10.1038/nmat876

[Toulemonde 1993] M. Toulemonde, E. Paumier, C. Dufour, Thermal spike model in the electronic stopping power regime, Radiation Effects and Defects in solide 126 (1993) 201-206

[Toulemonde 2012] M. Toulemonde, W.Assmann, C.Dufour, A. Meftah, C. Trautmann Nanometric transformation of the matter by short and intense electronic excitation: Experimental data versus inelastic thermal spike model, Nuc. Ins. Meth. B 277 (2012) 28-39

[Vaudey 2010 a] C.E.Vaudey, N.Toulhoat, N.Moncoffre, N.Bérerd, Chlorine speciation in nuclear graphite: consequences on temperature release and on leaching, Radiochim. Acta 98, 1–7 (2010) / DOI 10.1524/ract.2010.1767

[Vaudey 2010 b] Vaudey, C.-E. (2010). *Effets de la température et de la corrosion radiolytique sur le comportement du chlore dans le graphite nucléaire : conséquences pour le stockage des graphites irradiés des réacteurs UNGG.* Thèse de doctorat, Université Claude Bernard Lyon 1, IPNL. LYCEN T 2010-12

[Ziegler 1985] J-F.Ziegler et al., (1985) « The Stopping and Range of Ion in Solids », Pergamon Press, New York.

[Ziegler 2010] J.F. Ziegler et al., 2010. Srim – the stopping and range of ions in matter (2010). Nuclear Instruments and Methods in Physics Research Section B: Beam Interactions with Materials and Atoms, 268(11–12): 1818-1823.

CAST
Final report on results from Work Package 5:
Carbon-14 in irradiated graphite (D5.19)

Lithuanian Energy Institute (LEI)

1. TOULHOAT, N., NARKUNAS, E., ZLOBENKO, B., DIACONU, D., PETIT, L., SCHUMACHER, S., CATHERIN, S., CAPONE, M., VON LENSA, W., PINA, G., WILLIAMS, S., FACHINGER, J., NORRIS, S. Report D5.5. 2015. WP5 Review of Current Understanding of Inventory and Release of C-14 from Irradiated Graphite. CAST Project.

2. MAZEIKA, J., LUJANIENE, G., PETROSIUS, R., ORYSAKA, N., OVCINIKOV, S. 2015. Preliminary Evaluation of ^{14}C and ^{36}Cl in Nuclear Waste from Ignalina Nuclear Power Plant Decommissioning. *Open Chemistry*, Vol. 13(1), 177–186.

3. NARKUNAS, E., POSKAS, P. Report D5.17. 2017. Report on Modelling of C-14 Inventory in RBMK Reactor Core. CAST Project.

4. http://www.atomic-energy.ru

5. Technical description of RBMK-1500 reactor. Ignalina Nuclear Power Plant, 1985 (In Russian).

6. NARKUNAS, E., SMAIZYS, A., POSKAS, P., DRUTEIKIENE, R., DUSKESAS, G., GARBARAS, A., GUDELIS, A., GVOZDAITE, R., LUJANIENE, G., PLUKIENE, R., PLUKIS, A., PUZAS, A. Technical Report T-3.4.2. 2013. Assessment of Isotope-Accumulation Data from RBMK-1500 Reactor. CARBOWASTE Project.

7. NARKUNAS, E., POSKAS, P., BLACK, G., JONES, A., IORGULIS, C., DIACONU, D., PETIT, L., PONCET, B. Technical Report T-3.4.3. 2013. Modelling of Isotope Release Mechanism Based on Fission Product Transport Codes. CARBOWASTE Project.

8. MCNP – A General Monte Carlo N-Particle Transport Code, Version 5, (Vol. I-III.) Reports LA-UR-03-1987, LA-CP-03-0245, LA-CP-03-0284. Los Alamos National Laboratory. Los Alamos, New Mexico, 2003.

9. SCALE: A Comprehensive Modeling and Simulation Suite for Nuclear Safety Analysis and Design. ORNL/TM-2005/39, Version 6.1, Oak Ridge National Laboratory, Oak ridge, Tennessee, 2011.

Regia Autonoma pentru Activitati Nucleare – Institute for Nuclear Research (RATEN ICN)

Ahn, H.J., Song, B.C., Sohn, S.C., Lee, M.H., Song, K., Jee, K.Y. Application of a wet oxidation method for the quantification of ^{3}H and ^{14}C in low-level radwastes. 2013. Appl. Radiat. Isot., 81:62-6, 2013.

Carlsson, T., Kotiluoto, P., Vilkamo, O., Kekki, T., Auterinen, I. And Rasilainen, K. 2014. Chemical aspects on the final disposal of irradiated graphite and aluminium - A literature survey, VTT Technology 156, ISBN 978-951-38-8095-8.

Magnusson, A., Stenstrom, K., Aronsson, P.O. 2008. ^{14}C in spent ion-exchange resins and process water from nuclear reactors – A method for quantitative determination of organic and inorganic fractions. Journal of Radioanalytical and Nuclaer Chemistry, Vol. 275, No. 2, 261-273, 2008.

Petrova, E., Shcherbina, N., Williams, S. 2015. Definition of the scientific scope of leaching experiments and definition of harmonized leaching parameters (D5.4). Carbon-14 Source Term (CAST) Project, N° 604779, CAST – D5.4.

RIZZO, A., BUCUR, C., COMTE, J., Källström, K, LEGAND, S., RIZZATO, C, Večerník, P. 2017. Final Report on the Estimation of the Source Term and Speciation (D4.5). Carbon-14 Source Term (CAST) Project, N° 604779, CAST - D4.5.

Toulhoat, N., Narkunas, E., Ichim, C., Petit, L., Schumacher, S., Capone, M., Shcherbina, N., Petrova, E., Rodríguez, M., Lozano, E.M., Fugaru, V. 2015. WP5 Review of Current Understanding of Inventory and Release of C14 from Irradiated Graphite (D5.5). Carbon-14 Source Term (CAST) Project, N° 604779, CAST – D5.5.

Toulhoat, N., Narkunas, E., Ichim, C., Petit, L., Schumacher, S., Capone, M., Shcherbina, N., Petrova, E., Rodríguez, M., Lozano, E.M., Fugaru, V. 2016. WP5 Annual Progress Report – Year 3 (D5.9). Carbon-14 Source Term (CAST) Project, N° 604779, CAST - D5.9.

Agenzia Nazionale per le Nuove Technologie, L'Energia e lo Sviluppo Economico Sostenibile (ENEA)

Bourlinos, A. B., Georgakilas, V., Zboril, R., Steriotis, T. A. and Stubos, A. K. (2009), Liquid-Phase Exfoliation of Graphite Towards Solubilized Graphenes. Small, 5: 1841–1845. doi:10.1002/smll.200900242.

Choi, E.-Y., Choi, W. S., Lee, Y.B. and Noh, Y-Y, Production of graphene by exfoliation of graphite in a volatile organic solvent, Nanotechnology, 22 (2011), 365601 (6pp).

Hernandez, Y., V. Nicolosi, M. Lotya, F. Blighe, Z. Sun, S. De, I. T. McGovern, B. Holland, M. Byrne, Y. Gunko, J. Boland, P. Niraj, G. Duesberg, S. Krishnamurti, R. Goodhue, J. Hutchison, V. Scardaci, A. C. Ferrari, J. N. Coleman, High-yield production of graphene by liquid-phase exfoliation of graphite, Nature Nanotechnology, Vol. 3, September 2008, 563-568.

Khan, U., O'Neill, A., Lotya, M., De, S. and Coleman, J.N., High-Concentration Solvent Exfoliation of Graphene, Small 2010, 6, No.7, 864-871.

Forshungzentrum Juelich GmbH (FZJ)

1 Toulhoat, N. et al. D5.2. WP5 Annual Progress Report of EU project CAST, p. 45, 2014.

2 Bach, F.-W. BMBF-Abschlussbericht: Trennen von graphitischen Reaktorbauteilen; Universität Dortmund; Förderkennzeichen 02S7849, 2004.

3 Shcherbina, N. et al. Final evaluation of leach rates of treated and untreated i-graphite from the Rossendorf Research Reactor. D5.12 of EU project CAST, 2017.

4 Petrova, e. at al. Definition of the scientific scope of leaching experiments. D5.4 of EU project CAST, 2015.

5 Vulpius, D. et al. Thermal treatment of neutron-irradiated nuclear graphite. // Nucl. Eng. Des. 265, 294–309, 2013.

6 Kuhne et al. Entsorgung von bestrahltem Graphit (CarboDisp). Abschlussbericht, 2015.

7 Carroll, J.J., Slupsky, J.D., Mather, A.E. The solubility of carbon dioxide in water at low temperature. // J. Phys. Chem. Ref. Data, 20, 1201, 1991.

8   Brenneke, P. Anforderungen an endzulagernde radioaktive Abfälle (Endlagerungsbedingungen, Stand Dezember 2014), Technical report SE-1B-29/08-REV-I, 2014.

9   Burchell, T.D. Graphite: properties and characteristics. Chapter 2.10 in: Konings, R.J.M. (ed.) Comprehensive nuclear materials, 2, 285-305, 2012.

10 Engle, G.B., Kelly, B.T. Radiation damage of graphite in fission and fusion reactor systems. // J. Nucl. Mater. 122(1-3), 122-129, 1984.

11 Shcherbina et al. Final evaluation of leach rates of treated and untreated i-graphite from the Rossendorf Research Reactor D5.12 of EU project CAST, 2017.

Centro de Investigationes Energéticas Médioambientales y Tecnològicas (CIEMAT)

[1] ISO (International Organization for Standarization), "Long-Term Leach Testing of Solidified Radioactive Waste Forms", ISO 6961-1982(E).

[2] Reference ALD-F patent EP2347422

[3] J. Cobos, L. Gutiérrez, N. Rodríguez, E. Iglesias, G. Piña, E. Magro (CIEMAT). Irradiated Graphite Samples Bulk Analyses at CIEMAT. CARBOWASTE report (T.3.2.4).

[4] Proceedings of ICAPP 2011, Nice, France, May 2-5, 2011; Paper 11267: Impermeable graphite: A new development for embedding radioactive waste; J. Fachinger1, K.H. Grosse1, R. Seemann2, M. Hrovat2 1FNAG, 2ALD Vacuum technologies, Wilhelm Rohn Str. 35;63450 Hanau; Germany

[5] E. Magro, M. Rodríguez Alcalá, J. L. Gascón, G. Piña, E. Lara, L. Sevilla. WP5 CIEMAT Final Report on ^{14}C leaching from Vandellós I Graphite (D5.15)

[6] "Leaching methods for conditioned radioactive waste". R.Carpentiero, P.Bienvenu, A.G.de la Huebra, C.Dale, D.Grec, C.Gallego, M.Rodriguez, F.Vanderlinden, ºP.I.Voors, J.Welbergen, R.Maz, J.Fazs. Report WG-B-02, Abril 2004.

[7] J. Fachinger, W. von Lesa, T. Podruhzina. Decontamination of nuclear graphite. Nuclear Engineering and Design 238 (2008),3086-3091.

[8] R. Holmes, B. Marsden, A. Jones. Mechanisms Involved in the Removal of Radioisotopes from Nuclear Graphite. First year report of PhD study, University of Manchester.

[9] J. Cleaver. Thermal Treatment of irradiated Graphite for the Removal of ^{14}C.

Radioactive Waste Management (RWM)

AMEC report to RWM, Carbon-14 Project Phase 2: Irradiated Graphite Wastes, AMEC/200047/004 Issue 2, 2016, https://rwm.nda.gov.uk/publication/carbon-14-project-phase-2-irradiated-graphite-wastes/

Amec Foster Wheeler report to RWM, Specification for SMOGG Version 7.0: A Simplified Model of Gas Generation from Radioactive Wastes, AMEC/204651/001, Issue 2, https://rwm.nda.gov.uk/publication/specification-for-smogg-version-7-0-a-simplified-model-of-gas-generation-from-radioactive-wastes/, 2016a.

Amec Foster Wheeler report to RWM, User Guide for SMOGG Version 7.0: A Simplified Model of Gas Generation from Radioactive Wastes, AMEC/204651/002,

	CAST	
	Final report on results from Work Package 5:	
	Carbon-14 in irradiated graphite (D5.19)	

Issue 2, https://rwm.nda.gov.uk/publication/user-guide-for-smogg-version-7-0-a-simplified-model-of-gas-generation-from-radioactive-waste/, 2016b.

BASTON, G.M.N., CHAMBERS, A.V., COWPER, M.M., FAIRBROTHER, H.J., MATHER, I.D., MYATT, B.J., OTLET, R.L., WALKER, A.J. and WILLIAMS, S.J. 2004. The Release of Volatile Carbon-14 from Irradiated Graphite in Contact with Alkaline Water, Serco Assurance Report SA/ENV-0654.

BASTON, G.M.N., MARSHALL, T.A., OTLET, R.L., WALKER, A.J., MATHER, I.D. and WILLIAMS, S.J. 2012. Rate and Speciation of Volatile Carbon-14 and Tritium Releases from Irradiated Graphite, Mineralogical Magazine 76(8), 3293-3302, 2012.

BASTON, G., PRESTON, S., OTLET, R., WALKER, J., CLACHER, A., KIRKHAM, M. and SWIFT, B. 2014. Carbon-14 release from Oldbury Graphite, Amec report AMEC/5352/002 Issue 3.

HANDY, B.J. 2006. Experimental Study of C-14 and H-3 Release from Irradiated Graphite Spigot Samples in Alkaline Solution, NNC Report 11996/TR/001.

MARSHALL, T.A., BASTON, G.M.N., OTLET, R.L., WALKER, A.J. and MATHER I.D. 2011. Longer-term Release of Carbon 14 from Irradiated Graphite, Serco Report SERCO/TAS/001190/001 Issue 2.

McDERMOTT, L. 2011. Characterisation and Chemical Treatment of Irradiated UK Graphite Waste, PhD thesis, University of Manchester.

NUCLEAR DECOMMISSIONING AUTHORITY, 2012. Geological Disposal, Carbon-14 Project, Phase 1 Report, NDA Report NDA/RWMD/092.

RADIOACTIVE WASTE MANAGEMENT, Geological Disposal: Carbon-14 Project Phase 2: Overview report, NDA Report no. NDA/RWM/137, 2016, https://rwm.nda.gov.uk/publication/geological-disposal-carbon-14-project-phase-2-overview-report/.

SWIFT, B.T. and RODWELL, W.R. 2006. Specification for SMOGG Version 5.0: a Simplified Model of Gas Generation from Radioactive Wastes, Serco Report SERCO/ERRA-0452 Version 6.

The 2010 UK RADIOACTIVE WASTE INVENTORY: Main Report, URN 10D/985, NDA/ST/STY(11)0004, 2011.

State Institution "Institute of Environmental Geochemistry National Academy of Science of Ukraine" (IEG NASU)
[1]   T. Podruhzina "Graphite as radioactive waste: corrosion behavior under final repository conditions and thermal treatment." Doctoral Dissertation. 2004.
[2]   V.V. Skripkin, N.N. Kovalyukh, Recent Developments in the Procedures Used at the SSCER Laboratory for the Routine Preparation of Lithium Carbide. Radiocarbon 1998, V.40, pp.211-214.